超高層大気観測のための真空計開発に関する検討

大早田 翼 [1]; 阿部 琢美 [2]; 渡部 重十 [3]; 三宅 亙 [4]
[1] 東海大; [2] ＪＡＸＡ宇宙科学研究所; [3] 北大・理・宇宙; [4] 東海大・工

Development of ionization gauge for a study of the upper atmosphere

Tsubasa Oohayata[1]; Takumi Abe[2]; Shigeto Watanabe[3]; Wataru Miyake[4]
[1] Tokai Univ.; [2] ISAS/JAXA; [3] Cosmosciences, Hokkaido Univ.; [4] Tokai Univ.

In the Earth's atmosphere above 70 km, a part of the neutral atmosphere is ionized by various ionization processes. Since the electromagnetic force acts on the ionized atmosphere, the neutrals and charged particles mostly move in the different directions, then momentum is transferred each other due to collisions between these particles. It is thought that this momentum transport plays an important role in phenomena in this region. Thus, it is important to measure the neutral density and wind, which determine the momentum of the neutral particles, to understand such a basic process.

In this study, we try to develop an instrument to measure density of the neutral atmosphere and neutral wind in the lower thermosphere, assuming that it is installed on the sounding rocket. In particular, we focus on developing an ionization gauge which can be used for a pressure up to 10^{-4} Pa corresponding to that at 150 km altitude. Ionization gauge *MG-2F* made by Canon Anelva is considered as a candidate of applicable element.

In terms of measurement on the sounding rocket, the shape of the container in which the ionization gauge is housed is important. In the past measurement of atmospheric density using the ionization gauge, it was housed in spherical or cylindrical containers, but common understanding of an optimal shape has not been obtained. In this study, we use DSMC (Direct Simulation Monte Carlo) method which can simulate the rarefied gas flow for consideration of the shape of the container. When atmospheric pressure is low (e.g. lower thermosphere) and spatial scale of the gas flow is small, Navier-Stokes equation is not valid because the flow cannot be treated as continuum. The DSMC method can simulate the rarefied gas flow in such a situation through the calculation of motion and collision of sample particles.

First, in order to confirm a validity of the DSMC method to simulate the rarefied gas flow around the ionization gauge and accuracy of the calculation algorithm, we compare a result form the DSMC method with the experiment which is performed in the vacuum chamber. In the experiment, we demonstrate the upper atmosphere environment using the vacuum chamber in which wind is induced due to pressure difference. The pressure distribution around the wind flow is measured by MG-2F. On the other hand, the flow and the pressure around the experimental system are simulated by using the DSMC method. Since both of results mostly in a good agreement, validity of the DSMC method was confirmed.

There are two categories of the container for the ionization gauge; *open* type or *closed* type. For the former, atmospheric particles which enter the container flow outward after they pass through the ionization gauge. For the latter, they stay inside the container. We need to use properly the container type depending on background atmosphere density and measurement environment. In the case of *closed* type, a pressure value measured by the ionization gauge may be different from the background atmospheric pressure depending on the amount of inflow. Therefore, for accurate measurement, it is important to design the shape of the ionization gauge so that we can show a relation between the background pressure, the amount of inflow to the container, and pressure (neutral density) from the ionization gauge.

We are now considering the optimal shape of the container using the DSMC method, assuming that we use MG-2F. In this presentation, we will show the result of our comparison between the DSMC simulation and the measurement in the vacuum chamber, and will also explain the desirable shape of the container for MG-2F and an idea of measurement on sounding rocket.

地球の高度約 70km 以上の大気では、さまざまな電離過程によって中性大気の一部が電離して電離大気となる。電離大気は電磁気的な力を受けるために中性大気とは異なる方向に運動し、中性大気と電離大気の衝突によって運動量が輸送される。この運動量輸送が超高層大気領域固有の電子密度擾乱や電離圏ダイナモといった現象にかかわっていると考えられており、これらの現象を理解するためには中性大気の密度および中性粒子の運動である中性風の情報を精確に把握することが必要である。

本研究では観測ロケットに搭載することを前提に、熱圏下部での中性大気密度の測定および中性風に関する情報の検出を可能にする測定器の開発を目的とする検討を行う。具体的には高度約 150km に相当する、大気圧 10^{-4}Pa までの測定を可能にする電離真空計の開発を目的とし、現在は測定球の候補としてキャノンアネルバ社製の真空ゲージ MG-2F を考えている。

観測ロケット上での測定においては真空ゲージをどのような容器に収納するかが大変重要である。これまでに海外で行われた観測ロケット上での真空計による大気密度測定では球形や円筒形状の容器に真空ゲージが収められていたが、最適な形状についての共通的な理解は得られていない。本研究では収納容器の形状検討のため、希薄気体のシミュレーションが可能な DSMC（Direct Simulation Monte Carlo）法を用いる。熱圏下部のように低圧力の領域や流れの空間スケールが小さい領域では、気体を連続体として扱うことができなくなり、Navier-Stokes 方程式が有効ではなくなる。DSMC 法は 1 つで多数の気体粒子を表すサンプル粒子の運動と衝突の計算を通して希薄気体のシミュレーションを行う手法である。

まず、DSMC 法によって真空計周辺の流れのシミュレーションが可能か、また計算アルゴリズムの精度を確かめるた

め、室内での真空チャンバーを用いた実験とシミュレーションを比較することで DSMC 法の妥当性を検証した。室内実験では真空チャンバーに低圧力かつ気体の流れがある状況を作り出し、気体の流れによって生じる圧力分布を真空計で測定した。この実験を DSMC 法を用いてシミュレーション空間上で再現し、実験値とシミュレーション値を比較したところ、両者に概ね一致が見られたことから、我々が用いている DSMC 法の妥当性を検証することができた。

真空ゲージを収納する容器には開放型と閉鎖型が考えられる。前者では容器に入ってきた大気粒子が真空ゲージ付近を通過した後に外部に流れ出すのに対し、後者では容器内にいったん留まる。これらは測定対象である大気の密度や測定環境により使い分ける必要がある。閉鎖型の容器の場合には流入する大気の量によっては背景の大気密度と一致しない真空度が計測される可能性があって、精確な測定のためには両者の関係を定量的に理解しておくことが必要になる。このため、背景の大気密度および真空計を収納した容器への大気流入量と真空ゲージによって得られる真空度（大気密度）との関係が明確に示せるような形状の真空計を設計することが重要である。

我々は真空ゲージ MG-2F を用いることを前提に、上記の条件を満たす容器の最適形状について DSMC 法を用いて検討を行っている。本発表では DSMC 法の妥当性の検証結果、現在検討している MG-2F を収納する容器の形状、および観測ロケットに搭載した場合の真空度の測定方法について述べる。

観測ロケット搭載用イオンドリフト速度測定器の開発（１）

阿部 琢美 [1]; 渡部 重十 [2]; 齊藤 昭則 [3]
[1] ＪＡＸＡ宇宙科学研究所; [2] 北大・理・宇宙; [3] 京都大・理・地球物理

Development of ion drift velocity analyzer for sounding rocket (1)

Takumi Abe[1]; Shigeto Watanabe[2]; Akinori Saito[3]
[1] ISAS/JAXA; [2] Cosmosciences, Hokkaido Univ.; [3] Dept. of Geophysics, Kyoto Univ.

http://ssl.tksc.jaxa.jp/pairg/member/abe/index.html

Charged particles and neutral particles co-exist in the lower ionosphere. The charged particles tend to move in a direction different from neutral particles, because of a difference in those behaviors against the electromagnetic force. The ionospheric current and ambipolar electric field existing in this region are attributed to a difference in a collision frequency between ion and electron with neutral particles. Characteristic phenomena such as traveling ionospheric disturbance and electron density irregularity are significantly generated due to the diversity of the particles in this region. The momentum transfer between the charged and neutral particles plays an important role in generating these phenomena. Sounding rocket is only the platform which enables us to make in-situ measurement in this region because low-altitude satellite cannot be in orbit for a long time due to the atmospheric drag. Thus, it is desirable to make a direct measurement of charged and neutral particles by using instrument on the sounding rocket to further understand such unresolved phenomena.

Lithium Ejection System (LES) or Trimethyl Aluminum (TMA) instruments have been adapted for sounding rocket experiment to get the local information on neutral wind in the lower ionosphere. In contrast, no instruments to measure a drift of the ionospheric ions is now available in Japan, and it is not practical to estimate the ion drift with good accuracy from the electric field measurement. Therefore, our understanding of interaction between charged and neutral particles has not made much progress because of a lack of instrument for this purpose. Unfortunately, it is very difficult to reproduce a coupling between charged and neutral particles on the ground, and therefore direct measurements by sounding rocket in the lower ionosphere is only the way to provide quantitative information.

Under such a background, we have started developing an ion drift velocity analyzer which enables us to estimate the ion drift velocity and density so that it can be installed on the sounding rocket. It is well known that Ion Drift Meter (IDM) or Retarding Potential Analyzer (RPA) had been installed on low-altitude satellite, such as Dynamic Explorer-2 and Atmospheric Explorer series. Our instrument will be required to have both of these functions. It will also be possible to make simultaneous measurement of the ion drift and neutral wind in the sounding rocket experiment when our development succeeds in the future. Then, we will be able to conduct quantitative discussion on the coupling between charged and neutral particles.

As an actual schedule, a numerical simulation to design an internal structure of the instrument was already started. The prototype model will be made after we obtain a confident prospect that the instrument provides the ion density and velocity in a good accuracy. Then, we will evaluate a performance of this prototype instrument. The latest status of our instrument development will be explained in the presentation.

電離圏には電離大気と中性大気が共存している。電離大気は電気的磁気的な力を受けるために中性大気とは異なる独立した運動を行うが、これらの粒子間には衝突が起こりうるので大気粒子は運動量を交換しながら複雑な運動を行う。電離大気は磁力線方向に運動しやすい性質から粒子の運動が非等方的になり、また電子とイオンでは中性粒子との衝突周波数が異なるために電離圏電流や分極電場を生じる等、中性大気のみの場合とは異なる特徴的な性質をもつことが知られている。電離大気－中性大気間の運動量輸送は電離圏下部（高度約 80～300 km）において顕著であるが、人工衛星は大気ドラッグの影響のために、この領域を長時間飛行することは出来ない。ロケットの弾道飛行中に測定を行なう観測ロケットは衛星が飛行できない高度領域でのその場観測を可能にする唯一の手段である。下部電離圏には中規模移動性電離圏擾乱 (MS-TID) や電子密度イレギュラリティ、赤道スプレッド F 等、中性大気とプラズマの相互作用に起因して複雑な現象が多く存在するが、残された未解明の問題を解決するためには、観測ロケットに搭載可能な測定器を用いて電離大気と中性大気の精度良い観測を行なうことが必要である。

この領域に存在する大気粒子の運動の観測手段として、中性大気に関しては日本のリチウム放出器や米国研究者の提供による TMA（トリメチルアルミニウム）放出器が日本の観測ロケットに搭載され中性風に関する良好なデータを取得してきた。これに対し電離圏プラズマ中で観測が可能なイオンドリフトの測定器は現在日本に存在せず、電場計測によりイオンドリフトを推定する方法では精度良い測定値を得ることが容易ではないため、研究を進める妨げとなってきた。電離圏のような弱電離気体中の中性大気とプラズマの相互作用、特に運動量輸送については地上の実験では測定することが出来ず、宇宙空間で観測する以外に方法は無い。

このような背景のもと、我々は電離圏下部においてイオンドリフト速度および密度の推定を可能にする観測ロケット搭載用小型測定器の開発を 2018 年度に開始した。これまで海外では、測定器開口面接線方向の速度の推定が可能な Ion Drift Meter(IDM) や開口面に直交する速度成分の推定が可能な Retarding Potential Analyzer(RPA) が人工衛星に搭載されてきたが、本開発では小型でありながらこれら２つの機能を兼ね備え、イオン種毎の密度と、イオンドリフト速度をベ

クトルとして測定できる発展型測定器の実現を目指す。ここで開発する測定器は小型であるため、観測ロケットや小型衛星に中性大気観測の計測器とともに搭載することが可能であり、両者の相互作用の直接同時観測を実現し、下部電離圏領域の現象についての定量的議論に必要な数値データを提供することが期待できる。

電離圏中には複数種のイオンが存在するのに対し、本研究で開発する測定器は質量弁別機能をもたないが、イオンの熱速度よりも高速で移動するプラットホームの系においては質量比例のエネルギーで粒子が測定器に入ってくるように見えるため、およその区別が可能になる。第 1 段階では測定器により取得されたデータに加え電離圏 IRI モデルが提供するイオン組成比を参照することで、イオン種を同定し、電流値から各イオンの密度を推定することの妥当性を検討する。

開発計画としては、まず測定器の机上設計および数値シミュレーションにより研究をスタートさせ、見通しが得られた段階で第 1 次の測定器構造を設計し、その後測定器の試作に着手する予定である。試作完了後にスペースチェンバー内に設置してイオンの測定を行うことで基本性能を確認した後に、必要な改良点を洗い出す。これらの検討結果を試作品に反映させて、試作モデルの完成を目指す。測定器の構成としては、前段に RPA、後段に 16 枚の扇形平板からなる電流収集用コレクタ電極を配置するものを第 1 次案として考えている。シミュレーション空間で測定器内部の電位分布を表現し、ある速度と温度の分布関数で表されるイオンが外部から測定器に対し入射した場合の各々のコレクタ電極の電流値を計算する。入射角度、速度、温度等のパラメータを様々な値に変化させた場合の各電流値を計算し、各パラメータを推定する方法の妥当性を検討する。本講演においては最新の検討状況を報告する。

バリウム・ストロンチウムを用いたカスプ領域プラズマドリフト・熱圏風計測における高精度な解析手法の提案

渡邊 太郎 [1]; 山本 真行 [2]; 柿並 義宏 [3]
[1] 高知工科大・システム工・電子; [2] 高知工科大; [3] 苫小牧高専

Proposition of accurate analytical method for wind measurement of cusp region using Barium and Strontium chemical releases

Taro Watanabe[1]; Masa-yuki Yamamoto[2]; Yoshihiro Kakinami[3]
[1] Electronic, Kochi Univ. of Tech.; [2] Kochi Univ. of Tech.; [3] Tomakomai College

In the cusp region, there are phenomena such as aurora and density fluctuation of neutral atmosphere due to the energy input from outer space. The density fluctuation of neutral atmosphere causes global density fluctuation in thermosphere and affects altitude and orbital motion of low orbital satellites (LEO) and space debris. For safer operation of the satellites, accurate prediction of the density fluctuation of neutral atmosphere is indispensable. Recently, in the cusp region, density rising of neutral atmosphere was discovered, which presumed to be caused by Joule heating due to small scale fluctuation of the electric field. In order to support this phenomenon, there is a method of releasing Ba (to be ionized in a short time by extreme ultraviolet (EUV) from the Sun) and Sr (not ionized in a short time) from a sounding rocket, then observing resonance scattering emission of Ba^+ and Sr simultaneously from multiple sites so as to obtain fluctuation of the electric field and Joule heating.

In November 2014, we conducted a US-Japan joint rocket experiment called the Cusp Region Experiment 1 (CREX-1) in the Arctic region, but we could not observe the cusp region at that time. Currently, we are planning a space experiment, based on the CREX-1 results, using two sounding rockets of the Cusp Region Experiment 2 (CREX-2) and the Joint Japan-US Cusp Heating Investigation (CHI) aiming at observing of the cusp region in December 2019.

In CREX-1, at Andoya Rocket Range in Norway, we launched an sounding rocket equipped with 24 discerptible type small canisters that release Ba/Sr gases. Canisters released the both gases at multiple altitudes after separating from the rocket at planned altitudes. Resonant scattering emission of released Ba/Ba^+/Sr gases was optically observed from two points of Longyearbyen and Ny-Alesund in Svalbard, and the position of the multiple luminescent cloud was determined every successive moment by triangulation, and ion drift and neutral atmospheric wind speed were measured. Since the wavelengths of the emission are 553.5 nm for Ba, 455.4 nm for Ba^+ and 460.7 nm for Sr, respectively, two cameras for Ba and Ba^+/Sr with a bandpass filter with a width of 12 nm were installed at each site. The experiment was carried out in the morning with good S/N between the luminescent cloud and the background. As a result, 10 canisters in 24 successfully released Ba/Sr gases between the altitude of 393.82 km and 198.90 km (Kakinami et al., 2015), but they were released where deviated location from the cusp region, direct observation of the cusp region was not fulfilled at that time.

In the experiment scheduled in December 2019, simultaneous launches of the CREX-2 from Andoya and the CHI from Ny-Alesund are planned, with releasing Ba/Sr gases in a wide range of the cusp region to capture the cusp reliably, so as to measure the neutral atmospheric wind and ion drift. Also, to observe Ba^+ and Sr independently, we plan to install a 4 nm bandpass filter on the cameras. In addition, the time resolution will be improved by using a high sensitivity camera using the latest imaging sensor.

Currently, with the aim of establishing highly accurate observation methods and analytical methods for the CREX-2 and CHI, we are working on proposing/establishing a method to correct the lens distortion using the background stars, a method of measuring the position of weighted illuminating center of each tracer, and a method of obtaining the appropriate Ba^+ illuminating area of spreading along the direction of geomagnetic field lines, based on the CREX-1 data. In this presentation we will report initial results of the proposing methods.

References:

Y. Kakinami, S. Watanabe, M.-Y. Yamamoto, D. Kihara, M. Conde and M.F. Larsen, Measurement of thermospheric wind and plasma drift using barium strontium in cusp region, the 138th SGEPSS Meeting, 2015.

極域では，地球磁場の磁力線構造が宇宙空間に対して開いているカスプと呼ばれる領域が存在し，カスプ領域から流入する宇宙からのエネルギーによってオーロラや中性大気密度変動といった現象が起こる．中性大気密度変動は全球熱圏密度変動を引き起こし，低軌道周回衛星 (LEO) やデブリの姿勢および軌道運動に影響を及ぼすため，衛星の安全な運用にはその正確な予測が不可欠である．近年カスプ領域において，小さいスケールでの電場の変動によるジュール加熱が要因と推測される中性大気密度上昇が発見された．この裏付けを得るための宇宙実験の手法として，太陽極端紫外線により短時間でイオン化する Ba と短時間にはイオン化しない Sr を観測ロケットから放出し，Ba^+ と Sr の共鳴散乱発光をトレーサーとして，イオンドリフトおよび中性大気風を同時観測することで電場の変動とジュール加熱を求める手法がある．

電場の変動を観測するために，2014 年 11 月に Cusp Region Experiment 1(以下 CREX-1) と称した日米共同のロケット実験を北極域で実施したが，カスプ領域の観測は行えなかった．現在，CREX-1 の結果と課題を踏まえ，2019 年 12 月に

カスプ領域の観測を目指す Cusp Region Experiment 2(以下 CREX-2)，The Joint Japan-U.S. Cusp Heating Investigation(以下 CHI) の 2 機の観測ロケットを用いた宇宙実験を計画中である．

CREX-1 では，Ba/Sr ガスを放出する分離式小型キャニスター 24 個を搭載した観測ロケット 1 機をノルウェーのアンドーヤロケット実験場から打ち上げた．キャニスターは上空の計画高度でそれぞれロケットから分離の後に複数の高度においてガスを放出した．放出された Ba/Ba^+/Sr ガスの共鳴散乱光をスバールバル諸島ロングヤービン，ニーオルスンの 2 地点から光学観測し，三角測量によって複数の発光雲の時々刻々の位置を定め，イオンドリフトと中性大気風速を得る．Ba は 553.5 nm．Ba^+ は 455.4 nm，Sr は 460.7 nm で共鳴散乱するため，それぞれの観測地点には 12 nm 幅のバンドパスフィルタを取り付けた Ba 用と Ba^+/Sr 用の 2 台のカメラを設置して観測した．実験は，発光雲と背景光との S/N が良好な早朝に行われた．実験結果として，高度 393.82 km から 198.90 km の間で 24 個中 10 個のキャニスターが正常動作し Ba/Sr ガス放出に成功した (柿並 他, 2015) が，カスプ領域から外れた場所に放出されたため，カスプ領域の直接観測に至らなかった．

2019 年 12 月に予定される実験では，CREX-2 をアンドーヤから，CHI をニーオルスンから同時に発射し，カスプ領域の広範囲に Ba/Sr ガスを放出することで確実にカスプを捉え，中性大気風とイオンドリフトの計測を可能とする．また，Ba^+ と Sr を分離して観測するため，新たに 4 nm 幅のバンドパスフィルタを取り付ける．加えて，最新の撮像素子を用いた高感度カメラを用いることで，時間分解能を改善する．

CREX-1 には高知工科大学のメンバーを含む日本チームが参画し，地上および航空機からの光学観測および風速解析を行っており，CREX-2 および CHI にも参画する予定である．日米共同の観測チームでは，長年にわたって中性大気観測に取り組んできており，高知工科大学では撮像機器の開発に加え，2007 年の Li 放出実験から継続的に複数回の熱圏中性大気風の観測に参画し，これまで専用レンズ開発による S/N 向上や同時観測の運用精度の改善などを行ってきた．ロケットからのガス放出技術の確立に加え，広視野な特殊カメラを用いた同時観測による精密な位置計測とそれを基にした流れの精密解析のため，様々な観測条件に合わせた最適な解析手法の確立が課題である．

現在，CREX-2 および CHI に向けた観測手法や解析手法の高精度化の確立を目的とし，CREX-1 のデータを用いて，背景の星の座標を用いたレンズ歪みの補正方法や各トレーサーの重心位置を測定する手法，Ba^+ の磁力線方向の拡がりを求める手法を提案しその確立に取り組んでおり，本発表で初期結果を報告する．

参考文献：

柿並義宏, 渡部重十, 山本真行, 木原大城, M. Conde, M.F. Larsen, カスプ領域でのバリウム・ストロンチウムを用いた熱圏風・プラズマドリフト計測，第 138 回地球電磁気・地球惑星圏学会講演会, 2015.

EISCAT_3D（次世代欧州非干渉散乱レーダー）計画の進捗状況（７）

宮岡 宏 [1]; 小川 泰信 [1]; 西村 耕司 [1]; 中村 卓司 [1]; 野澤 悟徳 [2]; 大山 伸一郎 [3]; 藤井 良一 [4]; Heinselman Craig[5]
[1] 極地研; [2] 名大・宇地研; [3] 名大 ISEE; [4] 情報・システム研究機構; [5] EISCAT 科学協会

Recent progress of EISCAT_3D (Next-Generation Incoherent Scatter Radar Project for Atmospheric and Geospace Science) (7)

Hiroshi Miyaoka[1]; Yasunobu Ogawa[1]; Koji Nishimura[1]; Takuji Nakamura[1]; Satonori Nozawa[2]; Shin-ichiro Oyama[3]; Ryoichi Fujii[4]; Craig Heinselman[5]
[1] NIPR; [2] ISEE, Nagoya Univ.; [3] ISEE, Nagoya Univ.; [4] ROIS; [5] EISCAT

EISCAT_3D is the major upgrade of the existing EISCAT mainlamd radars, with a multi-static phased array system composed of one central active (transmit-receive) site and 4 receive-only sites to provide us 50-100 times higher temporal resolution than the present system. The construction of EISCAT_3D is planned to implement by 4-staged approach, starting from the core site with half transmitting power about 5MW and 2 receiving sites at Kaiseniemi (Sweden) and Karesuvanto (Finland) at the 1st stage. Sweden, Norway, Finland and UK have successfully secured their national funding for the construction of the 1st stage of EISCAT_3D by April 2017. After careful examinations and discussions on possible future funding scenarios, the EISCAT Council has officially started the implementation of the 1st stage of EISCAT_3D from 1st September 2017 to be completed by the end of 2021 including a commissioning of the whole radar system.

The EISCAT_3D program in Japan, on the other hand, was applied to the Master Plan 2017 of the Science Council of Japan as a part of 'Study of Coupling Processes in the Solar-Terrestrial System'(PI: Prof. Toshitaka Tsuda, Kyoto Univ./ROIS), and has been granted as one of 28 high-priority programs of Master Plan 2017. In parallel to funding proposals for EISCAT_3D to the Ministry since 2014, the National Institute of Polar Research has been developing the EISCAT 3D transmitter power amplifier (SSPA) modules to contribute in-kind for the verification test system at Tromso site and the 2nd stage of EISCAT_3D at the Skibotn core site. In this paper, we overview the current status of the project implementation and our development regarding the EISCAT 3D transmitter sub-system.

EISCAT科学協会（現加盟国：スウェーデン、ノルウェー、フィンランド、英国、日本、中国）が現在進めているEISCAT_3D（次世代欧州非干渉散乱レーダー）計画の進捗状況について報告する。EISCAT_3D計画は、送受信を担う主局と4箇所の受信局から成る多点フェーズドアレイレーダーシステムを整備して北極域大気への太陽風エネルギーの流入とその影響の全容解明を目指す国際共同プロジェクトである。昨年9月より第1段階の整備を開始し、主局が置かれるシーボトン（ノルウェー）、ならびに受信局が設置されるカイセニエミ（スウェーデン）、カレスバント（フィンランド）の敷地確保や電力線および光ファイバの敷設準備を進めるとともに、レーダー設備本体の整備をサブシステム毎に開始した。アンテナユニット、受信システムの国際入札はすでに完了し、現在送信機システムの入札を進めている。今後、さらにパルス制御システムおよびレーダーサイト建屋の入札を実施し、2019年より本格的な現地整備を開始する。2021年末までに第1段階の整備作業およびコミッショニング試験を完了して2022年より本格運用を開始する予定である。

これと並行して、トロムソ観測所において試験用サブアレイ（クロス八木アンテナ91本）1式からなるEISCAT_3D試験システムを用いた技術実証試験を進めている。日本は、第1段階用レーダー送信機10,000台（計約5MW）の開発・製造を分担する計画で予算要求を進めてきたが、2018年度予算として必要な整備予算が認められなかったため、これを各加盟国の分担金による国際入札に切り替え、第2段階用（2022年以降）の送信機10,000台の開発・製造を分担する計画に変更した。日本のEISCAT_3D計画は、大型研究計画「太陽地球系結合過程の研究基盤形成」の一部として、日本学術会議のマスタープラン2017重点大型研究計画（全28件）に採択された。本体予算はまだ措置されていないが、開発予算を用いて、上記の技術実証試験システムに使用する送信機の開発と製造を進めており、2016年度に19台、2017年度に55台を製造・提供した。本年度も国際入札で整備する最終仕様を満たす量産モデルの開発・製造を継続し、技術実証試験および第2段階整備に貢献する。本講演では、EISCAT_3D計画全体の最新の進捗状況と日本の取り組み状況を中心に報告する。

北欧に展開された3つの流星レーダーを用いた両極性拡散係数の異常増大

高橋 透 [1]; 堤 雅基 [1]; 小川 泰信 [1]; 野澤 悟徳 [2]; Hall Chris[3]; 宮岡 宏 [1]
[1] 極地研; [2] 名大・宇地研; [3] トロムソ大・TGO

Anomalous enhancement of ambipolar diffusion coefficient observed by three meteor radars installed in the polar region

Toru Takahashi[1]; Masaki Tsutsumi[1]; Yasunobu Ogawa[1]; Satonori Nozawa[2]; Chris Hall[3]; Hiroshi Miyaoka[1]
[1] NIPR; [2] ISEE, Nagoya Univ.; [3] TGO, UiT

Meteor radars detected echoes of meteor tails as a tracer of neutral wind from an altitude of 75 to 100 km (Hall et al., 2005). Using a decay time of the echo power, the meteor radar estimated the ambipolar diffusion coefficient, which depends on the ion and electron temperature. The ambipolar diffusion coefficient allows to estimate the neutral temperature because ion and electron temperatures are generally in thermal equilibrium with the neutral temperature. Recently, an anomalous enhancement of the ambipolar diffusion coefficient was observed by the meteor radar installed at Tromsoe, Norway (69.6N, 19.2E). This anomaly could not be explained by neutral temperature enhancement. A previous study compared the anomalous enhancement with ion velocity and ion and electron temperatures observed by EISCAT radar (Tsutsumi et al. 2017). They reported that the anomalous enhancement tended to appear usually at 16 UT and accompanied by an enhancement of ion velocity and electron temperature. During a case study, the anomalous enhancement was not seen during an event of high energy particle precipitation on November 17, 2012. This suggests that the anomalous enhancement is be generated by the intense electric field and high energy particle precipitation is not always necessary for its generation. Currently the generation mechanism of the anomalous enhancement is still unclear. To clarify this, we need to compare the spatial distribution of the anomalous enhancement with the convective electric field. Three meteor radars have been installed at Tromsoe, Bear island (74.5N, 19.0E), and Longyearbyen (78.2N, 16.2E). These meteor radars almost align on the same longitude line and provide spatial distribution of the anomalous enhancement. All meteor radars are a commercially produced VHF system (ENDR8-20) manufactured by ATRAD Pty Ltd. The antennas were produced by the Arctic University of Norway (Nozawa et al., 2012, JGR; Hall et al., 2002, GRL, Hall et al., 2006, JASTP).

Peaks of occurrence rate were seen at 20-22, 19-21, 16-19 MLT (˜UT+3) at Tromsoe, Bear island, and Longyearbyen latitudes, respectively. This indicates that the anomalous enhancement appeared sequentially from high to low latitudes. In the morning sector, the peak of occurrence rate was only seen at 2-6 MLT above Bear island. In the case of high geomagnetic activity (Kp>3), the evening peaks of the occurrence rate shifted to an earlier time. Clear occurrence peaks in the morning sector appeared at 3-5, 4-8, 7-10 MLT, respectively. The anomalous enhancement had a high probability of 90% 100 km south of Tromsoe. These characteristics at times of high geomagnetic activity showed good agreement with the geomagnetic activity dependences of convective electric field.

We also found that peak occurrence rate in the evening sector was larger than in the morning sector. This can be related to auroral arcs appearing with intense electric field mainly observed in the evening sector. Thus, the generation of anomalous enhancement seems to relate both the convective electric field and the appearance of auroral arcs.

We will show the spatial distribution, MLT and geomagnetic activity dependence of the anomalous enhancement and its comparison with the electric filed observed by EISCAT and EISCAT Svalbard radars.

流星レーダーは高度 75-100 km の流星飛跡からの反射波を観測し、そのドップラーシフトから風速測定を推定している (Hall et al., 2005)。それに加えて、反射波の強度減衰から両極性拡散係数も推定することができる。両極性拡散係数はイオン温度と電子温度に依存する係数ではあるが、イオンと電子が中性大気と衝突を介してほぼ熱平衡状態にあると考えられるため、中性大気温度を推定する情報源として活用されている。しかし、近年、国立極地研究所と名古屋大学の研究グループによってノルウェー・トロムソ（北緯 69.6 度、東経 19.2 度）に設置された流星レーダーで中性大気温度変動では説明できないほどの両極性拡散係数の増大現象（以下、異常増大）が見出された。

これまでの研究では、トロムソ流星レーダーで観測された異常増大と EISCAT(European Incoherent Scatter) レーダーで観測されたイオン速度及びイオン・電子温度とを比較した（堤他, 平成 28 年度大気圏シンポプロシーディングス, 2017）。これによると、イオン速度と電子温度の増大と同時に異常増大が観測されるケースが多く、特に 16 UT に集中して異常増大が発生していることが分かっている。また、1 例ではあるが高エネルギー粒子の降り込みとの比較も行われた。2012 年 11 月 17 日に発生した高エネルギー粒子の降り込みイベント時には異常増大は観測されなかった。これらのことから高エネルギー粒子の降り込みは異常増大の生成に大きく寄与をしていないものと考えられる。以上のように異常増大の基本的な描像は理解されつつあるが、トロムソの 1 地点の観測データでしか調査が行われていないため、その生成メカニズムの理解は未だ不十分である。異常増大のメカニズムを理解するためには異常増大の広域観測データと対流電場などのグルーバルな現象とを比較する必要がある。

北極域ノルウェー・トロムソ、ベアアイランド（北緯 74.5 度、東経 19.0 度）、ロングイヤビン（北緯 78.2 度、東経 16.2 度）には流星レーダーがほぼ同一経度線上設置されており、異常増大の空間分布の導出が可能である。これらの 3 つの流星レーダーは、アンテナはノルウェー北極大学製、コントロール系が ATRAD 製である (Nozawa et al., 2012, JGR;

Hall et al., 2002, GRL, Hall et al., 2006, JASTP)。本研究ではこの 3 つの流星レーダーを使って異常増大の空間分布及び発生確率を導出した。トロムソ、ベアアイランド、ロングイヤビンのそれぞれの観測点において、20-22, 19-21, 16-19 MLT（~UT+3）に発生頻度の極大が現れており、高緯度ほど異常増大が早い時間帯にピークを持っていた。また、この発生確率のピークはベアアイランのみで朝側 2-6 MLT にも見られた。

地磁気活動度で発生確率を分類すると、Kp> 3 の時の夕側の異常増大の発生頻度のピーク時間が 17-21, 15-19, 12-16 MLT と早い時間に異常増大の発生頻度のピークがシフトすることがわかった。また、3 つの観測点すべてで朝側にも発生確率のピークが出現し、それぞれの観測点で 3-5, 4-8, 7-10 MLT となり、夕側とは反対に低緯度から順にピークを迎えることが分かった。さらに、トロムソ天頂から約 100 km 低緯度側では 19-21 MLT に約 90%高い確率で異常増大が発生していた。地磁気活動度が活発な時に見られるこの特徴は対流電場の地磁気活動依存性と良い一致をする。

この一方で、地磁気擾乱時に朝側に見られる異常増大の発生頻度のピークは夕方側に比べて低い。これは、強い電場とともに出現するアーク状のオーロラが主に夕側付近に出現し、朝側では強い電場を伴わない脈動オーロラやパッチ状のオーロラが主に出現することに関連していると考えられる。即ち、異常増大は対流電場とオーロラの双方に影響を受け出現していると考えられる。

本発表では、異常増大の緯度分布、磁気地方時、地磁気活動度依存性についての解析結果を述べるとともに、EISCAT レーダーと ESR によって観測された電場強度との定量的な比較についても報告する予定である。

2017-2018 年における南極昭和基地での波長可変共鳴散乱ライダー観測

西山 尚典 [1]; # 江尻 省 [1]; 津田 卓雄 [2]; 津野 克彦 [3]; 阿保 真 [4]; 川原 琢也 [5]; 和田 智之 [6]; 中村 卓司 [1]
[1] 極地研; [2] 電通大; [3] 理研; [4] 首都大・システムデザイン; [5] 信州大・工; [6] 理化学研究所基幹研

Temperature and metallic atom variability near the mesopause by resonance scattering lidar at Syowa, Antarctica in 2017-18.

Takanori Nishiyama[1]; # Mitsumu K. Ejiri[1]; Takuo Tsuda[2]; Katsuhiko Tsuno[3]; Makoto Abo[4]; Takuya Kawahara[5]; Satoshi Wada[6]; Takuji Nakamura[1]
[1] NIPR; [2] UEC; [3] RIKEN; [4] System Design, Tokyo Metropolitan Univ.; [5] Faculty of Engineering, Shinshu University; [6] ASI, RIKEN

The National Institute of Polar Research (NIPR) is leading a prioritized project of the Antarctic research observations. One of the sub-project is entitled the global environmental change revealed through the Antarctic middle and upper atmosphere. Profiling dynamical parameters such as temperature and wind, as well as minor constituents is the key component of observations in this project, together with a long term observations using existent various instruments at Syowa, Antarctica (69S). As a part of the sub-project, we developed a new resonance lidar system with multiple wavelengths. The lidar has a capability to observe temperature profiles and variations of minor constituents such as Fe, K, Ca+, and aurorally excited N2+. The lidar system installed at the Syowa Station by the 58th Japan Antarctic Research Expedition (JARE 58) in January 2017 and then its observation has been continued. In this presentation, we will report temperature and metallic atom density variability in Mesosphere-Lower Thermosphere region based on 2-years observations from 2017 to 2018.

南極観測事業において国立極地研究所が推進する重点研究観測の中で、中層・超高層大気観測研究はサブテーマ 1 に位置付けられており、地表から超高層大気にいたる大気の変動をとらえる計画で、大型のレーダーやライダーなどの測器の開発・導入・観測を進めている。そのなかで、中間圏界面付近での大気重力波の活動や、オーロラ活動に伴うイオン化学反応を介した大気微量成分の組成変動など、超高層大気中の様々な力学・化学過程を通した大気の変動をとらえるべく、国内で波長可変共鳴散乱ライダーの開発を行ってきた。送信系には波長可変のアレキサンドライト・レーザーと第 2 高調波発生器を用いており、インジェクションシーダーの波長を波長計で制御することで、基本波として 768-788 nm、第 2 高調波として 384-394 nm のうち任意の波長のレーザーパルスを得ることが出来る。これにより南極昭和基地において、カリウム原子 (770 nm)、鉄原子 (386 nm)、カルシウムイオン (393 nm)、窒素イオン (390-391 nm) の原子とイオンを狙って、高度 80-100km の大気温度、原子やイオンの高度分布などを測定する。このライダーは、第 58 次南極地域観測隊により 2017 年 1 月に南極昭和基地に設置され、同年 3 月にカリウム原子密度観測に成功し、以降もカリウム層および鉄層を利用した温度・鉛直風観測を 2018 年も継続している。本講演では、これらの 2 年間の観測結果を報告する。

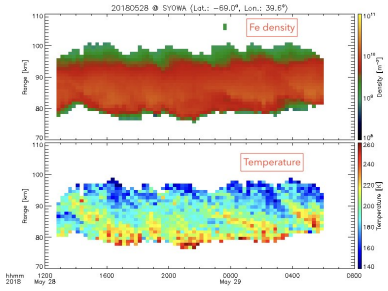

Horizontal temperature gradients in the polar MLT region above Tromsoe using sodium LIDAR data

Satonori Nozawa[1]; Yasunobu Ogawa[2]; Hitoshi Fujiwara[3]; Takuo Tsuda[4]; Takuya Kawahara[5]; Norihito Saito[6]; Satoshi Wada[6]; Tetsuya Kawabata[1]; Toru Takahashi[2]; Masaki Tsutsumi[2]; Chris Hall[7]; Asgeir Brekke[8]
[1] ISEE, Nagoya Univ.; [2] NIPR; [3] Faculty of Science and Technology, Seikei University; [4] UEC; [5] Faculty of Engineering, Shinshu University; [6] ASI, RIKEN; [7] TGO, UiT; [8] Science and Technology, UiT

We have analyzed 2700 hours of temperature data obtained with the Tromsoe sodium LIDAR over 7 winters between October 2012 and February 2018, and we have calculated horizontal temperature gradients in the polar mesosphere and lower thermosphere (MLT) region between 83 and 105 km. The sodium LIDAR operated at the EISCAT Tromsoe site (69.6 deg. N, 19.2 deg. E) has a capability of simultaneous five-directional measurements of temperature and sodium density with good (3 min/500 m) resolutions. Configurations of the sodium LIDAR observational directions are as follows: vertical position, south (Azimuth= 180 deg.), north (Azimuth = 0 deg.), west (Azimuth = 270 deg.), and east (Azimuth = 90 deg.). The elevation angle was set to be 77.5 degrees between 2013 and 2016 seasons, while it was 60 degrees for 2 seasons in 2012 and 2017. Here we call interval between October and March as season, since the LIDAR measurements were made only for the interval.

We made a statistical study of the temperature gradients. For the statistical study, we have used data sets with their length longer than 4 hours at each night, then we have 187 nights in total: winter (between October 21 and February 23) for 163 nights, and equinox for 24 nights. On average over the 163 nights, the northward temperature gradient is negative (i.e. it was warmer in the south than in the north), and about -0.004 K/km at maximum below 97 km in winter, while it was positive above 97 km. The positive meridional temperature gradient above 97 km is consistent with that of Maeda et al. (JGR, 2004JA010893, 2005) who derived temperature gradients utilizing ion temperature data obtained with two EISCAT radars at Longyearbyen (78.2 deg. N, 16.2 deg. E) and Tromsoe; the gradients were calculated in a much larger scale compared to that of this study. The averaged zonal temperature gradient was about zero between 85 and 96 km, and it was westward above 96 km. Year-to-year variations are also found: they are more significant above 97 km in the both directions. Southward temperature gradients below 97 km seem to be a common feature over the 6 years except for 2012 season.

Then, we have investigated variations of temperature gradients on nightly basis. In this talk, we will present results of case studies about the temperature gradients in the polar MLT region. In particular, we focus on effects of auroral activities as well as influence of Sudden Stratospheric Warming (SSW).

トロムソ観測点のファブリ・ペロー干渉計を用いた地磁気静穏時における高緯度熱圏平均風の研究

Xu Heqiucen[1]; 塩川 和夫 [1]; 大山 伸一郎 [2]
[1] 名大宇地研; [2] 名大 ISEE

Study of high-latitude quiet-time mean thermospheric winds with a Fabry-Perot interferometer in Tromsoe, Norway

Heqiucen Xu[1]; Kazuo Shiokawa[1]; Shin-ichiro Oyama[2]
[1] ISEE, Nagoya Univ.; [2] ISEE, Nagoya Univ.

In the previous study, we have studied thermospheric wind variations at the onsets of isolated substorms by using a Fabry-Perot interferometer (FPI) in Tromsoe Norway. In this research, we investigated nightside mean thermospheric winds during periods of geomagnetically quiet condition. The wind variations were measured from the Doppler shift of both red line (630.0 nm, altitudes: 200-300 km) and green line (557.7 nm, altitudes: 90-100 km) emissions with a time resolution of ˜13 min for deriving each wind vector. We used the X-component of local magnetometer data and Kp index to indicate the locally and globally quiet conditions, respectively. At first, we found that the wind pattern in Tromsoe can be affected by the geomagnetic activity even under quiet conditions (Kp < 1+ and the variation of X-component is less than 50 nT from 3 hours before the wind observation) when considering the typical tidal structures. We discussed these quiet-time results with our previous event study regarding effects of the substorm onset. We also investigated the dependence of quiet-time winds on various parameters, for example, the geomagnetic activity level, solar radiation, and interplanetary magnetic field conditions. At F-region height, we found that the quiet-time winds at duskside are more sensitive to the geomagnetic activity level than those at dawnside. With greater 10.7 cm solar radio flux (F10.7), the eastward wind changed its direction to the west in the post-midnight sector, while the northward wind shows a larger amplitude at the pre-midnight sector.

Can the SuperDARN radar make estimates of thermospheric neutral density?

Michael J. Kosch[1]; Nozomu Nishitani[2]
[1] SANSA; [2] ISEE, Nagoya Univ.

Using the ion-momentum equation in the F-region ionosphere, simplified for field-perpendicular ion motion only, we derive an expression for the ion-neutral collision frequency that depends primarily on the temporal and spatial variability of the ion velocity. The ion-neutral collision frequency is primarily a function of neutral density in the thermosphere. SuperDARN radars are very suited to this type of observation because of their large coverage of the F-region ionosphere, mesoscale range resolution and frequency agility. Trial observations have been performed on some SuperDARN radars using a special mode. These show that realistic estimates of thermospheric neutral density, compared to the MSIS model, can be obtained. Since HF radio wave propagation refracts in the F-region ionosphere, a functional comparison is only possible with reliable and accurate ray tracing. Problems with ray tracing and assumptions made are discussed.

Characteristics of the tropical tropopause inversion layer using high resolution temperature profiles by COSMIC GPS-RO

Noersomadi Noersomadi[1]; Toshitaka Tsuda[1]; Masatomo Fujiwara[2]
[1] RISH, Kyoto Univ.; [2] Hokkaido U.

Using long-term observation of COSMIC GPS-RO with 0.1 km vertical resolution in the upper troposphere and lower stratosphere (UTLS), we investigate global distribution of static stability (N^2) and the variation of tropical TIL, the sharp gradient of temperature profile which is related to N^2. We show the mean N^2 in the conventional height coordinate and relative to both Lapse Rate Tropopause (LRT) and Cold Point Tropopause (CPT) locations in the vertical. The double layers of strong N^2 appear in the tropics, within 1 km and near 2 km above LRT height. When the N^2 profiles are averaged relative to CPT height, it shows a single thin layer less than 1 km in thickness with maximum about 12.0 x 10^{-4} s^{-2}. The mean and standard deviation of TIL sharpness (S-ab) is (10.5 +- 3.7) x 10^{-4} s^{-2} and about 70% of TIL thickness (dH) are in the range 0.4 +- 0.04 km. Seasonal variations of S-ab and dH are closely related with the deep convections as shown by low Outgoing Longwave Radiation (OLR) values. S-ab anomaly (S-ab$^{\Lambda}$) has anti phase with OLR anomaly (OLR$^{\Lambda}$) both in 90-150E and 170-230E regions. The correlation between S-ab$^{\Lambda}$ and Sea Surface Temperature (SST) Nino 3.4$^{\Lambda}$ index over Pacific region is +0.88 which means during El-Nino Southern Oscillation (ENSO) warm event, warmer SST produces more deep convections which tend to force the air upward to the tropopause layer and enlarge the temperature gradient. Intraseasonal variation of S-ab$^{\Lambda}$ in the fast and slow episodes of Madden-Julian Oscillation (MJO) demonstrated that eastward propagations of positive S-ab$^{\Lambda}$ are associated with organized deep convections. This suggests convective activity in the tropics influence the variation of tropopause sharpness.

Evolution of aerosol profile and convective instability in the middle atmosphere on Mars

Hiromu Nakagawa[1]; Naoki Terada[2]; Nao Yoshida[3]; Hitoshi Fujiwara[4]; Kanako Seki[5]
[1] Geophysics, Tohoku Univ.; [2] Dept. Geophys., Grad. Sch. Sci., Tohoku Univ.; [3] Geophysics, Tohoku Univ.; [4] Faculty of Science and Technology, Seikei University; [5] Dept. Earth & Planetary Sci., Science, Univ. Tokyo

It is believed that Mars underwent drastic climate change, changing its environment from warm and wet to cold and dry. This gives rise to the idea that Mars may have hosted life in the past, and indeed, may do so even today. Atmospheric evolution is thus an important key to understanding the history of Martian habitability. However, precise estimates of past atmospheric inventories including water, and their loss mechanisms, are difficult to be obtained.

High-altitude (above 60 km) water vapor was first identified by SPICAM occultations onboard MEX (Maltagliati et al., 2011, 2013; Fedorova et al., 2018) especially in the southern summer, which happens to be a dusty season (at a solar longitude of 240 degree or later). Maltagliati et al. (2013) showed the links between such high-altitude water vapor and aerosols in their vertical profiles within a short time scale. This implies the importance of aerosols for key processes in the Martian water cycle and climate as a whole. Importantly, the new pathway of water loss proposed by recent studies implies higher loss to space, in addition to the diffuse-limited escape of H2 (Catling and Kasting, 2017).

One possible scenario for upward transport from the lower atmosphere is the enhanced diffusion caused by gravity waves (GWs) of lower atmospheric origin. GWs have significantly effects on large scale winds, thermal balance, and density in the upper atmosphere (e.g., Medvedev et al., 2011, Medvedev et al., 2016). Recent MAVEN data reveal that the atmospheric waves exist ubiquitously in the upper atmosphere (Bougher et al., 2015; England et al., 2017; Terada et al., 2017). The average amplitude of GWs in the Martian upper thermosphere is 10 % on the dayside and 20 % on the nightside, which is about 2 and 10 times larger than those on Venus and the low-latitude region of Earth. IUVS occultations onboard MAVEN suggest that observed wavelike perturbations likely represent propagating GWs of tropospheric origin (Nakagawa et al., under revision). Answering questions about the upper atmospheric sources of these waves and their possible links with those in the troposphere is a key to an understanding the efficient upward transport process from below.

The study presented here demonstrated for the first time the evolution of aerosol profile and convective instability resulting from superposition of various atmospheric waves during a martian year. More than hundreds-profiles obtained by IUVS stellar occultations with UV channel onboard MAVEN are retrieved, which covers the Mars Year (MY) 33-34 during March 2015 and October 2017. All profiles used in this study correspond to Level 2, version 06,07,12, revision 01 data provided by the Planetary Data System (PDS). The measured profiles exhibit drastic temporal variations and a greater variety of shapes, with the presence of detached layers. The aerosols were lofted higher into the middle atmosphere in the southern summer, whereas less aerosols in the southern winter. The higher detached layer above the persistent near-surface haze were identified in the southern summer. These results are consistent with previous studies (Montmessin et al., 2006; Maltagliati et al., 2013; Maattanen et al., 2013). Our results can also suggest correlated behavior between aerosols and convective instabilities layers. This highlights the role of the vertical mixing enhanced by the atmospheric waves in addition to the global circulation and the seasonal inflation/contraction. Related to changes in the homopause height, a fast vertical mixing at low pressure (high) altitude could be occurred in the southern summer. This potentially creates aerosol upsurges and influences the large scale vertical evolution. In this paper, the external penetration from above is also discussed as the potent source to generate the detached aerosol layers at 80-110 km altitudes.

赤道ライダーにより観測された赤道ケルビン波に伴う下降流による成層圏エアロゾルの鉛直輸送

阿保 真 [1]; 柴田 泰邦 [1]; 長澤 親生 [1]
[1] 首都大・システムデザイン

Downward transport of stratospheric aerosols associated with equatorial Kelvin waves observed by the equatorial lidar

Makoto Abo[1]; Yasukuni Shibata[1]; Chikao Nagasawa[1]
[1] System Design, Tokyo Metropolitan Univ.

The transport of substance between stratosphere and troposphere in the equatorial region makes an impact to the global climate change, but it has a lot of unknown behaviors. We have performed the lidar observations for survey of atmospheric structure of troposphere, stratosphere, and mesosphere over Kototabang (0.2S, 100.3E), Indonesia in the equatorial region since 2004. Kelut volcano (7.9S, 112.3E) in the Java island of Indonesia erupted on 13 February 2014. The CALIOP observed that the eruption cloud reached 26km above sea level in the tropical stratosphere, but most of the plume remained at 19-20 km over the tropopause.

In June 2014 (4 months after the eruption), aerosol transport from the stratosphere to the troposphere were observed by the polarization lidar at Kototabang. At the same time, we can clearly see down phase structure of vertical wind velocity observed by EAR (Equatorial Atmosphere Radar) and temperature profiles observed by radiosonde associated with equatorial Kelvin waves.

We investigate the transport of substance between stratosphere and troposphere in the equatorial region by data which have been collected by the polarization lidar at Kototabang and the EAR. Using combination of the ground based lidar and the atmosphere radar, we can get valuable evidence of equatorial transport of substance between the troposphere and the lower stratosphere.

我々は赤道直下のインドネシア・コトタバン（0.2S , 100. 3E）の EAR サイトにおいて、地球大気の熱収支に重要な影響を及ぼす赤道領域の対流圏の雲・エアロゾル分布の連続観測を、波長 532nm の小型ミーライダーを用いて 2004 年から現在まで 14 年間継続しており、さらに 2014 年からは対流圏上部から成層圏のモニターを目的に偏光ライダー観測を行っている。

2014 年 2 月 13 日に噴火したインドネシアジャワ島のケルート火山（7.9S, 112.3E）の多くの火山ガスは高度 19˜20km 付近の成層圏に注入された。衛星ライダーである CALIOP データからは火山起源のエアロゾルが噴火後緯度方向に広がり 5 日で赤道に達し、その後赤道上空では QBO による顕著な強い東向きの風により経度方向に輸送され、約 1ヶ月で地球を 1 周し、3 周まで周回する様子が見られた。4 周目に入る 6 月になると東向きの風が弱まり経度方向の動きは明瞭でなくなった。

成層圏に注入されたエアロゾルは鉛直方向については全体的に上方に輸送されていったが、インドネシア上空では 6 月にエアロゾルが下方に輸送される様子が赤道ライダーにより観測された。この時 EAR の鉛直風観測並びにラジオゾンデの気温プロファイルからは、赤道ケルビン波に伴う鉛直風並びに気温プロファイルの変調が見られた。これは赤道ケルビン波に伴い下降流が生じ、成層圏から対流圏へエアロゾルが鉛直輸送された様子を地上ライダーにより観測したものと考えられる。講演では解析結果と、異なる期間の観測データについても示す。

熱帯成層圏界面領域におけるハドレー型子午面循環と半年周期振動

冨川 喜弘 [1]; Harvey V. Lynn[2]; Knox John A.[3]; 藤原 正智 [4]
[1] 極地研; [2] UBC; [3] U. Georgia; [4] 北大

Stratopause Hadley circulation and semiannual oscillation around the tropical stratopause

Yoshihiro Tomikawa[1]; V. Lynn Harvey[2]; John A. Knox[3]; Masatomo Fujiwara[4]
[1] NIPR; [2] UBC; [3] U. Georgia; [4] Hokkaido U.

Stratopause Hadley circulation (S-Hadley) is a thermally-driven Hadley-type circulation in the tropical upper stratosphere and lower mesosphere. Its driver is meridional gradient of ozone heating in the solstitial seasons. It is well known that S-Hadley is closely related to stratopause semiannual oscillation (SAO) around the tropical stratopause through the absolute angular momentum transport. Their relationship has been studied in 2D General Circulation Model and using satellite observations. Recently several kinds of meteorological reanalysis data have been available for climate and atmospheric science studies. In this study, we investigate the relationship between S-Hadley and SAO using the latest reanalysis datasets. This study is performed as a part of the SPARC Reanalysis Intercomparison Project (S-RIP), which is a coordinated activity to compare all reanalysis datasets.

Real-time ionosphere 3-D tomography and its validation by MU radar incoherent scatter measurements

Susumu Saito[1]; Mamoru Yamamoto[2]; Akinori Saito[3]
[1] ENRI, MPAT; [2] RISH, Kyoto Univ.; [3] Dept. of Geophysics, Kyoto Univ.

Real-time ionospheric 3-D tomography with GEONET real-time data has been operated since March 2016. 3-D ionospheric density profiles over Japan are reconstructed every 15 minutes with about 6 minutes delay [Saito et al., NAVIGATION, 2017].

The reconstructed ionospheric density profiles are shown to be generally in agreement with the foF2 measured ionosondes. The 3-D tomography has also been compared with the electron density profiles measured by the MU radar (34.85N, 136.11E) incoherent scatter (IS) measurements on a few days to show good agreements in their heights and shapes around the F region peak. However, it has also been shown that the foF2 values estimated by the 3-D tomography are not always in good agreement with those observed by ionosondes.

To evaluate the performance of the 3-D tomography in terms of the F region peak height and shapes of the electron density profile, further comparison with the MU radar IS observations were conducted. MU radar IS observation data from 35 days from May 2016 to September 2017 are used. Trend in the agreements in the F region peak height and shapes of profiles in different seasons will be discussed. Based on the comparison, the way forward to improve the ionosphere 3-D tomography will also be discussed.

衛星ビーコン観測に基づくアジア域の電離圏赤道異常の日変化・季節変化の研究

坂本 悠記 [1]; 山本 衛 [1]; Hozumi Kornyanat[2]
[1] 京大・生存圏研; [2] NICT

Daily and seasonal variation of the equatorial anomaly in Asia, satellite-ground beacon experiment

Yuki Sakamoto[1]; Mamoru Yamamoto[1]; Kornyanat Hozumi[2]
[1] RISH, Kyoto Univ.; [2] NICT

Studies of ionospheric structures by the satellite-ground beacon experiment were conducted in southeast Asia. We have deployed a meridional chain of five beacon receivers from 8S to 27N along 100E meridian, they showed meridional distribution of total-electron content (TEC) of the ionosphere, and we revealed time and spatial variabilities of the equatorial anomaly in a certain period time (Watthanasangmechai et al., 2014, 2015). The data analysis was, however, not easy mainly because of difficulty in estimating bias of the measurement to get the absolute TEC.

In this study, we developed the method of bias estimation. As a result, we can get TEC distribution by computers automatically. Using this method, we analyzed latitude distribution of TEC from Thai to Indonesia in 2012-2015. It is valuable to measure such latitudinal distribution of TEC in the wide latitudinal range from the ground fixed sites.

Using these data, we classified TEC distribution with the equatorial anomaly. It shows some distribution patterns depends on season or time. Classifying the TEC distribution data of LT14-17 and LT20-23, assuming after the formation of the equatorial anomaly (EIA), we take the average in 2012-2015. The plasma fountain makes the 2 peaks (northern and southern of the magnetic equator) in the TEC-Lat graph. In the northern hemisphere summer, the northern peak is larger than the southern one. In winter, the southern peak is larger than the northern one. Classifying the data of LT10-13, assuming the right after formation of the EIA. It shows the opposite result. In summer, the southern one is larger. In winter, the northern one is larger. We will compare these analysis results with atmospheric parameters from the whole atmosphere model GAIA.

我々は東南アジア域を中心とした衛星-地上ビーコン観測によって，電離圏の構造に関する研究を行なってきた．南緯 8 度-北緯 27 度，東経 100 度沿いに観測環境を構築し，一定期間の電離圏全電子数 (TEC) の分布を明らかにし，2012 年 3 月の赤道異常の時間・空間構造を示すことに成功している (Watthanasangmechai et al., 2014, 2015)．しかしながら，TEC 値を得るためのバイアス値の推定が困難で，解析時間がかかりすぎるため大量のデータ解析は容易ではなかった．

本研究では，まず TEC 値を効率的に算出するためにバイアス推定法の開発を行なった．これによりコンピュータを用いて TEC 値の自動算出を可能とした．これによって 2012-2015 年の期間についてタイからインドネシア上空の TEC 値の緯度分布の解析を行った．

この結果は地上の固定された観測点から広い緯度範囲の TEC 値のデータとして利用価値があると考える．このデータを用いて赤道異常における TEC 分布の分類を行なったところ，季節や時間で分布パターンが現れることがわかった．赤道異常安定後の日中を想定した LT14-17 時と日没後である LT20-23 時のデータについて分類を行い，2012-2015 年の期間で平均をとった．プラズマファウンテンによって磁気赤道の南北に 2 つの TEC 値のピークが見られるが，北半球の夏季では磁気赤道の南側よりも北側の TEC 値が大きく，冬季では南側の TEC 値が大きいという傾向が得られた．赤道異常形成直後を想定した LT10-13 時に関しても同様の分類を行った．先ほどの時刻での結果と真逆の結果となり，夏季では南側が大きく，冬季では北側が大きいという結果になった．これらの結果と全大気のシミュレーションである GAIA からのデータを比較することにより背景現象の考察を行う．

GNU Radio Beacon Receiver 2 (GRBR2) の開発

山本 衛 [1]; 松永 真由美 [2]
[1] 京大・生存圏研; [2] 東京工科大・工

Development of GNU Radio Beacon Receiver 2 (GRBR2)

Mamoru Yamamoto[1]; Mayumi Matsunaga[2]
[1] RISH, Kyoto Univ.; [2] Tokyo Univ. of Tech.

GNU Radio Beacon Receiver (GRBR) is the very successful digital receiver developed for dual-band (150/400MHz) beacon experiment. We were successfully conducted observations of total-electron content (TEC) of the ionosphere over Japan and in southeast Asia. However, many beacon satellites is now aging, and its number is decreasing. We now have a project to start new satellite-ground beacon experiment with new satellite constellations. One of them is TBEx (Tandem Beacon Explorer), a project by SRI International, to fly a constellation of two 3U cubesats with triband beacon transmitters. Another one is a project of FORMOSAT-7/COSMIC-2 by Taiwan/USA. Well-known mission of COSMIC-2 is GNSS occultation experiment, but the satellites carry triband beacon transmitters. All of these satellites will be placed into low-inclination orbits by the same launch vehicle in 2018, which will give us great opportunities to enhance studies of the low-latitude ionosphere. In this presentation we report a new digital receiver, GRBR2, for these new satellite beacon. GRBR2 is a four channel receiver at 150/400/965/1067MHz beacon signals from two satellite constellations. The reveiver system was finally fixed, and we now conduct receive tests. GRBR2 will be soon deployed for the real experiment.

GNU Radio Beacon Receiver（GRBR）はデュアルバンド（150/400MHz）ビーコン実験用に開発された非常に成功したデジタル受信機である。日本および東南アジアにおいて、電離圏全電子数（TEC）の観測に成功してきた。しかし多くのビーコン衛星は老朽化してきており、その数は減少している。我々は、新しく打ち上げられる衛星群を用いた新しい衛星＝地上ビーコン実験を始めようとしている。それらの 1 つは、SRI International による TBEx（Tandem Beacon Explorer）であり、3U サイズの cubesate 2 機が予定されている。もうひとつの計画は、台湾/米国による FORMOSAT-7/COSMIC-2 のプロジェクトである。6 機編隊で構成される COSMIC-2 の第 1 のミッションは GNSS 波の掩蔽観測であるが、同衛星はビーコン送信機も搭載している。以上の衛星はすべて、2018 年内に 1 機の打上げロケットによって低軌道傾斜角の軌道に配置される。我々は現在、これらに対応して地上に配備されるビーコン受信機 GNU Radio Beacon Receiver 2 (GRBR2) を開発し、受信テストを実施している。GRBR2 は、周波数が 150/400/965/1067MHz の 4 バンドの信号を同期して受信できる。本発表では、GRBR2 の最終的な機器構成とテスト状況について報告する。

航空航法用 VHF 帯電波の異常伝搬現象を用いたスポラディック E 層空間構造の解析

木村 康択 [1]; 細川 敬祐 [1]; 坂井 純 [1]; 斎藤 享 [2]; 冨澤 一郎 [3]; 津川 卓也 [4]; 西岡 未知 [4]; 石井 守 [4]
[1] 電通大; [2] 電子航法研; [3] 電通大・宇宙電磁環境; [4] 情報通信研究機構

Analysis of Spatial Construction of Sporadic-E by Using the Abnormally Propagation of VHF for the Aircraft Navigation System

Kotaku Kimura[1]; Keisuke Hosokawa[1]; Jun Sakai[1]; Susumu Saito[2]; Ichiro Tomizawa[3]; Takuya Tsugawa[4]; Michi Nishioka[4]; Mamoru Ishii[4]
[1] UEC; [2] ENRI, MPAT; [3] SSRE, Univ. Electro-Comm.; [4] NICT

Sporadic-E (Es) is one of the outstanding phenomena in the mid-latitude ionosphere, during which the electron density in the bottom of E region extremely increases often greater than that in the F region. Generally, VHF radio waves, whose frequency is greater than 100 MHz, penetrate all the way through the ionosphere, but they are sometimes reflected by Es when they enter the ionosphere obliquely. The aircraft navigation system uses such VHF radios (> 100 MHz) for communications within the range of direct propagation. However, when Es appears, the radio waves propagate abnormally for a long distance through the reflection by Es, and then an interference between the desired and abnormal waves may take place.

We have been observing VHF radio waves in the air-band frequency range in Chofu, Tokyo and Kure, Hiroshima since 2014. In this study, we used the data from Chofu in 3 years from 2014 to 2016 and from Kure in 2 years from 2014 to 2015. In addition, we attempted to detect electron density irregularities in Es by using ROTI (Rate of TEC index) routinely derived from GPS-TEC database at NICT. We mapped these two data onto the geographic coordinate system and compared the spatial distribution of Es in ROTI with the occurrence of abnormal propagation of air-band VHF waves.

As a result of the mapping, we extracted a number of examples where the spatial distribution of Es in ROTI coincides well with the distribution of the reflection points of the abnormal propagation. This indicates that 2D mapping of E region irregularities by using ROTI can be used for visualizing the spatial distribution Es. At the same time, it was confirmed that the abnormal propagation of air-band VHF waves is directly associated with Es. In addition, we found that the mapping of the reflection points of the waves enables us to monitor the spatial distribution of Es even outside the coverage of GPS-TEC observations of GEONET. In the presentation, we will introduce a few examples of simultaneous mapping of Es by using ROTI and air-band waves, and then discuss the possibility of monitoring the spatial construction of Es in a wide area by combining the air-band VHF waves with ROTI.

電離圏 E 領域の下部において、電子密度が F 領域を超えるほど増大する現象がある。これをスポラディック E 層 (Es) という。Es は、夏季に集中して発生するという季節的特徴と、局所的に発生するという地理的特徴を持つ。Es の発生メカニズムには中性風のシアや大気重力波が関係していると考えられている。通常 100 MHz を超える周波数の VHF 帯電波は電離圏で直進するが、Es が発生すると E 領域の電子密度が F 領域よりも高くなるために、斜めに薄く入射した電波が反射され長距離異常伝搬する可能性がある。航空航法では、VHF 帯電波が電離圏を直進するという性質を利用した見通し範囲内の通信を行っている。しかし Es が発生した場合、見通し範囲内にのみ届く所望波に対して、Es により長距離伝搬した電波が干渉し、航空無線通信に混信が発生する可能性がある。

我々は、電気通信大学調布キャンパスと呉海上保安大学校の 2 箇所で、異常伝搬した航空航法用 VHF 帯電波 (VOR, ILS) の観測を行ってきた。受信信号に対しエアバンドフィルタを適用することで、帯域外の信号をカットして、VHF 増幅器を用いて信号を増幅する。出力に対しスペクトラムアナライザを用いて、受信局、日付、時刻 (時間分解能 10 秒)、受信周波数、受信信号強度を抽出し、観測データベースに記録している。本研究では、これまでの観測から得られた 2014 年から 2016 年の調布の観測データ、2014 年から 2015 年の呉の観測データを、航空航法用 VHF 帯電波の異常伝搬事例の解析に用いた。また、情報通信機構 (NICT) において算出されている、電離圏全電子数 TEC (Total Electron Content) の 5 分間での標準偏差を取った電子密度擾乱指数 ROTI (Rate of TEC index) を用いることで、Es の内部に存在する電子密度の細かい不規則構造を検出する。これら二つのデータを個々の事例ごとに地理座標上に重ねてマッピングすることで、Es の空間構造と Es による航空航法用 VHF 帯電波の異常伝搬の関連性について解析を行った。

マッピングの結果、ROTI に見られる Es の空間構造と、異常伝搬の中間反射点の分布が一致する事例が多数見られた。このことから、ROTI を用いて Es の不規則構造を検出することで、Es の空間分布を示すことが可能だということが示された。また、長期観測によって得られた航空航法用 VHF 帯電波の異常伝搬が、Es によって引き起こされたものであることを確認することもできた。加えて、マッピングされた中間反射点の分布から、ROTI の観測範囲外に発生した Es の空間分布を予測することができた。発表では、マッピングを行ったいくつかの事例について紹介し、VHF 帯航空航法電波と ROTI を組み合わせた Es の広域空間構造モニタリングの可能性について議論する。

電離圏のGNSS測位への影響調査のための磁気赤道域VHFレーダー及びマルチGNSS受信機設置計画について

津川 卓也 [1]; Hozumi Kornyanat[2]; Jamjareegulgarn Punyawi[3]; Supnithi Pornchai[4]; 斎藤 享 [5]; 大塚 雄一 [6]; 浜 真一 [7]; 直井 隆浩 [1]; 石井 守 [1]
[1] 情報通信研究機構; [2] NICT; [3] ＫＭＩＴＬ; [4] KMITL; [5] 電子航法研; [6] 名大宇地研; [7] ＮＩＣＴ

Installation of a VHF radar and multi-GNSS receivers at the magnetic equators to investigate ionospheric effects on GNSS

Takuya Tsugawa[1]; Kornyanat Hozumi[2]; Punyawi Jamjareegulgarn[3]; Pornchai Supnithi[4]; Susumu Saito[5]; Yuichi Otsuka[6]; Shinichi Hama[7]; Takahiro Naoi[1]; Mamoru Ishii[1]
[1] NICT; [2] NICT; [3] KMITL; [4] KMITL; [5] ENRI, MPAT; [6] ISEE, Nagoya Univ.; [7] NICT

NICT has observed ionosphere using Ionosondes and GNSS receiver networks in Japan and Southeast Asia for the nowcast and forecast of the ionospheric condition. Current condition and prediction level of major ionospheric phenomena such as ionospheric storm observed in Japan are mainly defined based on statistical observation results and proviced to general users. In recent years, inquiries about the ionospheric variations from GNSS users increased due to the progress of high precision GNSS positioning utilization. NICT have started a new research project to validate the ionospheric effect of precise positioning technique using GNSS including quasi-zenith satellite (QZSS) since 2017. In this project, we will investigate ionospheric effects on individual positioning techniques (single frequency, DGPS, and RTK-PPP) and consider methods to mitigate and/or prevent the positioning errors under sever ionospheric conditions. To expand TEC observation area and spatial resolution, we have tried to use multi-GNSS data including GPS and QZSS for routine data collection and processing. In the Southeast Asia, it is important to identify which satellite-receiver path suffers from plasma bubble structures for verifying the ionospheric effects on GNSS positioning. we have a plan to install VHF radar at Chumphon (Thailand) and multi-GNSS receivers at Chumphon, Bac Lieu (Vietnam), and Cebu (Phillipines) at the magnetic equator. In this presentation, we will show the project outline and report the current status.

情報通信研究機構（NICT）では、日本および東南アジアにおけるイオノゾンデ及びGNSS受信機網を利用した電離圏観測により、電離圏の現状把握及び予報に関する研究開発を行っている。日本で観測される電離圏嵐など主要な電離圏現象の現況及び予測レベルは、主に統計的な観測結果に基づいて定義され、一般的なユーザー向けに公開している。近年、高精度GNSS測位の利用が進み、電離圏のGNSS測位への影響について、より定量的に評価できる指標や測位誤差低減のための方策に対するニーズが高まっている。そこで、NICTでは2017年から準天頂衛星（QZSS）を含むGNSSを用いた高精度測位技術の電離圏効果を検証するための新しい研究プロジェクトを開始した。本プロジェクトは、GNSSを利用した様々な衛星測位技術（単一周波数、DGPS、RTK-PPP等）に対する電離圏の影響を調査し、電離圏変動が大きい条件下での測位誤差を低減・防止する方策を検討することを目的としている。本プロジェクでは、QZSSも含むマルチGNSSデータを利用し、これまでGPSデータのみを利用していた全電子数（TEC）観測の観測領域及び空間分解能を拡大する。また、東南アジア域における電離圏観測では、特にプラズマバブルによるGNSS測位への影響を検証するため、プラズマバブル構造を正確に把握可能なVHFレーダーを磁気赤道に近いタイ・チュンポンに設置する計画を進めている。また、GNSSシンチレーションを観測できるGNSS受信機をタイ・チュンポン、ベトナム・バクリウ、フィリピン・セブの磁気赤道域に設置する予定である。本発表では、本プロジェクトの概要を示し、現在の状況を報告する。

電離層電流と海洋中を流れる電流の電磁相互作用 (2) - Dp 場の場合-

竹田 雅彦 [1]
[1] 京大・理・地磁気センター

Electromagnetic interaction between currents flowing in the ionospheric and ocean - Dp field -

Masahiko Takeda[1]
[1] Data Analysis Center for Geomagnetism and Space Magnetism, Kyoto Univ.

Electric currents flowing in the ionosphere and land-ocean shell driven by the external currents were estimated for the period of 1 and 10 min. variation. Electromagnetic self and mutual induction effects were included by using spherical harmonics expansion of equivalent currents in the shells. It was shown that induction effect delays the ionospheric current system by more than 30 about 5 degrees for 1 and 10 min, period, respectively, and ionospheric current is affected by the land-ocean shell even for 10 min. period.

地磁気変化は誘導電場を生じる電流を流し、自分自身が作る誘導電場の効果を含めた電流系を評価するには、球関数展開を通じてそれが作り出す磁場を計算できる電流関数を用いるのが有効であるが、Dp 場の場合には電離層電流系は電離層外から電流が供給されるため電離層電流系単独では非発散ではないので電流関数で表現することはできない。しかしながらこの場合にも全磁場変化を表現する等価電流関数を用いることは可能であり (Takeda, M. (2008), JGR, doi:10.1029/2007JA012662)。

今回は、この手法を海陸分布を表現する薄層と固体地球を表現する導体球からなる 2 薄層 1 導体球モデルを使用し、電離層外から沿磁力線電流が供給される場合の電離層-海洋陸地電磁結合を考慮した場合の時間変化する電流系を 1 及び 10 分周期、各 UT について調べた。その結果、ずれの周期でも UT 変化は Dst 場に比べて大きくなること、周期 1 分では自己誘導場の効果で供給電流に比べ外部等価電流系は位相が 30 度以上遅れるとともに海陸分布の影響により UT によりかなり変化すること、周期 10 分でも 5 度程度の位相遅れが生じることがわかった。

GAIAモデルデータを用いたCO2二倍に対する超高層大気の応答

中本 雄介 [1]; Liu Huixin[2]; 三好 勉信 [3]; 垰 千尋 [4]
[1] 九大・理・地惑; [2] 九大・理・地惑; [3] 九大・理・地球惑星; [4] 情報通信研究機構

Response of the upper atmosphere to doubling CO2 with GAIA model

Yusuke Nakamoto[1]; Huixin Liu[2]; Yasunobu Miyoshi[3]; Chihiro Tao[4]
[1] Dept. Earth Planet. Sci, Kyushu Univ.; [2] None; [3] Dept. Earth & Planetary Sci, Kyushu Univ.; [4] NICT

Many observations and models show that increasing CO^2 would result in temperature decreases in thermosphere. Better understanding of this global cooling in thermosphere will benefit long-term satellite orbit prediction. The purpose of this study is to evaluate the effect of increasing CO^2 on thermospheric temperature and circulation. Using the GAIA model, two experimental simulations are performed. The first is for the year 1997 with observed CO^2 values, and the second is with douled CO^2. We examine the difference between these two simulation results by subtracting values of the first run from the second run (double CO^2 - base CO^2). Results indicate that the strong cooling peak (~-60K) in upper thermosphere occur between S45-N45 in equinox and this peak moves to summer hemisphere in solstice. Background meridional circulation with double CO^2 is stronger than one with base CO^2 by ~10m/s. For better understanding of those change, contribution of heating/cooling processes in thermosphere, such as solar radiation, infrared radiation and heat conduction, is examined. We found notable change of solar heating (200K/day) that affects cooling peak moving in solstice mainly. Combined with changes in the meridional circulation, these changes produces the thermosphere cooling. Furthermore, tidal changes are also examined, which reveals significant increase in amplitude of DW1 but decreases in SW2, and slight increases in DE3 above 150 km altitude.

近年、多くの観測やモデルを用いて CO^2 増加による熱圏の温度低下が研究されており、その「寒冷化」を理解することは長期的な人工衛星軌道予測精度向上につながる。本研究の目的は濃度を２倍にした CO^2 が熱圏の温度と循環に与える影響を他の関連する物理量と共に理解することである。CO^2 の影響を見るために GAIA モデルを用い、２つのシミュレーションを行った。１つ目は 1997 年の観測に基づいた CO^2 の値を用いたもので、２つ目はその CO^2 を２倍にしたものである。後者から前者を引くことで差を求め CO^2 ２倍の影響を調査した。（CO^2 ２倍－ CO^2 基準）以上の解析から、上部熱圏では、3 月と 9 月には南緯 45 度から北緯 45 度の間に強い寒冷化（～-60K）の領域を得られ、6 月と 12 月にはその領域が夏半球に移動するような季節変化が見られた。また、子午面循環は CO^2 ２倍のときが基準の CO^2 のときより 10m/s ほど強くなる結果が得られた。これらの変化をより深く理解するために、太陽放射、赤外放射と熱伝導の熱圏の熱収支について解析を行った。その結果、CO^2 ２倍すると太陽放射に著しい変化（～200K/day）が見られ、それが上で述べた寒冷化域の季節変化に影響していた。また、熱収支の変化と循環の変化がバランスすることで熱圏の寒冷化の領域を作り出していた。加えて、大気潮汐の解析を行うことで、DW1 振幅の著しい増加、SW2 の減少と 150km 以上の DE3 の比較的小さな増加が見られた。

フェーズドアレイ気象レーダーによって観測された局地的大雨の事例解析と将来の利用に向けたデータベース整備

磯田 総子 [1]; 佐藤 晋介 [1]; 牛尾 知雄 [2]; 村山 泰啓 [3]
[1] NICT; [2] 首都大; [3] 情報通信研究機構

Case study of localized heavy rainfall observed by Phased Array Weather Radar and data base arrangement for future utilization

Fusako Isoda[1]; Shinsuke Satoh[1]; Tomoo Ushio[2]; Yasuhiro Murayama[3]
[1] NICT; [2] Tokyo Metropolitan Univ.; [3] NICT

The Phased Array Weather Radar (PAWR), which was installed at Osaka University Suita Campus in 2012, is a rainfall observation radar that can scan for 30 seconds (10 seconds for detailed observation) at a radius of 60km (30 km in detailed observation). On the radar until then, the volume scan (to scan the three-dimensional structure of sky), it was taking a time of about 5 minutes by changing the elevation angle of the parabolic antenna is rotated many times (e.g., Ishihara, 2012, Radar echo population of thunderstorms generated on the 2008 Zoshigaya-rainstorm day and nowcasting of thunderstorm-induced local hevy rainfall-Part 1, Tenki 59, Kim et al., 2012, X-band dual-polarization radar observation of Precipitation core development and structure in a multi-cellular storm over Zoshigaya, Japan, on August 5, 2008, J. Meteor . Soc. Japan), The PAWR is capable of high-speed observation every 30 seconds by using the technology of Digital Beam Forming, it is suitable for the detailed observation of the development of localized heavy rainfall that develop in a short time (Yoshikawa et al., 2013, MMSE Beam forming on fast-scanning phased array weather radar, IEEE Trans. Geosci. Remote Sens., Ushio et al., 2015, Review of recent progress in lighting and thunderstorm detection techniques in Asia, Atmos. Res.). In this study, we analyze four cases of localized heavy rainfall by isolated cumulonimbus, which was observed on July 26, 2012. As a result, a basic investigation is required to examine the requirements for long-term database maintenance for the future rainfall research. I hope that I can contribute to the planning for the database development which is easy to use.

In the localized heavy rainfall observed in this study, it was found to bring a weak rainfall on the ground after 3-5 minutes from the first echo called a baby cell of torrential rains which appears in the altitude about 4-6 km, and to cause strong torrential rains on the ground after 10-15 minutes. It takes 40 to 70 minutes to converge the rainfall. In the case of torrential rains that take 70 minutes, the alternation of the precipitation core (especially the strong precipitation area) has taken place, and the precipitation duration of the entire system was elongated by the growth of precipitation core again after entering the dissipation phase.

As for the first echo mentioned earlier, a complex movement was observed, unlike the conceptual model (for example, fig. 10 of Kim et al., 2012), which describes a local heavy rainfall in a single core. In the conceptual model, it was thought that the precipitation would develop at the altitude of first echo, but in the PAWR observation, first echo lowered the altitude once in the first few minutes, and the appearance that the precipitation system developed upward rapidly.

From the results of the analysis of past events, it is expected to obtain useful knowledge about the PAWR observation data of the high time spatial resolution in future observation database management. For example, we think that there are some issues to consider about various aspects such as bibliographic information (annotation, metadata and identifiers), environmental information (background field of atmosphere, event extraction, event classification, etc.) We will discuss the data management and the improvement of the research process as expected in the new scientific research paradigm, such as open science and research data sharing. In addition, we would like to aim to contribute to the improvement of convenience and the applicability of the future data use in a timely as well as long lasting manner considering the direction of development of research such as meteorology and radar observation methods, and disaster prevention and mitigation apprication.

2012年に大阪大学吹田キャンパスに設置されたフェーズドアレイ気象レーダー（PAWR）は、30秒（詳細観測のときは10秒）で半径60km（詳細観測のときは30km）のボリュームスキャンができる降雨観測レーダーである。それまでのレーダーでは、ボリュームスキャン（上空の立体構造をスキャンする）には、パラボラアンテナの仰角を変化させて何度も回転させて5分程度の時間がかかっていたが（例えば、石原、2012、「2008年雑司が谷大雨当日における積乱雲群の振る舞いと局地的大雨の直前予測」、天気　59、Kim et al., 2012, X-band dual-polarization radar observation of precipitation core development and structure in a multi-cellular storm over Zoshigaya, Japan, on August 5, 2008, J. Meteor. Soc. Japan）、PAWRではデジタルビームフォーミングという技術を用いて30秒ごとの高速観測が可能となり、短時間で発展する局地的大雨の発展を詳細に観測するのに適している（Yoshikawa et al., 2013, MMSE beam forming on fast-scanning phased array weather radar, IEEE Trans. Geosci. Remote Sens., Ushio et al., 2015, Review of recent progress in lighting and thunderstorm detection techniques in Asia, Atmos. Res.）。本研究では、2012年7月26日に観測された孤立積乱雲による局地的大雨の4つのケースを事例として解析し、その結果から、今後の降雨研究のための長期間データベースの整備に求められる用件検討のための基礎調査を行いう。利用しやすいデータベース整備へ向けたプランニングに貢献できればと希望している。

本研究で観測された局地的大雨では、上空に現れる「豪雨のタマゴ」と呼ばれるファーストエコーから3-5分後には地上に弱い降水をもたらし、10-15分後には地上に強い豪雨をもたらすことがわかった。降雨の収束までには40-70分か

かる。70 分かかる豪雨の事例では、降水コア（特に降水の強い部分）の入れ替わりが起こっており、収束相に入った後も再び降水が発展することで全体の系の降水継続時間が長くなっている様子が捉えられた。

先に述べたファーストエコーについては、従来の単一コアで局地的大雨を説明する概念モデル（例えば、Fig. 10 of Kim et al., 2012）とは異なり、複雑な動きが観測された。従来のモデルでは、ファーストエコーの現れた高度で降水が発展すると考えられていたが、PAWR 観測ではファーストエコーは最初の数分間で一度高度を下げ、その後急激に降水システムが上方に発展する様子が捉えられた。

高時間空間分解能の PAWR 観測データについて、こうした過去イベントの解析結果から、今後の観測データベースマネジメントに有用な知見を得ることが期待される。例えば、アノテーション・メタデータ・識別子など書誌的情報、大気の背景場などの環境情報、イベント抽出、イベント分類などの情報整理方法、等、さまざまな側面について検討課題があるのではないかと考えている。また将来的にはこれらを通じて、オープンサイエンスや研究データ共有等の新たな科学研究パラダイムに期待されているような、データ管理・提供と研究プロセスの向上へ向けた議論を行う。さらには、今後の気象学・レーダー観測手法等の研究の発展方向性や、防災・減災の適時性、長期性の面からの有用性等も視野にいれながら、今後のデータ利用の利便性・応用性の向上に貢献することを目指せればと考えている。

アジア域雷放電検出網で観測された雷活動と台風強度発達との関係

佐藤 光輝 [1]; 高橋 幸弘 [2]; 山下 幸三 [3]; 久保田 尚之 [4]; 濱田 純一 [5]; Marciano Joel[6]
[1] 北大・理; [2] 北大・理・宇宙; [3] 足利大・工学部; [4] 北大・理; [5] 首都大・都市環境・地理; [6] ASTI, DOST

Relation between Typhoon Intensity and Lightning Activity Measured by the Asian Lightning Detection Network

Mitsuteru SATO[1]; Yukihiro Takahashi[2]; Kozo Yamashita[3]; Hisayuki Kubota[4]; Jun-ichi Hamada[5]; Joel Marciano[6]
[1] Hokkaido Univ.; [2] Cosmosciences, Hokkaido Univ.; [3] Engineering, Ashikaga Univ.; [4] Faculty of Science, Hokkaido Univ.; [5] Geography, Tokyo Metropolitan Univ.; [6] ASTI, DOST

Lightning activity is a good proxy to represent the thunderstorm activity and the precipitation and updraft intensities. Recent studies suggest that the monitoring of the lightning activities enables us to easily predict the maximum wind speed and minimum sea-level pressure of the tropical cyclone by one or two days before, though the prediction error of those typhoon intensities by the recent meteorological model becomes worse for the past 30 years. Many countries in the western Pacific region suffer from the attack of tropical cyclone (typhoon) and have a strong demand to predict the intensity development of typhoons. Thus, we have developed a new automatic lightning observation system (V-POTEKA) and installed this system in the Philippines, Guam and Palau since September 2017. V-POTEKA consists of a VLF sensor detecting lightning-excited electromagnetic waves in the frequency range of 1-5 kHz, an automatic data-processing unit, solar panels, and batteries. Lightning-excited VLF pulse signals detected by the VLF sensor are automatically analyzed at the data-processing unit, and the extracted information, such as the trigger time and pulse amplitude, is transmitted to a data server via the commercial 3G communications. We are now developing the lightning geolocation software using the time-of-arrival (TOA) technique. We have compared the relation between the lightning activities measured by the V-POTEKA network and the intensity variation of the typhoon occurred in 2017 and 2018. We confirmed that the time variation of the detected lightning event number and maximum wind speed are highly correlated and that the rapid increase of the lightning event number occurred just before the rapid intensification of the typhoon intensity.

雷放電は強い上昇気流に伴い発達した雷雲内で生じるため，雷雲活動度，降水量，鉛直対流強度などに対し良い指標となりうると指摘されている。中でもシビア気象の 1 つである台風に関して，最新の気象モデルをもってしても台風の規模予測精度は年々悪化しているのに対し，台風内部で発生する雷放電発生頻度を計測すると台風の最大風速や気圧を 1-2 日前に予測できるという先行研究も示されている。アジア域では，台風などのシビア気象による災害が毎年のように発生しているにもかかわらず，気象観測網や雷放電観測網は十分に整備されていない。海洋から大気へのエネルギー流入と台風発達過程において雷雲が重要な役割を果たしていると考えられることから，この地域での雷放電活動のリアルタイム監視体制を構築することが急務となっている。そのため我々は，新たな雷放電観測システム (V-POTEKA) を開発し，2017 年 9 月からフィリピン，グアム，パラオに設置した。この観測システムは，雷放電放射 VLF 帯電波受信器，データ処理装置，太陽電池パネル，蓄電池で構成される。雷放電電波を受信すると自動的に波形解析が行われて，波形トリガ時刻や振幅値がテキストデータとして 3G 電話回線でデータサーバに伝送される仕組みとなっている。これまで V-POTEKA は安定して動作しており，現在は，得られたデータから到来時間差法 (TOA) を用いて雷放電発生位置を推定するソフトウェアの開発を行っている。V-POTEKA のデータを解析し，2017 年 9 月から 2018 年にかけて発生した台風と雷活動の関係を調べた。その結果，雷放電発生数と台風の規模発達には高い相関が見られ，さらに，台風急速強化が発生する直前に雷放電発生数が急激に増加する兆候も確認された。講演では，これらの解析で得られた初期結果について詳しく紹介する。

Oscillations of atmospheric electric field during snowfall in the Kanto region, Japan, using 95-GHz cloud radar FALCON-I

Hiroyo Ohya[1]; Kota Nakamori[2]; Masashi Kamogawa[3]; Tomoyuki Suzuki[4]; Toshiaki Takano[5]; Kazuomi Morotomi[6]; Hiroyuki Nakata[7]; Kazuo Shiokawa[8]

[1] Engineering, Chiba Univ.; [2] Electrical and Electronic, Chiba Univ.; [3] Dept. of Phys., Tokyo Gakugei Univ.; [4] Education, Gakugei Univ.; [5] Chiba Univ.; [6] Japan Radio Co. Ltd.; [7] Grad. School of Eng., Chiba Univ.; [8] ISEE, Nagoya Univ.

It is known that cloud-to-ground lightning and precipitations generated from thunderclouds are a generator of global electric circuit (e.g., Williams, 2009). In the fair weather, the atmospheric electric field at the ground is generally 100 V/m and downward (positive). The atmospheric electric field varies during not only lightning/thunderstorms, but also snowfall/blizzard (Minamoto and Kadokura, 2011). In particular, variations in the atmospheric electric field during powder snow in Antarctica have been studied. However, variations in the atmospheric electric field during wet snow in the Kanto area, Japan, have not been revealed yet. In this study, we investigate the variations in the atmospheric electric field during snowfall of 23-24 November, 2016, using a field mill, the 95 GHz cloud radar, FALCON (FMCW Radar for Cloud Observations)-I, and X-band radar (9.4 GHz). We have observed the atmospheric electric field with a Boltek field mill, and cloud reflectivity and the Doppler velocity with the FALCON-I in Chiba University, Japan, (CHB, 35.63N, 140.10E). At 16.2 km southeast from the CHB, a phased array X-band radar operated by Japan Radio Corporation have observed precipitations/cloud. During snowfall of 23-24 November, 2016, periodic oscillations in the atmospheric electric field with periods of 70-90 minutes were observed at four observation sites; CHB, Kakioka (KAK, 36.23N, 140.19E), Tokyo Gakugei University (KGN, Kokubunji, Tokyo, 35.71N, 139.49E), and Seikei High School (MSN, Musashino, Tokyo, 35.72N, 139.57E). The distances of CHB-KAK, CHB-TGU, and CHB-SHS are 64.8 km, 55.9 km, and 49.0 km, respectively. This is the first observations of similar oscillations in the atmospheric electric field at four observation sites located at a long distance of 50-65 km. At the end of snowfall, the periods of the oscillations became shorter to be 20-50 minutes at all sites. Based on the FALCON-I and X-band radar observations, we found that the reflectivities of the snow cloud have the same period of 70 minutes at CHB at 2 km heights during the snowfall. In the presentation, we will discuss the cause of the long oscillations in the atmospheric electric field.

OHイメージャ観測を用いた、南極昭和・Davis基地上空の中間圏重力波の伝播特性比較

木暮 優 [1]; 中村 卓司 [2]; 冨川 喜弘 [2]; 江尻 省 [2]; 西山 尚典 [2]; 堤 雅基 [2]; Michael J. Taylor[3]; Yucheng Zhao[3]; Pautet P.-Dominique[4]; Damian Murphy[5]
[1] 総研大・複合・極域; [2] 極地研; [3] USU; [4] ユタ州立大学; [5] AAD

Comparison of gravity wave characteristics in the mesosphere over Syowa and Davis, the Antarctic, using OH airglow imagers

Masaru Kogure[1]; Takuji Nakamura[2]; Yoshihiro Tomikawa[2]; Mitsumu K. Ejiri[2]; Takanori Nishiyama[2]; Masaki Tsutsumi[2]; Taylor Michael J.[3]; Zhao Yucheng[3]; P.-Dominique Pautet[4]; Murphy Damian[5]
[1] Polar Science, SOKENDAI; [2] NIPR; [3] USU; [4] Utah State University; [5] AAD

Gravity waves transport momentum and energy from the lower atmosphere to the upper atmosphere, and drive the general circulation, which significantly change the temperature in the middle atmosphere [Fritts and Alexander, 2003]. To understand this role quantitatively will improve the modern general circulation models [Garcia et al., 2017].

The polar night jet region is known to have high gravity wave activity. However, their sources and propagation are only poorly understood because of the lack of observations. To understand those, our group has observed the gravity waves over Syowa (69S, 40E) using various instruments (e.g., lidar, OH imager, and MF radar). We recently compared the gravity waves over Syowa and Davis (69S, 79E), which have similar terrain and meteorological conditions, to show their horizontal variation over the East Antarctic. We found, from the lidar temperature observations, that vertical profile of gravity wave potential energy is similar between Syowa and Davis, except for a clear enhancement around 30-40 km over Davis [Kogure et al., 2017]. Horizontal propagation characteristics are more clearly observed by airglow imaging measurements of ˜90 km altitude. The comparison of four imagers' results between April-May 2013 have indicated that the major propagation directions were westward at three stations (Syowa, McMurdo, Halley), but at Davis GWs seems to propagate in all the directions, which is different from the other three. [Matsuda et al., 2017]. It seems like the GWs over Davis did not suffer wind filtering in the middle atmosphere.

The goal of this study is to reveal what causes the difference of the mesospheric gravity wave characteristic over Syowa and Davis. In this study, we will show the ground-based horizontal phase speed spectrum at ˜87 km altitude over the two stations derived from OH imagers in more details. We analyzed the OH airglow imager data obtained for eight months (from March to October in 2016) over the two stations with M-transform [Matsuda et al., 2014]. This included only the data without clouds and aurora contaminations continuously for at least one hour. The numbers of nights with such data sets are 40 at Syowa and 55 at Davis. In 2016, clear sky and aurora free data were available at both stations on ten nights. Comparison of phase velocity spectrum obtained on the same night showed very similar characteristics on only one night out of ten. On five nights, the spectra were quite different. On the other four nights, the spectral peaks with slow westward phase velocity (>50 m/s) were commonly observed, but additional spectral peaks were found over Davis and not over Syowa. We investigated, using raytracing method, where the gravity waves with common spectrum and additional spectrum on one of the four nights (29th Aug.), propagated from. This investigation suggested the common waves could propagate from the troposphere right below. On the other hand, the additional waves could propagate from the stratosphere over the sea. This presentation will show the results of OH imager observations and of the raytracing results, and we will discuss what causes the difference of the gravity wave characteristic over both stations.

下層大気起源の熱圏重力波により引き起こされた大規模伝播性電離圏擾乱

三好 勉信 [1]; 陣 英克 [2]; 藤原 均 [3]; 品川 裕之 [2]
[1] 九大・理・地球惑星; [2] 情報通信研究機構; [3] 成蹊大・理工

Traveling Ionospheric Disturbances excited by upward propagating gravity waves

Yasunobu Miyoshi[1]; Hidekatsu Jin[2]; Hitoshi Fujiwara[3]; Hiroyuki Shinagawa[2]
[1] Dept. Earth & Planetary Sci, Kyushu Univ.; [2] NICT; [3] Faculty of Science and Technology, Seikei University

It has been recognized that gravity waves (GWs) play an important role on the variability in the thermosphere/ionosphere. In this study, traveling ionospheric disturbances (TIDs) excited by upward propagating GWs are examined using a whole atmosphere-ionosphere coupled model (GAIA: horizontal resolution 100km). The GAIA contains the region from the ground surface to the upper thermosphere, so that we can simulate excitation of GWs in the lower atmosphere, their upward propagation into the thermosphere, and their impact on the ionosphere. We examine effects of solar activity on TIDs. Furthermore, the relationship between the TIDs and the lower atmospheric variability is also examined.

下層大気起源の大気重力波が、熱圏領域まで伝播し熱圏電離圏変動に多大な影響を及ぼしていることが、近年の数値モデル及び観測による研究で明らかになりつつある。本研究では、大気圏電離圏結合モデル GAIA の高水平分解能版 (水平解像度約 100km) を用いて、熱圏重力波が、電離圏変動におよぼす影響について調べてみた。本研究で使用する GAIA は、対流圏から熱圏上端までを含んでいるため、下層大気での重力波の励起、熱圏への鉛直伝播、熱圏での砕波などの一連の過程を再現することが可能である。また、中性大気と電離大気の相互作用過程を含んでいるため、熱圏重力波が電離圏変動におよぼす影響についても明らかにすることが可能である。本研究では、下層大気起源の熱圏重力波で励起される大規模伝播性電離圏擾乱（LSTID）について、太陽活動依存性や下層大気変動との関連性に注目して解析を行った。太陽活動依存性については、下層大気の状態を同じにして、太陽放射量のみを変えた二つの実験を行い、LSTID の発生頻度や規模の違いについて解析を行った。下層大気変動との関連については、成層圏突然昇温をはじめとする成層圏における極渦の時間変動と LSTID の発生頻度の関連について焦点を当てて解析を行う予定である。

GPS受信機網から得られる全電子数を用いた成層圏突然昇温の中規模伝搬性電離圏擾乱への影響の研究

大塚 雄一 [1]; 新堀 淳樹 [2]; Abadi Prayitno[3]; 津川 卓也 [4]; 西岡 未知 [4]
[1] 名大宇地研; [2] 名大・宇地研; [3] 名大 ISEE 研; [4] 情報通信研究機構

Effects of Stratospheric Sudden Warming on Medium-Scale Traveling Ionospheric Disturbances Based on GPS TEC Observations

Yuichi Otsuka[1]; Atsuki Shinbori[2]; Prayitno Abadi[3]; Takuya Tsugawa[4]; Michi Nishioka[4]
[1] ISEE, Nagoya Univ.; [2] ISEE, Nagoya Univ.; [3] ISEE, Nagoya Univ.; [4] NICT

In order to investigate effects of Stratosphere sudden warming (SSW) on the ionospheric disturbances, we have analyzed total electron content (TEC) data obtained from GPS receivers in the world. We have obtained perturbation component of TEC, which could be caused by MSTID, by subtracting 1-hour running average from the original TEC time series for each pair of satellites and receivers. Then, we have calculated the standard deviation of the perturbation TEC within 1 hour for each satellite-receiver path every hour. A ratio of the standard deviation to the 1-hour averaged TEC is defined as MSTID activity. In this study, we investigated the MSTID activity at mid- and high-latitudes before and after a major Stratospheric Sudden Warming (SSW) event that occurred on January 2009.

In East Asia, the daytime MSTID activity at latitudes higher than approximately 35^{o}N mostly exceeds 2.0% before January 24, 2009, whereas it is mostly below 2.0% after January 24, 2009. On the other hand, at latitude lower than approximately 35^{o}N, the daytime MSTID activity does not show distinct difference before and after January 24 although day-to-day variability of the MSTID activity exists. The daytime MSTID activity in Europe shows similar tendency, but the transition of the daytime MSTID activity from high to low values appeared on January 18, 2009. It occurred 6 days earlier than in East Asia. Amplitude of the decrease in the daytime MSTIDs is larger at latitude lower than 55^{o}N compared to that at latitudes higher than 55^{o}N.

The daytime MSTIDs could be caused by gravity waves propagating upward from below into the thermosphere. Recent simulations suggest that these gravity waves are secondary waves generated from dissipation of the primary waves in the MLT region. Miyoshi et al. (2015) have reported that the generation of secondary GWs is more active when the strato-mesospheric jet is strong, and that the generation of secondary waves is inactive when the strato-mesospheric jet is attenuated or becomes westward. Consequently, low MSTID activity after January 24 could be caused by weaker generation of secondary gravity wave during weaker or westward strato-mesospheric jet.

これまでの研究から、成層圏突然昇温が超高層大気の温度や電離圏電子密度に影響を及ぼすことが明らかにされてきた。本研究では、電離圏電子密度の波状構造である中規模伝搬性電離圏擾乱 (Medium-Scale Traveling Ionospheric Disturbance; MSTID) に対する影響を調べる。中緯度において、MSTID は冬季の昼間と、夏季または冬季の夜間に発生頻度が高いことが明らかになっており、昼間の MSTID は下層大気から上方伝搬する大気重力波が原因であり、夜間の MSTID はプラズマ不安定の一種である Perkins 不安定が原因と考えられている。本研究では、世界各地の GPS 受信機網で得られたデータから全電子数を算出した。各衛星と受信機で得られた全電子数の 1 時間移動平均からの偏差を MSTID による全電子数変動とし、1 時間平均値で規格化した値を MSTID 活動度と定義し、成層圏突然昇温の前後で MSTID 活動度の変化を調べた。

2009 年 1 月に発生した成層圏突然昇温では、東アジアの北緯 35-45 度において、MSTID 活動度は、2009 年 1 月 24 日以前は 2.0%をほぼ超えていたが、1 月 24 日以降は、2.0%以下であった。一方、北緯 35 度よりも低緯度では、このような変動は見られなかった。ヨーロッパでは、 1 月 18 日以降に MSTID 活動度が低下することが分かった。近年の研究より、電離圏・熱圏における大気重力波は、下層大気から伝搬してきた大気重力波が中間圏・下部熱圏において消散する際に生じた二次波と考えられている。成層圏突然昇温に伴って中間圏における東向き風が弱まり、また西向きになると、二次波の生成は弱まることから、電離圏における昼間の MSTID の活動度が成層圏突然昇温時に弱まったと考えられる。

陸別・信楽・アサバスカ・マガダンの大気光画像を用いた中間圏大気重力波・中規模伝搬性電離圏擾乱の水平波数分布の長期統計解析

土屋 智 [1]; 塩川 和夫 [1]; 大塚 雄一 [1]; 中村 卓司 [2]; 山本 衛 [3]; Connors Martin[4]; Schofield Ian[5]; Shevtsov Boris[6]; Poddelsky Igor[6]
[1] 名大宇地研; [2] 極地研; [3] 京大・生存圏研; [4] Centre for Science, Athabasca Univ.; [5] Athabasca University, Canada; [6] IKIR

Statistical analysis of wavenumber distribution of mesospheric and ionospheric waves in airglow images in Japan, Canada and Russia

Satoshi Tsuchiya[1]; Kazuo Shiokawa[1]; Yuichi Otsuka[1]; Takuji Nakamura[2]; Mamoru Yamamoto[3]; Martin Connors[4]; Ian Schofield[5]; Boris Shevtsov[6]; Igor Poddelsky[6]
[1] ISEE, Nagoya Univ.; [2] NIPR; [3] RISH, Kyoto Univ.; [4] Centre for Science, Athabasca Univ.; [5] Athabasca University, Canada; [6] IKIR

Airglow imagers are a powerful tool to obtain two-dimensional images of waves in the upper atmosphere. Atmospheric gravity waves (AGWs) in the mesosphere and medium-scale traveling ionospheric disturbances (MSTIDs) in the ionosphere are typical wave structures seen in the 557.7-nm (emission altitude: 90-100 km) and 630.0-nm (200-300 km) airglow images, respectively. Investigation of the horizontal characteristics of AGWs and MSTIDs is essential for understanding the dynamical variation of middle and upper atmosphere.

Takeo et al. [JGR, 2017] studied horizontal parameters of AGWs and MSTIDs over 16 years by using airglow images obtained at Shigaraki, Japan (34 N, 136 E). Tsuchiya et al. [JGR, 2018; JpGU, 2018] have applied the same spectral analysis technique to the airglow images obtained at Rikubetsu, Japan (43 N, 143 E), Athabasca, Canada (54 N, 246 E), and Magadan, Russia (60 N, 150 E). However, comparison of characteristics of horizontal wavenumber at different locations over 10 years has not yet been conducted.

In this study, we have applied the 3-dimentional FFT spectral analysis technique to the 557.7 nm and 630.0 nm airglow images at Rikubetsu and Shigaraki, Japan, Magadan, Russia, and Athabasca, Canada, focusing on their wavenumber distributions over ten years. For MSTIDs seen in the 630-nm airglow images in the thermosphere, the power spectrum density is strongest in summer compared to other seasons at all stations. We confirmed that this is not because of the 630-nm airglow layer thickness, since the difference of the thickness between summer and winter calculated based on IRI and MSIS models is not significant. When the solar activity is low, the power of longer wavelength waves is higher at Rikubetsu, but lower at Shigaraki. This solar activity dependence at Rikubetsu is consistent with the consideration of faster AGW dissipation for smaller scale waves by molecular viscosity in the upper atmosphere (e.g., Vadas and Fritts, JGR, 2006; Yigit and Medvedev, JGR, 2010), while that at Shigaraki may be due to latitudinal gradient of F-layer plasma density and associated 630-nm airglow intensity through spectral contamination to the lower wavenumber region. In the presentation we will also show characteristics of AGWs in the mesopause region observed in the 557.7-nm airglow images.

熱圏鉛直風によるプラズマバブルシーディング

横山 竜宏 [1]; 陣 英克 [1]; 品川 裕之 [1]
[1] 情報通信研究機構

Seeding of equatorial plasma bubbles by vertical neutral wind

Tatsuhiro Yokoyama[1]; Hidekatsu Jin[1]; Hiroyuki Shinagawa[1]
[1] NICT

Equatorial plasma bubble (EPB) is a well-known phenomenon in the equatorial ionospheric F region. As it causes severe scintillation in the amplitude and phase of radio signals, it is important to understand and forecast the occurrence of EPBs from a space weather point of view. The development of EPBs is presently believed as an evolution of the generalized Rayleigh-Taylor instability. We have already developed a 3D high-resolution bubble (HIRB) model with a grid spacing of as small as 1 km and presented nonlinear growth of EPBs which shows very turbulent internal structures such as bifurcation and pinching. In previous studies, initial plasma density perturbation, which should be a primary factor of the day-to-day variability of EPB occurrence, was applied manually at the beginning of the simulation. Although atmospheric gravity waves have been considered as a seeding source of EPBs for a long time, no direct evidence is presented so far. In this study, we focus on the vertical wind component in the theremosphere as a seeding source of the lower F region. Overall, vertical wind perturbation with an amplitude of a few meters per second can work as a seeding of EPBs.

赤道電離圏においては、赤道スプレッド F/プラズマバブルと呼ばれる現象の研究が古くから行われている。プラズマバブルに伴う局所的なプラズマ密度の不規則構造が発生した場合には、電波の振幅、位相の急激な変動（シンチレーション）が生じるため、GPS 等による電子航法に深刻な障害を及ぼすことが知られている。現在までに、プラズマバブルの複雑な内部構造を再現可能な 3 次元数値モデルを開発し、非線形成長過程について明らかにすることに成功してきた。プラズマバブルの東西非対称性や、プラズマバブル内部の磁場変動等、これまでに観測されてきたプラズマバブルの特徴も良く再現されてきた。一方、これまでのシミュレーションでは、プラズマ密度の初期変動を人為的に与えた状態から計算を開始していたが、プラズマバブルの成長過程はこの初期変動の与え方に強く依存しており、発生の日々変化の主な要因と考えられている。初期変動を作り出す主な要因として大気重力波が古くから考えられてきたが、現在までに明確な証拠は得られていない。そこで、大気重力波による風速変動の鉛直風成分に着目し、簡単化した条件の下で、鉛直風による電離圏 F 領域下部の変動生成、すなわちプラズマバブルのシーディングについて検討を行った。波面が地球磁場に並行な大気重力波に近い条件を考え、経度方向に変化し、ある緯度範囲内で一様な鉛直風変動を考え、高度 200km 以上に一様に印加した。鉛直風変動の振幅、波長、変動を与える緯度範囲に応じて、プラズマバブルの成長速度に差が見られたが、概ね数 m/s の鉛直風変動であっても、プラズマバブルのシーディングとして十分に役割を果たせることが明らかとなった。大気重力波に伴う鉛直風成分が、プラズマバブル発生の日々変動において重要な役割を担っていると考えられる。

都道府県規模インフラサウンド観測網の紹介

山本 真行 [1]
[1] 高知工科大

Introduction of infrasound observation network in prefectural level

Masa-yuki Yamamoto[1]
[1] Kochi Univ. of Tech.

Infrasound is known as pressure waves in atmosphere with its frequency lower than the human audible limit of 20 Hz. Due to its distant propagation characteristics without large attenuation, the infrasound can be used as a remote-sensing tool for the huge scale geophysical events closely coupled with atmospheric environment. Here we show the current situation of infrasound observation network in prefectural level, that has been established in Kochi.

Kochi prefecture is located in Shikoku island and, at along the southern coast of Kochi, we have many dangerous sites of tsunami invasion once a huge earthquake happens in Nankai Trough in the pacific ocean, just near the southern coast of Japan.

Infrasound observation network has been installed in Kochi region since 2016 for disaster prevention, taking account mainly for tsunami disasters. In 2017 we expanded our sites to be 15 in Kochi pref. The infrasound sensor arrays reveal us some important feature of the detected signals coming from Typhoons, volcanic eruption of Mt. Aso/Kirishima/Sakurajima, thunders, fireball (large meteor) events.

As the network is one of the densest infrasound observation schemes in such specific small area in a nation, we need appropriate analyzing method than that applied for usual arrayed infrasound sensors. In this talk, we will introduce our observation design of the network as a model case and the obtained datasets for consideration of tsunami and the other disaster preventions.

TEC and pressure changes by the 2015 Kuchinoerabujima eruption: comparison with energy distribution by ray-tracing

Yuki Nakashima[1]; Kiwamu Nishida[1]; Yosuke Aoki[1]; Kosuke Heki[2]
[1] ERI, Univ. Tokyo; [2] Hokkaido Univ.

Our objective is to interpret atmospheric perturbation excited by a Kuchinoerabujima volcano eruption on 29 May 2015. We observed a large GNSS-TEC and near-surface pressure perturbations at the same time. In this talk, we will show comparing the observation results with energy distribution expected by ray-tracing.

Kuchinoerabujima is a volcanic island that is located to the 100 km south of Kyushu. The volcano erupted at 0:59 UT (9:59 LT) May 29, 2015, with the eruption magnitude VEI 3. The volcanic eruption caused significant pressure changes. The lowest frequency part of them (less than ˜0.01 Hz) can go up and reach the ionosphere due to less viscosity attenuation. Such waves are sometimes detected as ionized atmosphere perturbations, and various kinds of responses to near-surface phenomena including volcanic eruptions have been reported so far.

We use the broadband seismometer array, F-net deployed by NIED, and the barometer array installed by AIST to find the wave propagating in the lower atmosphere. At the same time, we succeeded to detect ionospheric perturbation by GNSS-TEC derived from the 1 Hz sampling GNSS carrier phase data from Japanese dense GNSS array, GEONET. The three observations show similar perturbation signals in 0.01–0.02 Hz band, which come from the one volcanic air blast. However, observations near the surface and in the ionosphere have different physical units (Pressure and TECU), and it is difficult to compare them directly.

We are now trying to estimate energy distribution using ray-tracing from the source to the ionosphere to interpret the whole of the observation quantitatively and simultaneously. The ray-tracing method is assumed high-frequency approximation and seems slightly hard to use in our project. Nevertheless, we checked and already reported in past meetings, the travel time curve drawn by that is consistent with the propagation observed in the ionosphere and near the surface. From the calculation of the energy, we can estimate pressure changes and electron density perturbations. The quantitative comparison will characterize the further physical processes of the eruption.

熱帯の強い降雨時にSwarm衛星が東南アジア上空で観測した磁場変動

家森 俊彦 [1]; 青山 忠司 [2]; 山田 彬泰 [3]; Hozumi Kornyanat[4]; 中西 邦仁 [5]; 横山 佳弘 [6]; 佐納 康治 [7]; 小田木 洋子 [8]; Jarupongsakul Thanawat[9]; Pangsapa Vijak[10]
[1] 京大; [2] 京大・理; [3] 京大・理; [4] NICT; [5] 京都大学理学研究科; [6] 京大理; [7] 朝日大・経営; [8] 京大・理・地磁気センター; [9] チュラロンコン大・理; [10] チュラロンコン大・理

Magnetic variations observed by the Swarm satellites over south-east Asia during strong tropical rainfall

Toshihiko Iyemori[1]; Tadashi Aoyama[2]; Akiyasu Yamada[3]; Kornyanat Hozumi[4]; Kunihito Nakanishi[5]; Yoshihiro Yokoyama[6]; Yasuharu Sano[7]; Yoko Odagi[8]; Thanawat Jarupongsakul[9]; Vijak Pangsapa[10]
[1] Kyoto Univ.; [2] Graduate School of Science, Kyoto Univ.; [3] Faculty of Science, Kyoto University; [4] NICT; [5] Graduate School of Science, Kyoto Univ; [6] Grad school of Science, Kyoto Univ.; [7] Asahi Univ.; [8] WDC for Geomagnetism, Kyoto Univ.; [9] Faculty of Science, Chulalongkorn Univ.; [10] Chulalongkorn Univ.

Cumulative convection is expected to generate acoustic mode atmospheric waves, and they are expected to generate Magnetic Ripples. They are observed as a small scale magnetic variation. That is, their typical amplitude is less than a few nT with period around 10-30 seconds. They are observed by low-altitude satellites almost always along the orbit in low and mid latitudes. From the Swarm satellite observation, it was confirmed that they are spatial structure of short scale field-aligned currents[(1)]. Various case studies and statistical analyses strongly suggest that the main source is the cumulative convection[(2),(3)] in lower atmosphere. However, it is still not yet very clear probably because the cumulative convection exists everywhere. To show the generation process of magnetic ripples more directly, we have been making geomagnetic and micro-barometric observations, GPS-TEC and meteorological observations such as rain-fall, wind velocity, temperature etc. in Phimai, north-east of Thailand and in Nakanoshima Island South-West Japan. In this paper, we show the results of Swarm satellite observation over South-East Asia, GPS-TEC and ground observations during conjunction events. The polar orbits of Swarm-A and –C satellites are shifted about 1.4 degree in longitude, i.e., Swarm-C flies about 1.4 degree East of Swarm-A with around 10 seconds delay, and hence, they fly parallel with maximum distance about 140 km near the equator.

[(1)] Iyemori et al. (2015), Geophys. Res. Lett., 41, doi:10.1002/2014GL062555.
[(2)] Nakanishi et al. (2014), Earth Planets Space, 66:40, doi:10.1186/1880-5981-66-40.
[(3)] Aoyama et al. (2017), Earth, Planets and Space, 69:89, DOI 10.1186/s40623-017-0679-2.

低高度極軌道衛星が中低緯度でほぼ常に観測する磁気リップルと名付けられた小振幅の短周期磁場変動は、微細な沿磁力線電流の空間構造であることが、2013年11月に打ち上げられたESAのSwarm-A,-B,-C 3機編隊による精密磁場観測データの解析から明らかになった[(1)]。振幅の地理的、季節的分布や緯度分布、Local Time依存性の統計的解析や、全球雲画像、台風との対応など、様々な状況証拠から、下層大気中の積雲対流から放射される音波モードの大気重力波動による電離層でのダイナモ作用が原因であると推測される[(2),(3)]。しかし、どの積雲対流が発生源となっているのかなど、より直接的な対応をつけることはできていない。そこで、この発表では、熱帯域でのスコールに伴うような急な激しい降雨現象が発生したときに上空を経度方向に約1.4度平行して飛翔したSwarm-AとSwarm-Cの磁場観測データ、タイ東北部Phimaiやトカラ中之島で同時観測した地磁気、微気圧、降雨、風速およびGPS-TECデータなどを相互に比較した結果を報告する。

[(1)] Iyemori et al. (2015), Geophys. Res. Lett., 41, doi:10.1002/2014GL062555.
[(2)] Nakanishi et al. (2014), Earth Planets Space, 66:40, doi:10.1186/1880-5981-66-40.
[(3)] Aoyama et al. (2017), Earth, Planets and Space, 69:89, DOI 10.1186/s40623-017-0679-2.

放射伝達コードJACOSPARの火星limb観測への適応

豊岡 雅士 [1]; 岩渕 弘信 [2]; Mahieux Arnaud[3]; 青木 翔平 [3]; 中川 広務 [1]; 笠羽 康正 [4]
[1] 東北大・理・地球物理; [2] CAOS, Tohoku Univ.; [3] BIRA-IASB; [4] 東北大・理

Modification of the retrieval tool JACOSPAR for the Martian limb observations

Masashi Toyooka[1]; Hironobu Iwabuchi[2]; Arnaud Mahieux[3]; Shohei Aoki[3]; Hiromu Nakagawa[1]; Yasumasa Kasaba[4]
[1] Geophysics, Tohoku Univ.; [2] CAOS, Tohoku Univ.; [3] BIRA-IASB; [4] Tohoku Univ.

A fully spherical radiative transfer (RT) code with multiple scattering is extremely computationally expensive. To reduce the computational time, some approximations are usually needed. Smith et al., (2013) applied the 'pseudo-spherical' approximation (Spurr, 2002; Thomas and Stamnes, 1999) to the retrieval of the vertical distribution of dust and water ice aerosols. It was found that the computed radiance under the pseudo-spherical approximation was accurate within a few percent and was two orders of magnitude faster than the exact Monte Carlo(MC) calculations. However, there are still some potential demands to treat fully spherical systems for the atmosphere under the multiple scattering conditions.

JACOSPAR considers refraction and multiple scattering of light by aerosols in a fully spherical atmosphere (Iwabuchi et al, 2006, 2009a, 2009b). It calculates the radiance and Jacobians effectively with requested accuracy by adopting 'backward Monte Carlo method' and 'Dependent sampling method' (Marchunk 1980) with reduced calculation costs. JACOSPAR was applied to the Earth's observation of O3 and NO2(Irie et al., 2012). Recently, EU UPWARDS project (D1.1) applied JACOSPAR to the limb observation of Mars. The radiance computed by JACOSPAR was compared with those computed by the independent MC code. In the altitude range from 0 to 80km (80 layers) the calculated radiances of both codes showed a good agreement with the uncertainty of less than 1 % on average. In this study, we performed a further optimization of JACOSPAR for the limb observation of Martian atmosphere. We conducted radiative simulations as following settings.

The absorption coefficients of Martian gases (CO2, H2O, and CO) were calculated with the line-by-line method under their mixing ratio profiles. The single scattering properties of dust and water ice were calculated with the Mie theory (Wiscombe 1980) and integrated with the modified gamma distribution (Warren 1984). The refractive indices of dust and water ice are referred to from Wolff and Clancy (2003) and Warren (1984), respectively. The mixing ratio of the gases in the Martian atmosphere were assumed to be 95.32% of CO2 at 0-79km, 300 ppm of H2O at 0-79 km, and 800 ppm of CO at 0-79 km, respectively. The vertical temperature pressure profiles were selected from the solar EUV average conditions of Mars Climate Database (Forget et al., 1999).

For this application, we modified two points of JACOSPAR code in order to stably calculate the radiance in the thin atmosphere of Mars. (1) In the upper atmospheric layer of Mars where the multiple scattering rarely happens, the radiance can vary 20-30% depending on whether the observed light is the single scattered one or multiple one. This can cause unstable computation results. Thus, we modified the threshold to decide the occurrence of the scattering event. (2) When considering the finite size of Field-of-View (FOV), the radiance is averaged by taking the number of line of sights(LOSs) within the FOV. The LOSs were selected randomly in JACOSPAR. However, a slight difference of LOSs can cause significance on the number of scatterings in the limb geometry. We modified to set the LOSs uniformly within the FOV.

Based on these modifications, we conducted the test simulations for the geometry of OMEGA/MEx limb observations in the altitude range from 0 to 60 km with 6 layers. The analytical Jacobians for the absorption and the scattering by aerosols were compared with numerically calculated Jacobians by giving perturbations to the optical depth of each layer. The analytical and numerical Jacobians for absorption agreed well within 2%. Meanwhile, those for the scattering are within 10%.

Influence of MJO on the Turbulence Kinetic Energy in the Tropical Tropopause Layer observed from Equatorial Atmosphere Radar data

Noersomadi Noersomadi[1]; Hiroyuki Hashiguchi[2]
[1] RISH, Kyoto Univ.; [2] RISH, Kyoto Univ.

We investigate the turbulence kinetic energy (TKE) near the tropical tropopause using long-term dataset of Equatorial Atmosphere Radar (EAR) version 02.0212 from July 2001 to June 2018. TKE is estimated from the observed spectral width data in the northward beam to reduce the effect of strong zonal wind shear. We analyze the variation of TKE and the mean zonal wind (U) at 17 km, which is considered as the mean height of the tropical tropopause, as well as the phase propagation of Madden Julian Oscillation (MJO) from the Real-time Multivariate MJO index (RMM). We discuss the relationship between TKE and U in the active and inactive period of MJO (MJOa and MJOi), on the basis of the amplitude RMM, at Phase 3 and Phase 4 (P3 and P4) when MJO propagates from Indian Ocean to Maritime Continent. The results show that both during MJOa and MJOi, TKE is found larger up to 1.0-1.5 $(m/s)^2$ associated with strong westward wind than with eastward wind (about 0.5 $(m/s)^2$). The magnitude interval of westward wind in MJOa is larger than in MJOi, particularly at P4. The variation of TKE and U in seasonal MJOa at P4 indicates contrast between northern hemisphere winter and summer. Our analysis describes large turbulence occurred associated with strong westward wind especially during the active period of MJO.

栃木県足利市における雷雲観測を目的とした静電界計測網の構築

山下 幸三 [1]; 高橋 幸弘 [2]; 佐藤 光輝 [3]
[1] 足利大・工学部; [2] 北大・理・宇宙; [3] 北大・理

Construction of electrostatic measurement network for thunderstorm observation in Ashikaga City, Tochigi Prefecture

Kozo Yamashita[1]; Yukihiro Takahashi[2]; Mitsuteru SATO[3]
[1] Engineering, Ashikaga Univ.; [2] Cosmosciences, Hokkaido Univ.; [3] Hokkaido Univ.

In the recent, lightning observation has been considered as an effective and low-cost tool to carry out early detection and short-term forecast of thunderstorm which causes extreme weather events, such as tropical cyclone, torrential rainfall, etc. Previous studies indicated that detection of intracloud (IC) lightning discharge which occurs before cloud-to-ground (CG) lightning discharge was a key technology for nowcast of extreme weather events.

Detection of thunderstorm electrification before IC based on electrostatic measurement is also focused on as an effective method for early detection and nowcast of thunderstorm activity. However, preceding studies also pointed that not only thundercloud but also charge nearby sensor could be detected in electrostatic measurement due to high sensitivity. Although electrostatic measurement would be effective especially for nowcast of lightning discharge, it remains at the research stage because of the difficulty of operation.

In this study, we have newly deployed simple and low-cost electric field mill (EFM) to construct multiple electrostatic measurement network in Ashikaga city, Tochigi Prefecture. Previous meteorological research indicated that Tochigi prefecture is one of the most intense regions for thunderstorm activity in Japan. In this area, several isolated thunderclouds could be monitored during a summer. If isolated thundercloud can be observed by multiple electrostatic measurement, development of electrification in cloud would be derived quantitatively as an inversion problem. In this presentation, details of test observation and status of EFM deployment is summarized.

This work was supported by JSPS KAKENHI Grant Number 15K16314, 18K13970 and by Japan International Cooperation Agency (JICA) and JST under SATREPS.

MFレーダーデータ共有実験によるオープンサイエンス推進のための検討

磯田 総子 [1]; 村山 泰啓 [2]; 今井 弘二 [2]; 国武 学 [2]
[1] NICT; [2] 情報通信研究機構

A study for the promotion of Open Science by the MF Radar data sharing experiment

Fusako Isoda[1]; Yasuhiro Murayama[2]; Koji Imai[2]; Manabu Kunitake[2]
[1] NICT; [2] NICT

Open Science is being actively discussed increasingly, in various aspects including acceleration of research through the sharing of research data. It is considered that highly intellectual value data of various research institutions is considered as the result of scientific research, and that it will be important to be shared, used and re-sued in the general society in the future (e.g., Cabinet Office of Japan, 2015).

As an incentive for researchers to share their data, recent investigation and practice promotes that minting a digital object identifier (DOI) to a dataset and citing the dataset in a research paper when it is used in the paper (e.g., Force 11, Joint Declaration of Data Citation Principles, 2014, doi:10.25490/a97f-egyk). In Japan, as the first case of DOI registration experiments, the neutral wind data of the Alaska Poker Flat MF Radar (MFR) of NICT (doi: 10.17591/55838DBD6C0AD) has been granted (e.g., Japan Link Center, DOI Registration guidelines for research data ", 2015, doi: 10.11502/Rd_guideline_ja), which are actually cited in papers (e.g. Kinoshita. et al, JGR, 2015, doi:10.1002/2014JD022647).

This Poker Flat MF Radar data file has been stored and managed on-premises (servers in the organization) and has been provided by FTP and HTTP to registered collaborating researchers. On the other hand, in recent years, Web archive collected by the National Diet Library (NDL) Warp (Web ARchive Project) is an attempt to store data in the role of a research institution and an information storage organization (Kimezawa and Murayama, 2017, doi:10.18919/jkg.67.9_459).

Taking into consideration the above, we plan to study unresolved techniques and methodology of data sharing based on an experimental sharing of data of the MFR. In these cases, we will need to investigate proper design, technique, and practice possibility of storage, management, and use/reuse of the data. The result is expected to contribute to long-term or future utilization across multidisciplinary fields. A case study is currently assumed to use horizontal neutral wind datasets in the mesosphere and lower thermosphere of MFRs at Wakkanai (1998-present), Yamagawa (1998-2009) and Poker Flat (1998-2012).

Also the data sharing policy and an incentive for researchers and experts in charge of managing and producing data will be necessary subjects for further consideration. It will be necessary to discuss roles of functions of stakeholders including researchers, research institutions, scientific societies and the academic publishers (and their journal editorial policy). As for the incentives, the data citation by DOI has potential to be useful to evaluate and recognize data-producers' contribution, hopefully resulting in shedding light on inaccessible datasets. The study of the evaluation mechanism will need to be discussed at the associations or communities.

Open science is said to change the way of scientific research. In particular, it is important to aim for new concept and paradigm of research data management, preservation, sharing and re-use, as much as possible for each researcher, community, and in society. It is still at developing stage not only in Japan but also in Europe, America and other countries/regions who are interested in. We aim at making its progress based on experiments, consideration and investigation using our own observation datasets.

研究データをコミュニティや外部と共有することを通じて研究を加速する、という考え方が、いわゆるオープンサイエンスの議論の中で検討されている。例えば、内閣府では「さまざまな研究機関が持つ専門性の高い・知的価値の高いデータは科学研究の成果とみなす、また、社会での共有、利用に供されることが今後重要になる」といわれている（内閣府、「我が国におけるオープンサイエンス推進のあり方について」、2015など）。

データ共有をすすめるインセンティブの1つとして、データにも論文と同じようなデジタルオブジェクト識別子（Digital Object Identifier ; DOI）をつけ、データ利用時に引用することが検討されている（例えば、Force 11 Joint Declaration of Data Citation Principles, 2014, doi:10.25490/a97f-egyk）。DOI登録実験の第一号としては、NICTのアラスカ・ポーカーフラットMFレーダー（MFR）の中性風データにDOI（doi:10.17591/55838dbd6c0ad）が付与されており（ジャパンリンクセンター、「研究データへのDOI登録ガイドライン」、2015、doi:10.11502/rd_guideline_ja）、実際に論文引用されている（例えば、Kinoshita. et al, JGR, 2015, doi:10.1002/2014JD022647）。

このポーカーフラットMFレーダーのデータファイルは、オンプレミス（機関内サーバ上）で保管・管理されてきて、登録されたユーザーに対してFTPおよびHTTPで提供されてきた。一方で近年は、国立国会図書館WARP（Web Archive Project）事業で収集している公的機関Webアーカイブの一部として収蔵されたデータファイルに対してDOIを付与することで、研究機関と情報保管機関との役割をわけたデータ保管の試みもされている（木目沢・村山、2017、doi:10.18919/jkg.67.9_459）.

上記のことを考慮しながら、MFRの稚内、山川、ポーカーフラットのデータの公開実験を行うことで、具体的事例に基づく考察を進める。データを適切に保存、管理し、利用に供する将来の「研究データエコシステム」に有用な仕組みを検討し、長期間の、分野横断的な利活用を進めるためのコンセプトや手法、などの調査・検討に寄与していきたい。

具体的には、稚内（1998 年－現在）、山川（1998-2009 年）、ポーカーフラット（1998-2012 年）の期間の中間圏・下部熱圏の水平中性風のデータを対象として考えている。

また、今後の課題として、データ共有ポリシーを検討すること、データを作成・整備した研究者・担当者へのインセンティブとなりうる具体的な仕組みについての議論・考察を行うこと、が挙げられる。いずれも研究者・研究機関・ユーザーをふくめた科学コミュニティ・学協会や学術出版社・ジャーナル編集ポリシー等科学研究のステークホルダー全体の役割、機能に関連する議論が必要と考えられる。後者については、DOI を使ったデータ引用によって、データを作成・整備した者の活動評価につながる可能性がある。引用手法、引用情報の検索や評価の方法、実践のあり方などについては、科学コミュ二ティ・学協会での議論が今後必要となると考えられる。

オープンサイエンスは科学研究のあり方を変えると言われる。とくに専門的研究データの新しい取扱い、研究者やコミュニティ、社会の全体においてできるだけそれぞれがメリットのある方法を目指すことが重要である。現在は日本だけでなく、欧米でも試行錯誤・検討段階であり、本研究における自らが取得した観測データによる実験およびそれをもとにした考察が有益・有効であると考えている。

大気光イメージ観測による関東平野上空の山岳波動の研究

石井 智士 [1]; 鈴木 秀彦 [2]
[1] 明大・理工・物理; [2] 明治大

Study of Mountain waves above Kanto plain by airglow imaging

Satoshi Ishii[1]; Hidehiko Suzuki[2]
[1] Meiji Univ.; [2] Meiji univ.

Atmospheric gravity waves (AGWs) transport momentum from the lower atmosphere to the upper layer and drive the global circulation in the upper atmosphere. Major excitation sources of AGWs are local convective activities in the troposphere and local disturbances caused by interaction of mountain topography and tropospheric wind. Especially, topographical AGWs (mountain waves) are considered to be one of important factors giving local variabilities on middle atmospheric circulation.

We have observed OH airglow since Dec. 2015 in Kawasaki, Japan (35.613^{o}N,139.549^{o}E) to reveal the excitation and propagation processes of mountain waves. A mountain area including Mt. Fuji exists in the western side from the observation point which is sited in middle part of the Kanto plain. This would make easy to compare the observed results with simple model and would contribute to reveal the excitation and propagation processes of mountain waves. Although many mountain wave events were expected to be observed by the airglow imager, only five events which have no ground phase velocity (i.e. possible mountain wave events) had been observed during the period between Dec. 2015 and Dec. 2017. Moreover, it is shown that three of them are likely to be a ripple structure which is kind of an unstable structure or evanescent waves [Okuda, Master thesis, 2018]. Therefore, in order to improve the detection rate of mountain wave events, we have changed the objective lens of the imager to make its f.o.v. wider since May 2018. We also have developed an image processing procedure to extract mountain wave structures with small amplitude and various wavelengths from an airglow image.

In this presentation, we introduce the new analytical method to extract mountain waves from an airglow image. Mountain wave events during June to July 2018 newly identified by this new analysis method are reported and its excitation and propagation processes are discussed based on background atmospheric parameters.

大気重力波は下層大気から上層へ運動量を輸送し、超高層大気における地球規模の大気循環を駆動する。大気重力波の励起源としては、対流圏の活発な対流活動、山岳地形により大気が強制的に上昇させられることによって生じる局所的な擾乱によるものがある。特に地形性の大気重力波は励起源が地上に固定されているため、季節変動する下層大気の風速との関係で中層大気循環の強度に一定の規則を与える重要な因子の一つと考えられている。

そこで、本研究では山岳地形と下層の風の相互作用によって発生する、対地位相速度がゼロである山岳波の励起伝搬特性の解明を目指し、2015年12月より神奈川県川崎市にある明治大学生田キャンパス（35.613°N,139.549°E）においてイメージャーによるOH大気光のイメージング観測を継続している。この観測拠点においては、関東平野上空の大気重力波の振る舞いを観測することができるが、西部には富士山をはじめとした山岳地形があり、これらを励起源とする地形性の大気重力波（山岳波）が多数観測されることが期待される。山岳地域と平野部の対比が明瞭な観測拠点における山岳波の振る舞いに関する観測的な知見は、モデルとの比較が容易であり山岳地形と下層の風による山岳波の励起および伝搬過程の解明に貢献すると考えられる。しかし、2015年12月から2017年12月までの観測では、対地位相速度をもたない山岳波動であると考えられるイベントの検出は5例のみに留まっている。しかもそのうち3例については、背景大気の風速分布が鉛直伝搬条件を満たさないことや、その水平スケールと継続時間の特徴から不安定構造の一種であるリップル構造である可能性が高いことが示されている（奥田ほか、2017）。そこで、山岳波動の検出率を向上させるため、2018年5月よりイメージャーの対物レンズを交換し、観測視野を拡大した観測を継続している。これにより上空へ伝搬しやすい、より長波長の山岳波動を補足可能になると期待される。また、同時に長波長の山岳波動を抽出するための解析手法の開発を行った。山岳波は励起源が地上に固定されていて対地位相速度を持たず、空間構造が時間変動しない特徴があるため、その構造を明瞭にするためには、イメージデータを時間方向に積算すればよい。しかし、全視野と同程度のスケールの水平波長構造を検出しようとすると、単純に積算しただけでは大気光強度の天頂角依存性（van Rhijn効果）やカメラ感度の空間不均一性（フラット特性）などが突出してしまい、振幅の小さい大気波動をデータから発見することが困難になる。そこで、本研究では、フラット補正を慎重に行ったイメージデータより、強度が天頂角に依存する成分を除去し、大気波動による擾乱を大気光イメージデータから強調する手法を新たに開発した。

本発表では、更新されたイメージャーによるデータより長波長の山岳波動を抽出する解析手法の紹介を行うとともに、2018年6月から7月に検出された山岳波動イベントについて、背景大気パラメータとの比較によりその励起伝搬過程について考察した結果を報告する。

Neutral and plasma density perturbations in the top-/bottom-side ionosphere associated with MSTIDs

Shin Suzuki[1]; Jaeheung Park[2]; Yuichi Otsuka[3]; Kazuo Shiokawa[3]; Huixin Liu[4]; Hermann Luehr[5]
[1] Aichi Univ.; [2] GFZ; [3] ISEE, Nagoya Univ.; [4] None; [5] GeoForschungsZentrum Potsdam

Medium-scale traveling ionospheric disturbances (MSTIDs) are a well-known wavy structure in the F-region ionosphere. They typically have a horizontal wavelength of several hundred kilometers and a periodicity of about one hour. Although, the MSTIDs were considered to be caused by atmospheric gravity waves, recent studies have suggested that the generation of the MSTID in nighttime is highly associated with coupling processes between the E- and F-region electrodynamics. To confirm the different processes in the MSTID generation in daytime and nighttime, CHAMP satellite measurements would be greatly helpful; CHAMP plasma and neutral density data obtained in the day- and night-side sector can monitor the phase relations between the neutral (i.e., atmospheric gravity wave) and ionospheric plasma perturbations simultaneously at the top-side F-region (approximately 400 km).

As the first step in the abovementioned research, we compared the MSTID signatures between the CHAMP and ground-based 630-nm airglow measurements to validate the MSTID detection by CHAMP. Airglow imaging is a quite useful technique to investigate two-dimensional characteristics of the nighttime MSTIDs. Horizontal parameters of the MSTIDs (such as wavelengths, motions, and their spatial extent) can be estimated directly with a high spatial and temporal resolutions through the 630-nm airglow emission in the bottom-side F-region. Previous study by Park et al. [2009, JGR] made an investigation of spatial signatures regarding one MSTID event using airglow images along the CHAMP orbit. The Institute for Space-Earth Environmental Research, Nagoya University, have operated airglow imaging network, as the OMTI system, around the world since 2000; this network gives much more chance to make coordinated measurements with CHAMP.

In this presentation, we will report the statistics of conjugate MSTID measurements at mid-latitude Japanese stations (Rikubetsu: 44N, 144E, Shigaraki: 35N, 136E, and Sata: 31N, 131E) with CHAMP and the ground-based optical network in 2005-2008.

電離圏擾乱時における電離圏鉛直2次元構造の観測ロケット実験

芦原 佑樹 [1]; 山本 衛 [2]; 石坂 圭吾 [3]; 熊本 篤志 [4]; 白澤 秀剛 [5]; 阿部 琢美 [6]
[1] 奈良高専・電気; [2] 京大・生存圏研; [3] 富山県大・工; [4] 東北大・理・地球物理; [5] 東海大・情報教育センター; [6] ＪＡＸＡ宇宙科学研究所

Sounding rocket experiment of the vertical 2-D electron density profile in ionosphere

Yuki Ashihara[1]; Mamoru Yamamoto[2]; Keigo Ishisaka[3]; Atsushi Kumamoto[4]; Hidetaka Shirasawa[5]; Takumi Abe[6]
[1] Elec. Eng., NIT Nara; [2] RISH, Kyoto Univ.; [3] Toyama Pref. Univ.; [4] Dept. Geophys, Tohoku Univ.; [5] ICT Edu. Center, Tokai Univ.; [6] ISAS/JAXA

Various sounding rocket experiments has carried out for ionosphric observation before. In situ observation is most effective, e.g., the Langmuir probe is the most popular method to measure electron densities by sounding rocket. However, because it is in situ observation, it can not observe the spatial structure of electron densities in the ionosphere.

For observing the vertical 2-D electron density profile, we have proposed Rocket GPS-TEC Tomography method(GPS), which applies tomography analysis on the TEC values observed by rocket observation. We have been planning an sounding rocket experiment by using GPS, Dual Band Beacon(DBB), LF/MF Receiver(LMR), Ne (electron number density) measurement by Impedance probe(NEI), Sun Acquisition Sensor/Horizon Sensor(SAS/HOS). In this paper, we deliver the progress status of the experiment preparation.

これまで電離圏観測を目的した観測ロケット実験が種々行われている。観測ロケット実験における電子密度測定手法としては、ラングミュアプローブやインピーダンスプローブを用いたプローブ法を用いることが多い。プローブ法は精密な観測ができるが、その場観測であるために観測ロケット周辺の電子密度空間構造はわからない。一方で、中緯度電離圏における沿磁力線不規則構造 (Field-Aligned Irregularity: FAI) や中規模伝搬性電離圏擾乱（Middle-Scale Traveling Ionospheric Disturbance: MSTID）等の電離圏擾乱現象を把握するためには、電子密度の空間構造観測が必要となる。

観測ロケットによる電離圏空間構造の観測手法として、ロケット GPS-TEC 観測を提案する。本手法では、観測ロケット機上で観測した GPS-TEC データをトモグラフィ解析することで、電離圏の空間構造を推定する。我々は、新規開発するロケット GPS-TEC 観測（GPS）に加えて、2 周波数ビーコン観測（DBB）、長中波帯電波観測（LMR）、インピーダンスプローブ（NEI）、太陽・地平線センサ（SAS・HOS）を用いた観測ロケット実験を計画しており、準備状況について報告する。

Study of the characteristics of growth of Nighttime-MSTID in mid-latitude observed by GNSS

Takafumi Ikeda[1]; Akinori Saito[1]; Takuya Tsugawa[2]; Hiroyuki Shinagawa[2]
[1] Dept. of Geophysics, Kyoto Univ.; [2] NICT

We think two mechanism, E-F coupling and Perkins Instability, will relate to growth for nighttime-MSTID in mid-latitude [Tsunoda and Cosgrove., 2001 ; Perkins., 1973]. Linear growth rate of perturbation intensity of Pedersen conductivity expected from E-F coupling is around 15 minutes [Yokoyama et al., 2009], which is far shorter than one expected from Perkins Instability [Fukao and Kelley, 1991 ; Miller et al., 1997 ; Shiokawa et al., 2003]. However, Es layer's spatial and temporal scale is less than 100km and 15min [Maeda et al., 2013 ; S.Saito et al., 2007]. They are different from MSTID's ones, which are 200-400 km and around 2hours [Otsuka et al., 2011]. To decide which instability is responsible for growth of nighttime MSTID, the growth rate of MSTID was observationally determined with ground-based GPS network data.

We analyzed the statistical characteristics of nighttime MSTID in mid-latitude at 2014 observed by GNSS. We applied two-space and time spectral analysis to calculate MSTID's growth rates. We compared growth rate observed with linear growth rate of Perkins Instability for two method. We calculated latter using by ion temperature, neutral wind velocity, electric field and O mass density of GAIA model [Jin et al., 2008] and magnetic field of IGRF model. First, we compared maximum growth rate observed in one day with maximum growth rate of Perkins model in one day. Observed maximum growth rate was 0.13-8.7 $*10^{-4}s^{-1}$, which was similar to maximum linear growth rate of Perkins instability. Second, we compared observed growth rate with one of Perkins instability about seasonal dependence in 2014. Observed growth rate was 1.0-6.0 $*10^{-4}s^{-1}$ during 1800LT-0600LT in summer (May-Jun-Jul-Aug). In winter (Nov-Dec-Jan-Feb) growth rate was 1.0-6.0 $*10^{-4}s^{-1}$ during 1800LT-2400LT, after than growth rate was less than 1.0 $*10^{-4}s^{-1}$. Linear growth rate of Perkins instability was larger in summer. Observed growth rate in summer was not related to Es layer intensity [Ogawa et al., 2002] observed by Ionozonde at Kokubunji. Linear growth rate of Perkins Instability is decided to F-region neutral wind, so nighttime MSTID's growth in mid-latitude would be decided by Perkins Instability and F-region neutral wind, not E-F coupling.

ISS-IMAP/VISI観測による中間圏大気重力波の活動度とプラズマバブル発生との関係性について

岡田 凌太 [1]; 齊藤 昭則 [2]; 池田 孝文 [2]; 品川 裕之 [3]; 津川 卓也 [3]; 坂野井 健 [4]
[1] 京大・理・地球惑星; [2] 京都大・理・地球物理; [3] 情報通信研究機構; [4] 東北大・理

Relationship between mesospheric gravity wave activities observed by ISS-IMAP and occurrence of equatorial plasma bubbles

Ryota Okada[1]; Akinori Saito[2]; Takafumi Ikeda[2]; Hiroyuki Shinagawa[3]; Takuya Tsugawa[3]; Takeshi Sakanoi[4]
[1] Earth and Planetary, Kyoto Univ.; [2] Dept. of Geophysics, Kyoto Univ.; [3] NICT; [4] Grad. School of Science, Tohoku Univ.

In this study we investigate relation between occurrence of equatorial plasma bubbles observed by GPS-Total electron content (TEC) data ,linear growth rate of the Rayleigh-Taylor instability in the ionosphere obtained with GAIA and mesospheric gravity wave activities observed by ISS-IMAP/VISI.

赤道電離圏において電子密度が大きく減少した領域が観測されることがある。この領域のことをプラズマバブルと呼ぶ。電離圏底部の微小擾乱がレイリー・テイラー不安定性によって成長するという発達機構が考えられている。先行研究からはこの微小擾乱としては中規模（~600km）の大気重力波が有力視されている。大気重力波の発生には経度や季節による変動が予想されており、また数日程度の短周期の変動があると考えられている。そのような大気重力波の変動が、プラズマバブルの発生においてレイリー・テイラー不安定性の成長率だけでは説明できない変動の原因となっていると考えられる。大気重力波の経度による変動としては、Ionosphere, Mesosphere, upper Atmosphere and Plasmasphere mapping mission from the ISS の Visible and near Infrared Spectral Imager(ISS-IMAP/VISI) の 762nm 大気光データを用いて同心円上大気重力波の分布を示した先行研究によりアフリカ西部地域の方が東部地域よりも同心円上重力波が多く見られることが報告されており、近接する地域でも発生が大きく異なることが知られている。

そこで GPS-Total Electron Content（TEC）データから算出した Rate of TEC Index (ROTI) によりアフリカ磁気赤道帯での東西それぞれの観測点におけるプラズマバブルの発生率を月ごとに解析した。その結果以下のような特徴が見られた。プラズマバブルの発生率はアフリカ西側の方が東側よりも全体的に高い。10月～3月の時期には西側、5月～8月の時期には東側での発生率の方が高くなる傾向が見られた。プラズマバブルの発生率は春分秋分に高く、夏至冬至に低い。それぞれの地域での発生率のピークの時期は西側で２、３月と10、11月、東側で３、４月と８、９月に見られた。先行研究のプラズマバブル発生率の季節・経度依存性にもこれらと似たような傾向が見られた。西側の発生率のピークは季節による違いはあまり見られなかったが、東側の発生率のピークは８、９月の方が３、４月に比べて大幅に低い傾向が見られた。この結果は先行研究のプラズマバブル発生率の季節・経度依存性には見られない傾向である。これらの GPS-TEC データによるプラズマバブル発生の様子と大気圏・電離圏統合モデル GAIA の結果から算出して得られたレイリー・テイラー不安定性の線形成長率との関係性に ISS-IMAP/VISI の 762nm 大気光データから得られる高度約 95km の大気重力波の様子がどのように関わるのかについて調べた結果を報告する。

石垣島で取得された630.0 nm大気光観測データを用いたプラズマバブルの形状解析

高見 晃平 [1]; 細川 敬祐 [2]; 斎藤 享 [3]; 小川 泰信 [4]; 塩川 和夫 [5]; 大塚 雄一 [5]
[1] 電通大; [2] 電通大; [3] 電子航法研; [4] 極地研; [5] 名大宇地研

Estimating the shape of plasma bubbles by using 630.0 nm airglow observations in Ishigaki

Kohei Takami[1]; Keisuke Hosokawa[2]; Susumu Saito[3]; Yasunobu Ogawa[4]; Kazuo Shiokawa[5]; Yuichi Otsuka[5]
[1] none; [2] UEC; [3] ENRI, MPAT; [4] NIPR; [5] ISEE, Nagoya Univ.

Plasma bubbles are regions in the nighttime equatorial F-region ionosphere where the electron density is significantly depleted. Plasma bubbles are known to affect the accuracy/stability of GNSS (Global Navigation Satellite Systems) because the steep gradient and small-scale irregularities within or in the vicinity of bubbles can disturb GNSS signals propagating through the ionosphere. Plasma bubbles usually evolve along geomagnetic meridian and change their shape during the eastward motion. The changes in the shape of plasma bubbles are closely related to the background neutral winds and ionospheric conductivity. However, there has been no definite conclusion on how bubbles change their shape during the propagation. In this study, we analyze the shape of plasma bubbles by using 630.0 nm airglow observations and discuss their temporal evolution.

In this study, we make use of the Optical Mesosphere Thermosphere Imagers (OMTIs) and the WATEC imager both which have been operated in Ishigaki (24.4 deg N, 124.1 deg E) station. The exposure time and optical filter of OMTIs are severally 160 s and 630.0 nm, respectively. The WATEC imager consists of a small camera (WAT-910HX), a fisheye lens and an optical filter for the 630.0 nm airglow. Both the exposure time and temporal resolution of the measurement is 4 s. One of the problems of the WATEC imager is its low S/N ratio due to thermal noises because the CCD of the camera is not cooled. To minimize this effect, we removed the thermal noises by integrating its raw images for 2 minutes.

We have detected plasma bubbles on 63 nights from March 26, 2014 to December 25, 2016. On March 13, 2015, we detected plasma bubbles changing their shape when their eastward moving velocity gradually decreased. The eastward drift velocity estimated, with an assumed emission altitude of 250 km, changed from 93 m/s to 49 m/s at 17 deg geographic latitude, and from 103 m/s to 49 m/s at 20 deg geographic latitude. Besides, the offset angle between the bubble and the geomagnetic meridian changed from -5 to 5 degrees. In the presentation, we demonstrate the eastward drift velocity and the shape of 63 bubble cases and compare them with models of neutral wind. In addition, we discuss the shape of plasma bubbles extracted by using Sobel filter and Histogram of Oriented Gradient (HOG) method.

赤道電離圏において、F 領域の電子密度が局所的に大きく減少した領域が観測されることがある。この領域のことをプラズマバブルと呼ぶ。プラズマバブルは、周囲との間に極端に大きな電離圏全電子数の勾配と小規模不規則構造を作り出すため GPS 測位の精度や安定性に影響を及ぼすことが知られている。プラズマバブルは通常磁力線に沿った形状で発達し東向きに移動する過程で、形状が変化する。プラズマバブルの形状の変化は中性風や電気伝導度に起因すると考えられているが、明確な研究結果は報告されていない。本研究では大気光イメージャを用いた長期間のプラズマバブルの観測による形状解析を行い、プラズマバブルの形状の時間変化について考察を行う。

本研究で用いる観測機器は石垣島 (24.4 N, 124.1 E) に設置されている OMTIs(Optical Mesosphere Thermosphere Imagers)、及び WATEC イメージャである。OMTIs は、露光時間 160 秒、透過中心波長 630 nm の光学フィルターを用いた大気光観測を行っている。WATEC イメージャは、中心波長 632 nm、半値幅 10 nm の光学フィルターを用い、約 4 秒の露光時間 (時間分解能も同じ) で、同じく 630.0 nm 大気光を観測している。WATEC イメージャでは非冷却 CCD を用いており、画像に熱雑音ノイズが多く含まれる。プラズマバブルを観測する際の障害となるノイズを軽減するため、4 秒の原画像を 2 分間にわたって積分したデータを使用した。

2014 年 3 月 26 日- 2016 年 12 月 25 日の期間の 63 晩においてプラズマバブルが観測された。2015 年 3 月 15 日には、プラズマバブルの東向きの移動速度が徐々に遅くなり、バブルの形状にも変化が見られた。その事例について解析したところ、発光高度を 250 km と仮定した場合、12 UT から 16 UT の間で地理緯度 17 度では 93 m/s から 49 m/s、地理緯度 22 度では 103 m/s から 49 m/s まで速度が減少していることが分かった。また、磁気子午線とバブルの延伸方向の間の角度は (時計回りを正とした場合) -5 度から 5 度に変化していた。発表ではプラズマバブルが観測された全 63 晩について速度及び形状解析を行い、モデルを用いた中性風の速度と比較を行う。形状解析については Sobel Filter を用いたエッジ検出、HOG(Histogram of Oriented Gradient) を用いた特徴量抽出によって得た結果を報告する。

Plasma blobs and bubbles concurrently observed by muti-instruments in low latitude ionosphere in the Asian-Oceanian sector

Zheng Wang[1]; Huixin Liu[2]
[1] Atmos.,Kyushu University; [2] None

With simultaneous ionospheric observation data from ROCSAT-1 Satellite and ionosondes, three cases of concurrent plasma blobs and bubbles were observed around 22:30 in the same magnetic meridian at low latitude in Asian-Oceanian sector. Plasma blobs insitu-observed were near 600 km height, above the ESFs observed by ionosondes. Scintillations were also observed near the same magnetic meridian. Considering that both plasma bubbles and blobs are field-aligned elongated structures, these concurrent detections of plasma blobs and bubbles provide direct observational evidence for the proposed blob formation in the intermediate stage of plasma bubble generation.

A network of low-cost airglow imaging system for monitoring plasma bubble in wide area

Keisuke Hosokawa[1]; Susumu Saito[2]; Yasunobu Ogawa[3]; Mamoru Ishii[4]; Yuichi Otsuka[5]; Takuya Tsugawa[4]; Chia-Hung Chen[6]
[1] UEC; [2] ENRI, MPAT; [3] NIPR; [4] NICT; [5] ISEE, Nagoya Univ.; [6] Earth Science, NCKU

Plasma bubbles are regions in the nighttime equatorial F-region ionosphere where the plasma density is significantly depleted. Plasma bubbles affect the accuracy of GPS positioning since they have a steep gradient in the electron density in the F region and can disturb GPS signals propagating through the ionosphere. 630.0 nm airglow observations with ground-based all-sky imagers have been used for imaging the two-dimensional structures of plasma bubbles in the last two decades. However, such systems tend to be expensive and not easy to handle; thus, it has been difficult to visualize the large-scale structure of plasma bubbles by setting up multiple imagers at different stations. For this purpose, we recently developed a low-cost airglow imager which consists of a small camera (WAT-910HX), fisheye lens and optical filter. We then evaluated the feasibility of observations of plasma bubbles by using the low-cost airglow imager and confirmed its capability for imaging the spatial structure of plasma bubble. Following this result, we started deploying the system at low and equatorial latitude regions since 2017. As of August 2018, we have installed the Low-Cost Airglow imaging System (LCAS) into four stations: Ogimi and Ishigaki both in Okinawa, Tainan, and Chumphon within a framework of international collaboration and data sharing. In the presentation, we present the overview of the system and share the current status of the project.

GPS電波掩蔽観測を用いた地震に伴う電離圏擾乱の高度分布解析

井上 雄太 [1]; 中田 裕之 [2]; 大矢 浩代 [3]; 鷹野 敏明 [4]
[1] 千葉大・融合理工; [2] 千葉大・工・電気; [3] 千葉大・工・電気; [4] 千葉大・工

Examination of vertical distributions of coseismic ionospheric disturbances using GPS occultation observation

Yuta Inoue[1]; Hiroyuki Nakata[2]; Hiroyo Ohya[3]; Toshiaki Takano[4]
[1] Grad. School of Sci. and Eng., Chiba Univ.; [2] Grad. School of Eng., Chiba Univ.; [3] Engineering, Chiba Univ.; [4] Chiba Univ.

It is reported that ionospheric disturbances are caused by large earthquakes. One of the causes is the infrasound wave excited by surface waves propagated on the ground from the epicenter. The characteristics of horizontal propagation of the ionospheric disturbances after large earthquake have been examined by using a network of ground-based GPS receivers. On the other hand, the vertical propagation of coseismic ionospheric disturbances are rarely reported.

In this study, to examine the vertical propagation of the ionospheric disturbances, we have examined electron density profiles observed by GPS radio occultation measurements of FORMOSAT-3/COSMIC satellites.

We analyzed the density profile data in association with Tohoku Earthquake (M9.0) occurred at 5:46:18 on 11th March 2011 (UTC). The density profiles located within 30 degrees both of latitude and longitude one hour of the earthquakes were used.

The fluctuation of the density profile is determined by the difference of the observed profile and the Chapman layer model fitted to the observed profile. Then, long period fluctuation which seems to be caused by the earthquake over altitude 200 km to 400 km was obtained. From propagation velocity and propagation time of the perturbations from the epicenter to the observation point, it is confirmed that the disturbances are occurred due to the earthquake.

大規模な地震発生により，電離圏擾乱が発生することが報告されている。これは，地面変動や津波により生じた音波や大気重力波が電離圏高度まで伝搬するためである。地震発生後の電離圏擾乱の水平方向の伝搬特性は，GPS-TEC観測などを用いて明らかにされつつあるが，鉛直方向の伝搬特性を捉えた例は少ない。そこで，本研究では，地震に伴う電離圏擾乱の変動について，特に高度方向の分布に注目し，FORMOSAT-3/COSMIC衛星によるGPS電波掩蔽観測で得られる電子密度の高度プロファイルデータの解析を行った。

2011年3月11日5時46分18秒（UTC）に東北沖で発生したM9.0の東北地方太平洋沖地震を解析対象とし，震央を中心として緯度経度幅30度以内の地震発生後約1時間までに取得されたデータを抽出し，解析を行った。

観測された変動成分を詳しく解析するため，解析された高度分布をチャップマンモデルを用いてフィッテングし，それらのずれを変動成分として抽出した結果，高度200 km～400 kmにわたって地震による変動と思われる長周期（波長50km）の変動を確認した。震央から観測点までの距離から伝搬速度と伝搬時間を求めたところ，これらの変動は地震による変動であると考えられる。

LF 帯標準電波観測と GPS-TEC により観測された電離圏変動の相関

町 康二郎 [1]; 中田 裕之 [2]; 大矢 浩代 [3]; 鷹野 敏明 [4]; 西岡 未知 [5]; 津川 卓也 [5]
[1] 千葉大・融合理工; [2] 千葉大・工・電気; [3] 千葉大・工・電気; [4] 千葉大・工; [5] 情報通信研究機構

The relationship between the ionospheric variation observerd by Low Frequency Standard-time and GPS-TEC

Kojiro Machi[1]; Hiroyuki Nakata[2]; Hiroyo Ohya[3]; Toshiaki Takano[4]; Michi Nishioka[5]; Takuya Tsugawa[5]
[1] Grad. School of Sci. and Eng., Chiba Univ.; [2] Grad. School of Eng., Chiba Univ.; [3] Engineering, Chiba Univ.; [4] Chiba Univ.; [5] NICT

Low Frequency (LF) radio waves are reflected in the lower ionosphere. The phases of the received LF radio wave vary with the length of ray path when the reflection height moves vertically. Therefore, the height variation of the ionosphere is observed by the variation of the phase of received LF radio wave. Since the LF observation is one of the useful methods for the observation of the lower ionosphere, it is expected that it supplies important data for examining the lower ionosphere. This study examines the characteristics of the phase change of the LF Standard-time. The observation target is the standard radio wave of 60 kHz, which are transmitted from Hagane-yama station. The radio waves are observed by crossed loop antenna at Sugadaira, Nagano Prefecture.

In sunrise and sunset time, it is expected that the phase of the sky wave varies as the height of ionosphere varies. Therefore, the sky wave was separated using the polar coordinate representation of the received radio wave. The variation of the ionospheric height was estimated from the phase variation of the sky wave.

In this study, we analyzed the height variation of the ionosphere observed by LF obserbation and detected the fluctuation whose frequency is about 0.4 mHz. This frequency corresponds to that of TID. Using the wavehop method by the ITR-U model, the LF wave is considered to propagate from Mt.Hagane to Sugadaira with a single reflection at the ionosphere. We examined the TEC variation in the mid-point between Mt.Hagane and Sugadaira, and found the TEC variation with a same frequency as the fluctuation of LF waves. Therefore, there is a relationship of ionospheric fluctuation between the lower ionosphere and the F-region which affects the variation of GPS-TEC.

LF 帯電波は下部電離圏で反射する。電離圏擾乱によって電離圏高度が変化すると電波の反射高度が変動し, 電波の伝搬経路長が変化する。この時, 受信される電波の位相も変化するため, LF 帯電波の位相変動を観測することで電離圏高度の変動を観測することができる。下部電離圏を観測する方法は極めて少なく, LF 帯電波観測は有用な観測法の 1 つであり, 下部電離圏を研究する上で重要なデータを提供することが期待される。そこで本研究では LF 帯電波の位相変化を用いて LF 帯電波の電離圏における反射高度変化を観測し, 低高度電離圏の高度変動の導出を行なった。観測対象は 60 kHz の標準電波で, 送信点は佐賀県と福岡県の県境のはがね山である。 本研究では, 長野県上田市菅平高原に Crossed Loop Antenna を設置し, 観測を行った。

送受信点間の距離約 880 km であることから, 送信点から地表付近を伝搬し, 直接アンテナに到達する地表波と, 電離圏で反射して到来する空間波の両方が受信される。そこで, 日の出, 日の入付近では電離圏高度分布が大きく変化することから, 地表波と空間波の両方を含む受信波の日の出, 日の入のデータを極座標表示することで空間波を分離した。

空間波の位相変化より, 2016 年 6 月 23 日 の昼間の時間帯では, 0.4 mHz ほどの周期の波が観測された。この周期は TID に相当するものである。ITR-U モデルによる波線法の結果より, はがね山 - 菅平での観測は, 1 回反射で伝搬していることが考えられる。はがね山 - 菅平の中点での TEC 変動においても LF 観測と同様の周期の波が確認できた。LF 帯電波の反射する低高度電離圏と GPS-TEC 変動の影響が大きい F 領域で同様の変動が発生していることがわかる。

火山噴火後のLF/VLF帯標準電波強度変動

丸山 慶 [1]; 大矢 浩代 [2]; 土屋 史紀 [3]; 山下 幸三 [4]; 高橋 幸弘 [5]; 中田 裕之 [6]; 鷹野 敏明 [7]
[1] 千葉大・工・電気電子; [2] 千葉大・工・電気; [3] 東北大・理・惑星プラズマ大気; [4] 足利大・工学部; [5] 北大・理・宇宙; [6] 千葉大・工・電気; [7] 千葉大・工

Variations in intensity of LF/VLF standard radio waves after volcanic eruptions

Kei Maruyama[1]; Hiroyo Ohya[2]; Fuminori Tsuchiya[3]; Kozo Yamashita[4]; Yukihiro Takahashi[5]; Hiroyuki Nakata[6]; Toshiaki Takano[7]
[1] Electrical and Electronic, Chiba Univ.; [2] Engineering, Chiba Univ.; [3] Planet. Plasma Atmos. Res. Cent., Tohoku Univ.; [4] Engineering, Ashikaga Univ.; [5] Cosmosciences, Hokkaido Univ.; [6] Grad. School of Eng., Chiba Univ.; [7] Chiba Univ.

Several studies for the F-region ionosphere associated with volcanic eruptions based on GPS-TEC data have been reported so far (e.g., Heki, 2006; Dautermann et al., 2009; Heki et al., 2010). These studies reported that acoustic waves excited by volcanic eruptions reached up to the F-region height, and caused F-region disturbances. However, little studies on the D-region ionosphere associated with volcanic eruptions have been reported. In this study, we investigate the D-region variations after eruptions of Sakurajima (31.59N, 130.66E) and Shin-moedake volcanos (31.91N, 130.89E), Japan, and Kelud volcano (7.93S, 112.31E), Indonesia, using intensity and phase of low frequency (LF) and very low frequency (VLF) transmitter signals. The LF and VLF propagation paths are JJY 60 kHz - Tainan (TNN, Taiwan), BPC (68.5 kHz) – TNN, and NWC (19.8 kHz) – Pontianak, Indonesia. The Sakurajima volcanic eruptions occurred at 04:11 UT on 6 June, 2014. Based on wavelet spectra, the both LF intensities had a period of 3-5 minutes during 04:12-04:20 UT after the eruptions. We compared the LF intensities with atmospheric pressure data obtained by an infrasonic meter observed by Sakurajima Volcano Research Center, Kyoto University, and seismic waves in the NIED F-net data (FUK, STM, and SBR) located close to the Sakurajima volcano. The atmospheric pressure had the similar period of 3-5 min during 04:18-04:42 UT. The vertical velocity of the seismic waves had a period of 2-5 min during 04:12-04:47 UT. The similar period of the LF intensities, atmospheric pressure, and seismic waves could be caused by acoustic resonance between the Earth surface and lower thermosphere. In the presentation, we will also show variations in the LF/VLF signals after the Shin-moedake and Kelud volcanic eruptions in detail.

これまで火山噴火発生後のF領域電離圏に関する研究は、GPS-TECによるTEC変動などで報告されている (e.g., Heki, 2006; Dautermann et al., 2009; Heki et al., 2010)。これらの研究では火山噴火によって生じた音波がF領域電離圏まで到達し、F領域電離圏の変動を生じさせていることを示す。しかし、火山噴火に関連するD領域電離圏の変動についての研究はほとんどない。そこで、本研究ではLF/VLF帯標準電波の強度および位相データを用いて、桜島 (31.59N, 130.66E)、新燃岳 (31.91N, 130.89E)、およびケルート山 (7.93S, 112.31E) 噴火後のD領域電離圏変動を調べる。LF/VLF伝搬パスは、JJY-60kHz-台南 (TNN)、中国 (BPC-68.5kHz)-TNN、および NWC (19.8 kHz)-ポンティアナ（インドネシア）である。桜島の噴火は、2014年6月6日 04:11 UTに発生した。ウェーブレット解析の結果、4:12-4:20UTにかけてJJY60kHz-TNNおよびBPC-TNNパスのLF波の強度に3-5分の周期成分が検出された。京都大学防災研究所付属火山活動センター桜島火山観測所が観測する桜島の空振計による地表の気圧変化、防災科学技術研究所による広帯域地震観測網 (F-net) による地震計の上下動速度の観測データと比較したところ、空振計では4:18-4:42UTにかけて3-5分、地震計では4:12-4:47UTにかけて2-5分の周期が見られた。LF波強度、地表の気圧および地震波に見られたこれらの似た周期は、地表―下部熱圏間の音波の共鳴によるものである可能性がある。発表では、新燃岳およびケルート山噴火後のLF/VLF帯標準電波の変動についても報告する。

桜島噴火の規模とGPS-TEC変動との相関

庄子 聖人 [1]; 中田 裕之 [2]; 大矢 浩代 [3]; 鷹野 敏明 [4]; 津川 卓也 [5]; 西岡 未知 [5]
[1] 千葉大・工・電気電子; [2] 千葉大・工・電気; [3] 千葉大・工・電気; [4] 千葉大・工; [5] 情報通信研究機構

Relationship between the magnitude of Sakurajima eruptions and the disturbance of GPS-TEC

Kiyoto Shoji[1]; Hiroyuki Nakata[2]; Hiroyo Ohya[3]; Toshiaki Takano[4]; Takuya Tsugawa[5]; Michi Nishioka[5]
[1] Electrical and Electronic, Engineering, Chiba Univ; [2] Grad. School of Eng., Chiba Univ.; [3] Engineering, Chiba Univ.; [4] Chiba Univ.; [5] NICT

It is reported that ionospheric disturbances are caused by ground and atmospheric perturbations, e.g. earthquakes, typhoons and volcanic eruptions. Even though the volcanic eruptions excite the atmospheric waves, there little reports of ionospheric disturbances caused by volcanic eruptions. Therefore, in this study, we analyzed the ionospheric disturbances caused by volcanic eruption using GPS - TEC (Total Electron Content).

We analyzed TEC data observed in GNSS Earth Observation Network (GEONET) which is maintained by Geospatial Information Authority of Japan. In this study, we assumed that the ionospheric pierce point IPP is located at the altitude of 300 km. The 30-second TEC data used in this study is obtained in 1200 points of GEONET. The mask angle is 30 degrees. In this study, we analyzed three events which are Sakurajima eruptions at 7:45 UT on Oct.-3-2009, 1:07 UT on Sep.-19-2012 and 20:25 UT on Dec.-9-2012. The magnitudes of the eruptions are estimated by the infrasound meter located at Higash-Korimoto.

The TEC disturbances are larger as the large, fluctuations are observed by the infrasound meter.

It is expected that the TEC disturbance is inversely correlated with the distance from the crater as the energy of the atmospheric wave decays according to the distance from the crater. Therefore, we examined the relationship between TEC disturbances and distance of IPP from the crater. As a result, there was an inverse correlation with the distance in one events out of three events. However, no correlation was found in the other two events. This may be due to the direction of the magnetic field and the wave normal of the disturbance according to the GPS satellite-receiver. In order to eliminate these effect, we calculated the coupling coefficients using the directions of the atmospheric wave from the calculational results of the acoustic ray tracing and the magnetic field data determined by the IGRF-12 model.

An inverse correlation between TEC disturbances and the distance from the crater was appeared in two events.

From the above results, it was confirmed that when the influence of the magnetic field and the deviation peculiar to the observation method are fixed, the TEC disturbances associated with the eruptions have

inverse correlations with the distance from the crater.

地震や台風、火山噴火などの下層の現象に伴い、大気波動が生じ、これによって電離圏擾乱が引き起こされることが知られている。火山噴火に伴い、大気波動が生じることは知られているが，火山噴火に伴う電離圏擾乱の観測事例はそれほど多くない。そこで本研究では、火山噴火に伴う電離圏の変動について、GPS-TEC(Total Electron Content) を用いて解析を行った。

本研究では、国土地理院の GNSS 連続観測システム (GNSS Earth Observation Network : GEONET) より導出されたデータを使用した。また、電離圏貫通点は 300km と仮定した。解析に用いたデータは、GEONET の受信点 1200 点、衛星仰角 30 度以上の 30 秒値である。解析対象は 2009 年 10 月 3 日 7 時 45 分 (UT)、2012 年 9 月 19 日 1 時 7 分 (UT)、2012 年 12 月 9 日 20 時 25 分 (UT) に桜島で発生した火山噴火 3 事例である。噴火の規模は東郡元における空振計データにより評価した。

それぞれの事例において TEC 変動を抽出したところ、空振計の圧力変動が大きいほど、TEC 変動が大きい事例が多かった。

エネルギーが火口からの距離応じて減衰していくため電離圏の変動が火口からの距離と逆相関関係を取ると考えられる。そのため、TEC 変動と貫通点の火口からの距離との相関を求めた。その結果、3 事例中 1 事例で距離との逆相関関係はみられたが、2 事例は相関関係がみられず、かつ全事例で火口に近い貫通点における電離圏の変動が距離との逆相関関係から外れたデータとなった。これは TEC 変動に対する磁場の影響と変動の波面と衛星－受信機の視線方向とが直角でないことによるものであると考えられる。これらの影響を取り除くために音波レイトレーシングのデータと IGRF-12 モデルより算出した磁場データより係数を算出し補正行った。

補正したデータから相関係数を求めたところ、3 事例中 2 事例で TEC 変動と火口からの距離との強い逆相関関係が確認された。

以上の結果より、磁場の影響と観測法特有のずれを補正した場合、火山噴火の規模が大きいほど TEC 変動は大きくなり、また距離と逆相関関係を持つと考えられる。

HFドップラー及びGPS-TECを用いた異なる高度での地震に伴う電離圏擾乱の解析

大野 夏樹 [1]; 中田 裕之 [2]; 大矢 浩代 [3]; 鷹野 敏明 [4]; 冨澤 一郎 [5]; 細川 敬祐 [6]; 津川 卓也 [7]; 西岡 未知 [7]
[1] 千葉大・工・電気電子; [2] 千葉大・工・電気; [3] 千葉大・工・電気; [4] 千葉大・工; [5] 電通大・宇宙電磁環境; [6] 電通大; [7] 情報通信研究機構

Examination of ionospheric disturbances at different altitudes associated with earthquakes using HF Doppler and GPS-TEC

Natsuki Ono[1]; Hiroyuki Nakata[2]; Hiroyo Ohya[3]; Toshiaki Takano[4]; Ichiro Tomizawa[5]; Keisuke Hosokawa[6]; Takuya Tsugawa[7]; Michi Nishioka[7]
[1] Electrical and Electronic, Chiba Univ.; [2] Grad. School of Eng., Chiba Univ.; [3] Engineering, Chiba Univ.; [4] Chiba Univ.; [5] SSRE, Univ. Electro-Comm.; [6] UEC; [7] NICT

Many studies have reported that ionospheric disturbances occur after giant earthquakes. One of the causes is the infrasound wave excited by ground motions.The infrasound wave can produce perturbations of electron density in the ionosphere. Such perturbations were detected by a network of ground-based GPS receivers. The TEC perturbations shown in GPS-TEC those of horizontally propagation in ionosphere from the epicenter. However, characteristics of vertical propagation of infrasound were rarely reported.

In this study, the coseismic ionospheric disturbances in the different altitudes are examined using HF Doppler and GPS-TEC. The HF Doppler sounding system is operated by the University of Electro-Communications and enable to observe the vertical speed of the ionosphere in the different altitudes.

We analyzed earthquakes whose magnitudes are larger than M 6.5 occurred in Japan since 2003. In the 2011 Tohoku earthquake (M 9.0), Sugadaira and Kiso observatories fluctuations in the Doppler shift with a period of 3 to 4 minutes in 8.006, 9.595 MHz. We confirmed these fluctuations due to the earthquake by using the ground velocity data observed by the seismograph around the HFD observation point.

Among the earthquakes, only in one case the Doppler shift fluctuation with the period of 3 to 4 minutes has been confirmed. We will report the results for further analysis.

多くの研究により，大規模な地震の発生後に電離圏において擾乱が起こることが報告されている．これは，地面変動や津波により生じた音波や大気重力波が電離圏高度まで伝搬するためである．地震発生後の電離圏中での水平方向の伝搬特性については，GPS 観測などを用いて明らかにされつつあるが，鉛直方向の伝搬を捉えた例は多くない．電気通信大学の運営する HF ドップラー (HFD) では， 異なる送信周波数 (5.006，6.055，8.006，9.595 MHz) の電波を用いることで複数の高度での変動を観測することが可能である．国土地理院の GNSS 連続観測システム (GNSS Earth Observation Network : GEONET) により導出される GPS-TEC のデータと合わせて，地震に伴う電離圏擾乱の変動について高度方向の変化に注目し, 解析を行った.

2003 年以降に日本列島近辺で起きた M6.5 以上の地震を研究対象とし解析を行ったところ，2011 年 3 月 11 日に発生した M9.0 の東北地方太平洋沖地震において，菅平，木曽受信点の両データ (8.006，9.595 MHz) に周期約 3〜4 分のドップラーシフトの変動が確認された．得られた観測データと HFD 観測点直下付近の地震計により観測された地面変動速度データから，これらが地震による変動であることを確認した.

解析対象とした地震の中でも周期約 3〜4 分のドップラーシフトの変動が確認されたのは 1 事例だけである．この変動について，他の受信点の HFD データと GPS-TEC データを用いて比較・解析を行っており，発表ではその結果について報告する予定である.

HFドップラーと微気圧計を用いた台風に伴う電離圏変動の統計解析

益子 竜一 [1]; 中田 裕之 [2]; 大矢 浩代 [3]; 鷹野 敏明 [4]; 冨澤 一郎 [5]; 細川 敬祐 [6]; 長尾 大道 [7]
[1] 千葉大・融合理工; [2] 千葉大・工・電気; [3] 千葉大・工・電気; [4] 千葉大・工; [5] 電通大・宇宙電磁環境; [6] 電通大; [7] 統数研

Statistical analysis of ionospheric and atmospheric disturbances associated with typhoons using HFD and a microbarometer

Ryuichi Mashiko[1]; Hiroyuki Nakata[2]; Hiroyo Ohya[3]; Toshiaki Takano[4]; Ichiro Tomizawa[5]; Keisuke Hosokawa[6]; Hiromichi Nagao[7]
[1] Grad. School of Sci. Eng., Chiba Univ.; [2] Grad. School of Eng., Chiba Univ.; [3] Engineering, Chiba Univ.; [4] Chiba Univ.; [5] SSRE, Univ. Electro-Comm.; [6] UEC; [7] ISM

It is reported that ionospheric disturbances due to the effects of the lower atmosphere are excited. Although the extreme climate phenomena, such as typhoons and tornados, also excites the ionospheric disturbances, the studies of these kind disturbances are very few. In this study, therefore, we have examined ionospheric and atmospheric variations associated with typhoons using HF doppler sounding system (HFD), which is maintained by the University of Electro-Communications, microbarometers located at Sugadaira, Nagano Prefecture and Numata, Gunma Prefecture, and reanalysis data (JRA-55) provided by Japan Meteorological Agency. This study utilizes HFD data where HF wave transmitted from Chofu Campus is received at Sugadaira observatory.

It is found that spectral intensities of the disturbances both of HFD data and microbarometer data at frequency from 15 mHz to 45 mHz were enhanced in 5 of 8 events where typhoons come closer to Japan. Those 5 typhoons approached the observation point more than 250 km.

These ionospheric disturbances were caused by the acoustic mode of internal gravity wave in association with typhoons. The acoustic mode of internal gravity wave propagates vertically, and thus spectral intensity were enhanced when the typhoons were close to the observation point. In some typhoons which were close to the observation point, however, ionospheric disturbances were not observed. In order to reveal the cause of this phenomenon, we make analyses of wind velocity of the reanalysis data. As a result, it was found that the vertical neutral winds influence the propagations of the internal gravity wave.

下層大気からの影響により電離圏変動が発生することが報告されており，台風や竜巻等の激しい気象現象においても電離圏擾乱の発生が確認されている．しかし，これらに関する研究は未だ十分ではないことから，本研究では，台風に伴う電離圏変動や大気波動について解析を行った．用いたデータは，電気通信大学の運営するHFドップラー（HFD）観測データ，菅平と沼田に設置された微気圧計，気象庁による再解析データ（JRA-55）である．HFDについては電通大調布キャンパスより電波を送信したHF帯電波を菅平にて受信したデータを用いている．

2004年から2016年の間に発生した発生した台風の中から，調布－菅平中間点付近に接近したもの19個を対象としHFDデータの解析を行った．また，2012年から2016年までの8個の台風においては微気圧計データとの比較も行った．それぞれの台風においてHFD，微気圧計データにFFTを施し，スペクトル強度の比較を行った．その結果，HFDと微気圧計のデータにおいて15 - 45 mHzの帯域で台風接近に伴いスペクトル強度が上昇することが明らかになった．また，8個中5個の台風でHFDと微気圧計，両方のデータにおいても静穏日と比べ，スペクトル強度の上昇が確認された．

台風接近に伴い15 - 45 mHzの帯域でHFDのスペクトル強度の上昇が確認されたが，これは台風により接近した内部重力波の音波モードが電離圏に到達することで変動が起きていると考えられる．また，HFDと微気圧計の比較について，観測点に250 kmよりも接近した台風において共に変動が見られたが，これは内部重力波の音波モードは鉛直方向に伝搬するためである．今回，対象とした台風の中には観測点に250 kmよりも接近したにも関わらずHFドップラーに変動が現れていないものも存在した．そこで変動の有無について再解析データ（鉛直速度データ）を用いて解析を行った．その結果，HFドップラーと微気圧計，どちらのデータでも変動が観測された2つの台風ではどちらも鉛直上向きの風が発生していることがわかった．また，微気圧計の変動に対してHFドップラーであまり変動が大きくなかった台風において鉛直下向きの風が起こっていた．これらより内部重力波の伝搬には中性風の上下方向の風向きが影響していると考えられる．

Free oscillations of the earth observed by HF Doppler sounding

Hiroyuki Nakata[1]; Keisuke Hosokawa[2]; Ichiro Tomizawa[3]
[1] Grad. School of Eng., Chiba Univ.; [2] UEC; [3] SSRE, Univ. Electro-Comm.

Any elastic bodies support standing waves known as free oscillation or normal mode. The frequencies of the excited mode of these oscillation is less than 20 mHz since the oscillations are usually low orders of the eigen oscillation. The atmosphere also has resonant oscillations with similar frequencies. Therefore, there are normal modes in the combined system of the solid earth. The upper boundary of the normal modes is considered to be located at the upper ionosphere, as several hundreds km above the ground. This means that the a certain ionospheric sounding system can observe this normal modes. In fact, associated with some large impact events, such as the massive earthquakes, volcanic eruptions, the ionospheric disturbances whose frequencies are about several mHz have been observed. Since the earth shows this free oscillation due to various sources of seismic sources but the atmospheric and tidal sources, ionospheric disturbances with a coupled frequencies can be observed in the quiet days for the ionosphere. In this study, therefore, the ionospheric disturbances with frequencies of the coupled oscillation are examined using HFD ionospheric sounding system. The merit of the HFD sounding system used in this study is to obtain the ionospheric disturbances at up to four different altitudes. Selecting geomagnetically quiet days, the spectrum of the ionospheric disturbances in these quiet days are determined. In the presentation, we will report the result of the intensity of the coupled mode oscillation.

S-310-44号機観測ロケットによって観測されたVLF帯波動の解析

中村 龍一郎 [1]; 三宅 壮聡 [1]; 石坂 圭吾 [2]; 阿部 琢美 [3]; 熊本 篤志 [4]; 田中 真 [5]
[1] 富山県大; [2] 富山県大・工; [3] ＪＡＸＡ宇宙科学研究所; [4] 東北大・理・地球物理; [5] 東海大・情教セ

Analysis of VLF band waves observed by S-310-44 Sounding Rocket

Ryuichiro Nakamura[1]; Taketoshi Miyake[1]; Keigo Ishisaka[2]; Takumi Abe[3]; Atsushi Kumamoto[4]; Makoto Tanaka[5]
[1] Toyama Pref. Univ.; [2] Toyama Pref. Univ.; [3] ISAS/JAXA; [4] Dept. Geophys, Tohoku Univ.; [5] Tokai Univ.

The Sq current system, which occurs in the lower ionosphere in the winter daytime, causes the specific plasma phenomena such as electron heating and strong electron density disturbance. S-310-44 sounding rocket experiment was carried out to the special phenomena near the Sq current focus, at 12:00 JST on January 15th, 2016. The rocket passed through the Sq current focus, and all the scientific instruments onboard the rocket worked successfully. In this experiment, the Electric Field Detector (EFD) observed the VLF band AC electric fields up to 6.4 kHz in the altitude from 100km to 160km. We made the altitude profile of the electric field spectra, and found clear VLF band waves with the frequencies from 2kHz to 3kHz at the altitude about 100km. These VLF waves are observed during only the rocket ascent. The Fast Langmuir Probe (FLP) observed that the electron temperature increase about 150K larger than the background in this region, and the frequency variation of the VLF band waves shows good correlation with the electron temperature.

According to the polarization analyses, the electric fields of the VLF band waves are almost perpendicular to the magnetic field. The frequency range of this VLF band waves is consistent with the ion cyclotron frequency. These results suggest that the VLF band waves observed in this experiment are one of the ion cyclotron harmonic waves whose frequencies vary with the temperature ratio of the electron and the ion (Te/Ti).

In addition, we are going to investigate further the VLF waves observed by the rocket experiment, and clarify the observation parameters and generation mechanism of these VLF waves, in order to clarify the heating mechanism of the electrons near the Sq current focus.

冬季の電離圏下部領域で発生するSq電流系は，電子加熱や強い電子密度擾乱といった特異な現象を引き起こす．Sq電流系の中心付近で起こるこれらの現象のメカニズムを解明するため，S-310-44号機観測ロケットが2016年1月15日12時00分（JST）に打ち上げられた．ロケットはSq電流系中心を通過し，搭載された観測機器はすべて正常に動作した．電場観測装置（EFD）は高度100kmから160kmにかけて6400HzまでのVLF帯交流電界を観測した．電界スペクトルの高度分布から，上昇時のみ高度100km付近で2〜3kHzの周波数帯のスペクトル強度が強くなっており，VLF帯波動が観測された．また，高速ラングミューアプローブ（FLP）の観測結果から，電子温度が高度100km付近で150Kほど上昇しており，電子温度上昇とVLF帯波動の周波数変化に良い相関が見られた．

また，偏波解析の結果から，観測されたVLF帯波動は磁場に対してほぼ垂直であり，周波数帯がイオンサイクロトロン周波数と一致した．これらの解析結果から，この波動は電子温度とイオン温度の比 (Te/Ti) によって周波数が変化するイオンサイクロトロン高調波である可能性が考えられる．

さらに詳しい解析を行うことで，ロケット実験で観測されたVLF帯波動の発生条件や発生メカニズムを明らかにし，Sq電流系中心付近に発生する高温電子領域の発生メカニズムの解明を目指す．

S-310-44号機観測ロケットによるSq電流系付近のDC電場観測

森 俊樹 [1]; 石坂 圭吾 [2]; 阿部 琢美 [3]; 田中 真 [4]; 熊本 篤志 [5]
[1] 富山県大・工; [2] 富山県大・工; [3] ＪＡＸＡ宇宙科学研究所; [4] 東海大・情教セ; [5] 東北大・理・地球物理

DC Electric Field Measurements in Sq Current by S-310-44 Sounding Rocket

Toshiki Mori[1]; Keigo Ishisaka[2]; Takumi Abe[3]; Makoto Tanaka[4]; Atsushi Kumamoto[5]
[1] Toyama Pref Univ.; [2] Toyama Pref. Univ.; [3] ISAS/JAXA; [4] Tokai Univ.; [5] Dept. Geophys, Tohoku Univ.

The region called Sq current occurs in the lower ionosphere at altitude of about 100km in the winter daytime. The Sq current focus is appeared the specific plasma phenomenon such as electron heating, strong electron density disturbance. The physical quantity for the investigation of the specific phenomenon was observed by S-310-44 sounding rocket launched in January 2016. The attitude data which we need to analyze electric field was changed. Therefore, we analyze DC electric field data observed by S-310-44 sounding rocket, again.

The rocket passes through the magnetic field, so it observes the induced electric field (v x B). Therefore, the observed electric field includes the DC electric field in the ambient plasma and the v x B electric field, so it is necessary to subtract the v x B electric field. Accordingly, the v x B electric field was calculated using the rocket attitude data, magnetic field data and so on. In addition, we converted the v x B electric field from the geographical coordinate system to the spin coordinate system using the spin component, and subtracted the v x B electric field of the spin coordinate system from the observation data. Furthermore, we removed the spin component from the subtracted data, and we removed pulse noise by photoemission using the moving average. Then, we derived the DC electric field vector in the ionosphere.

In this report, we will explain about DC electric field analyzed anew and the relationship between the high temperature region observed in this experiment and plasma waves during the rocket ascent.

冬期昼間において高度100km付近の電離圏下部ではSq電流系と呼ばれる領域が発生し、その中心付近には電子加熱、強い電子密度擾乱等の特異なプラズマ現象が生じている。2016年1月に打ち上げられたS-310-44号機観測ロケットにおいて、特異現象の解明のための鍵となる物理量が観測された。今回、ロケットの電場解析を行う上で必要となる姿勢データが修正されたため、改めてS-310-44号機観測ロケットの電場の解析を行う。

ロケットが観測する電場は、自然電場とロケットが磁場を通過した際に生じる誘導電場の合成電場である。そのため、自然電場を求めるためには、磁場データとロケットの飛翔速度から誘導電場の値を算出する。そして、誘導電場を地理座標系からスピン座標系に変換するために、アンテナの角度、ロケット方位角、ロケット天頂角、偏角を用いてスピン(アンテナ)成分を求める。電場の観測値からスピン座標系の誘導電場を減算することで自然電場を求める。求めた自然電場からスピン成分を取り除き、光電子放出によるパルス性ノイズを取り除くための移動平均を行う。これらの手順から、地理座標系での電離圏中のDC電場のベクトルを導出する。

本報告では新たに解析したDC電場について説明し、ロケット上昇時に観測された高温度領域及びプラズマ波動との関係について説明する。

地磁気Sq場の成分別季節変化の地域性

竹田 雅彦 [1]
[1] 京大・理・地磁気センター

Locality of geomagnetic Sq field of each element and its seasonal variation0000

Masahiko Takeda[1]
[1] Data Analysis Center for Geomagnetism and Space Magnetism, Kyoto Univ.

Geomagnetic Sq field in the Y and Z components were examined for some regions in the world. It was found that seasonal variation of Sq field at an observatory may be different for each element, and a peculiar seasonal variation pattern exists in the East Pacific region More detailed features of the variations will be discussed in the presentation.

世界各地域での地磁気Sq場の変化を成分別に調べその季節変化の地域性を調べた。同じ観測所でもY成分とZ成分とでは季節変化にかなり相違が見られるが、また、東太平洋地域では南北両半球ともそれぞれの夏の終わりに極大が現れるといった特徴的な変化も見いだせる。
学会時には、各成分についての地域特性とUT変化との関連などについても議論する予定である。

IRIモデルによる理論イオノグラムと観測との比較

深見 哲男 [1]; 長野 勇 [2]; 東 亮一 [1]
[1] 石川高専; [2] 金沢大

Comparison of Observation and Theoretical Ionograms using the International Reference Ionosphere

Tetsuo Fukami[1]; Isamu Nagano[2]; Ryoichi Higashi[1]
[1] NIT Ishikawa Col.; [2] Kanazawa Univ.

Ionograms are effective data to know the lower ionospheric conditions. The ionogram is made by pulse waves of the ionosonde and shows frequency characteristics for delay time T from transmitted time to received time by the same antenna after travelling in the ionosphere. So, the ionograms have information of both apparent heights and reflection coefficients on observation frequencies. The apparent height h' is $cT/2$ where c is light speed, and is not the actual reflection height. The theoretical delay time is calculated by the ionospheric condition. We suggest a method that estimate the delay time from the electron density profile and the collision profile by the full wave calculation [1]. Our method can simultaneously obtain the reflection coefficients. We checked the availability of our method from the simultaneous experiment of the rocket and the ionogram at Kagoshima Space Center [2].

On the other hand, The International Reference Ionosphere (IRI-2016) can give the electron density profile at latitude, longitude and time [3]. And we can input special parameters of *foE*, *foF2* and the sun spot number.

We investigate difference between measured and theoretical ionogram at the Kokubunji site. Figure show the observed ionogram at 6:00UT in 1917/05/20 [4]. In this ionogram, the Es layer did not appear. For the theoretical ionogram, we obtained the electron density profile of IRI-2016 for *foE* = 3.0 MHz, *foF2* = 6.7 MHz of this ionogram, and used the collision frequency profile of reference [5]. In this figure, we show the theoretical apparent heights for both the ordinary (O) and the extraordinary (X) waves. The theoretical h' values of the E and F2 layer is nearly agreement with the observed h' values, but the theoretical h' values of the F1 layer is not agreement.

[1] Fukami, T., I. Nagano and J. MacDougall: Proc. of ISAP 1996, 685-688 (1996).
[2] Fukami, T., I. Nagano and R. Higashi: PIERS 2018 in Toyama, 4P0, p2060 (2018).
[3] https://ccmc.gsfc.nasa.gov/modelweb/models/iri2016_vitmo.php
[4] http://wdc.nict.go.jp/ISDJ/ionospheric-signal.html
[5] Mambo, M., I. Nagano, T. Fukami and Y. Kagawa: IEEE Trans. on A&P, AP-34, 10, pp.1214-1222 (1986).

イオノグラムは，下部電離層を定常観測する有効な資料である。イオノグラムは，周波数毎の見かけ高さ (h') と反射係数を測定した図である。我々は，電子密度分布と衝突回数分布を与えれば full wave 計算法を用いて見かけ高さ (h') を算出する理論計算法を提案した [1]。そして，その有効性をイオノグラムとロケットによる同時実験で確かめた [2]。

他方，IRI モデルは，希望場所と時間の電子密度分布を与える [3]。そして，パラメータとして*foE*や*foF2*や太陽黒点数等を指定入力できる。ただし，IRI モデルには，Es 層はない。

我々は，情報通信研究機構の電磁波研究所が行っている国分寺のイオノグラム [4] を使って調査する。今回は，図に示した Es 層が無さそうである 1917 年 5 月 20 日 15:00LT のイオノグラムを用いる。理論イオノグラムを得るため，電子密度分布は，図の*foE*=3.0MHz，*foF2*＝ 6.7MHz を使って IRI 電子密度分布を得た。また，衝突回数分布は，過去に日本国内の中波帯の理論電界強度計算に用いた分布 [5] を使った。これらを用いて正常 (O) 波と異常 (X) 波に対して得られた理論イオノグラムを図中に示す。イオノゾンデのアンテナ感度が分らないので，今回は反射係数が 0.01 より大きい場合のみを図示した。IRI による理論値と観測値を比較すると，E 層と F2 層では，ほぼ合っていると思われる。しかし，F1 層では，両者の形状が異なっていることが分る。

今後，両者がほぼ合う電子密度分布を推定したい。

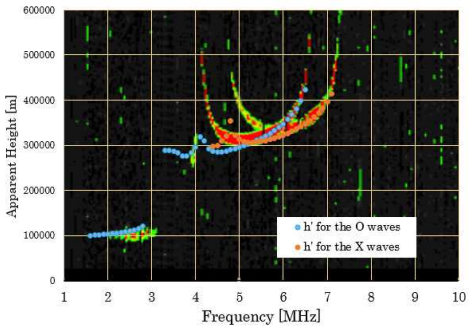

Obseaved ionogram and Calculated ionogram
using theIRI model (1917/05/20 06:00 UT)

SuperDARN近距離エコーの再評価

行松 彰 [1]
[1] 国立極地研究所/総研大

Reassessment of SuperDARN near range echoes in SENSU data

Akira Sessai Yukimatu[1]
[1] NIPR/SOKENDAI

SuperDARN is a powerful and unique tool primarily contributed to space weather research by providing global (polar and mid-latitude) ionospheric plasma convection and electric field potential map in high temporal resolution of ~1-2 min in quasi real time with its global coverage of international HF radars' FOVs. It also contributes to vertical coupling of ionised and neutral atmosphere in middle and upper atmosphere by observing TIDs (traveling ionospheric disturbances), neutral winds, and PMSE/PMWE etc in MLT (mesosphere and lower thermosphere) or MTI (mesosphere, thermosphere and ionosphere) regions.

SuperDARN near range echoes are the important targets especially for lower altitude echoes like those in D and E regions and those in MLT region. As typical range resolution of SuperDARN radars is rather coarse and HF ray paths bend in ionosphere, obtaining precise height/altitude information is key to understand the physics in the region correctly.

These years SuperDARN community tried to improve and re-establish the method of interferometer calibration (in several ways). Some radars have also started to try higher range resolution using imaging (SDI/FDI) and pulse coding technique etc.

We here try to re-calibrate the interferometer and elevation angles in our Antarctic Syowa SuperDARN SENSU radar data and to reassess the height information of the near range echoes.

Some recent papers related to this issue proposed near range echoes in summer midday obtained in Canadian SuperDARN radars data seems not from mesopause region altitude but from slightly higher altitude so those echoes might not be PMSEs. Results of reassessment of near range echoes in Syowa SENSU radars and origins of the echoes will be shown and discussed.

南極昭和基地ミリ波放射分光計による中間圏一酸化窒素カラム量の変動解析

長濱 智生 [1]; 水野 亮 [1]; 中島 拓 [1]; 大山 博史 [1]; 児島 康介 [1]; 江尻 省 [2]; 冨川 喜弘 [2]; 堤 雅基 [2]; 中村 卓司 [2]; 佐藤 薫 [3]
[1] 名大・宇地研; [2] 極地研; [3] 東大・理

An analysis of variations of the mesospheric column of nitric oxide observed with a millimeter-wave spectral radiometer at Syowa

Tomoo Nagahama[1]; Akira Mizuno[1]; Taku Nakajima[1]; Hirofumi Ohyama[1]; Yasusuke Kojima[1]; Mitsumu K. Ejiri[2]; Yoshihiro Tomikawa[2]; Masaki Tsutsumi[2]; Takuji Nakamura[2]; Kaoru Sato[3]
[1] ISEE, Nagoya Univ.; [2] NIPR; [3] Graduate School of Science, Univ. of Tokyo

Since 2011, the ISEE and NIPR started a joint research project on monitoring the composition changes in mesosphere and lower thermosphere (MLT) by using a millimeter-wave spectroscopy technique, and installed a millimeter-wave spectral radiometer operated in 250 GHz band at Syowa station in Antarctica (69S, 40E) for measuring the emission spectrum of nitric oxide (NO) in January 2012. The partial column of NO ranging from 75 to 100 km in altitude is retrieved from the observed emission spectrum. The mesospheric chemical composition largely varies caused by environmental changes of the earth inside and outside. Enhancement of NO_x and HO_x and consequence ozone depletion in the polar mesospheric region caused by precipitating the energetic particles such as a solar proton and an electron were reported. From the dataset observed with the radiometer in more than 6 years, we detect that the NO column amount shows the maximum in winter and sporadic enhancement of the NO column amount. Especially in case of 2016 fall, the NO column increased 3-4 times larger than the monthly average. In the presentation, we report the features of temporal variations of the observed NO column amount and the detail comparison with physical properties of precipitating high energy electrons, especially from the radiation belt.

名古屋大学宇宙地球環境研究所と国立極地研究所は 2011 年から共同して南極昭和基地に 250 GHz 帯高感度超伝導受信機を用いた小型ミリ波放射分光観測装置を設置し、2012 年 1 月より中間圏・下部熱圏の一酸化窒素（NO）から放射されるスペクトルの観測を行っている。中間圏の大気微量分子組成は大気密度が小さいことから地球内外の環境変動の影響を受けやすく、さらに地球の磁場構造により、太陽活動に起因する荷電した高エネルギー粒子は磁力線に沿って極域上空に降り込み、それによって中間圏や下部熱圏中性大気とのイオン分子反応により NO_x や HO_x の増加とそれに伴うオゾン減少等の大気組成変動をもたらすことが知られている。観測されたスペクトルの解析から 1 日以下の時間分解能で高度 75 から 105 km の NO カラム量を得ている。これまでに我々が取得した太陽極大期を含む 6 年間以上のミリ波観測データにより、極域中間圏の NO カラム量の季節変化は光化学反応が起こらない冬季に増大するが、その年々変動は大きいことがわかった。また 2015-2016 年には太陽活動と関連した数週間程度の周期的な NO カラム量増減が有意に見られた。特に、2016 年 8 月から 10 月にかけて、NO カラム量が月平均値より 3-4 倍に増加するイベントが数回検出された。NO カラム量の急増イベントでは、これまでに高エネルギー電子の降り込みとの相関が指摘されており（例えば、Isono et al. 2014）、これらのイベントにおいても高エネルギー電子との関連が見出された。発表では観測で得られた中間圏 NO カラム量の季節変化と急増イベントを中心に時間変動の特徴とそれらと高エネルギー電子の降りこみとの関連の詳細を報告する。

南極・昭和基地における中層大気多分子同時観測のための広帯域なミリ波分光計の開発

岩田 裕之 [1]; 小瀬垣 貴彦 [1]; 佐谷 昂樹 [2]; 原谷 浩平 [1]; 中島 拓 [3]; 長濱 智生 [3]; 水野 亮 [3]; 佐藤 薫 [4]; 堤 雅基 [5]; 渡邊 一世 [6]
[1] 名大・工・電気; [2] 名大・理・素粒子宇宙; [3] 名大・宇地研; [4] 東大・理; [5] 極地研; [6] 情報通信研究機構

Development of a millimeter-wave spectrometer for simultaneous observation of multi middle atmospheric molecules in Syowa station

Hiroyuki Iwata[1]; Takahiko Kosegaki[1]; Koki Satani[2]; Kohei Haratani[1]; Taku Nakajima[3]; Tomoo Nagahama[3]; Akira Mizuno[3]; Kaoru Sato[4]; Masaki Tsutsumi[5]; Issei Watanabe[6]
[1] Electrics, Nagoya Univ.; [2] Particle Astrophysics, Nagoya Univ.; [3] ISEE, Nagoya Univ.; [4] Graduate School of Science, Univ. of Tokyo; [5] NIPR; [6] NICT

Atmospheric environment on the Earth is changed by various factors. For example, in the polar regions, when energetic particles precipitate into the atmosphere during solar proton events or geomagnetic storms, nitrogen oxides(NO_X) increase, and the NO_X destroys ozone through catalytic reaction. On the other hand, the NO_X is photo-dissociated by solar UV radiation, and then the ozone depletion does not proceed further. But if the NO_X is transported downward, UV is absorbed in the upper atmosphere, and that prolongs the photochemical lifetime of NO_X and keeps destroying ozone for a long time. Moreover, ultraviolet ray has a direct impact not only on NO_X but also on generation and destruction of ozone. As mentioned above, atmospheric compositions are intricately changed by various physical and chemical factors. That is why we are monitoring atmospheric molecules at Syowa station, Antarctica in order to understand that the change of atmospheric composition can be dominantly caused on what condition by what physical or chemical interaction.

We are using millimeter-wave spectroscopy for monitoring. By this technique, the abundance of and vertical distribution of atmospheric molecules can be derived by receiving and dispersing millimeter-wave spectrum, radiated by themselves because of rotation transition. In our conventional millimeter-wave spectrometer, the observation frequency band is only 1 GHz, so we have observed O_3(237.146 GHz) and NO(250.796 GHz) by switching frequency. As described above, however, these two molecules are important on understanding change of atmospheric composition by energetic particle precipitation and atmospheric molecules are intricately interacting. That is why we are developing a new millimeter-wave spectrometer, which can observe five molecules including CO, NO_2, HO_2 in addition to O_3 and NO at the same time, in Syowa station since 2019.

In achieve that, we have been developing (1) frequency-independent beam transmission optical system which can efficiently collect signals from atmospheric molecules over broad frequency band, (2) a multiplexer which can distribute signals from optical system depending on observation frequency and lead to each detector and (3) Intermediate Frequency(IF) system which can lead signal from detectors to back-end digital Fourier transform spectrometer. As for (1), we designed the optical system which aperture efficiency is 39.3(+-)1.7 % between 179-254 GHz, 71 GHz-band, by using beam transmission simulator(GRASP). As for (2), we designed and produced the multiplexer which can distribute signal from 179-254 GHz to four channels by using electromagnetic simulator(HFSS). And we checked frequency dependency almost same as designed by using vector network analyzer in National Institute of Information and Communication Technology(NICT) (though we also checked 1-2 dB of insertion loss in the lowest frequency band). As for (3), we designed the circuit which can obtain five molecules spectrum at the same time by distributing 2 GHz band of new digital Fourier transform spectrometer to three IF bands. Now we are assembling components we have developed as an equipment and assessing phased performance.

In this presentation, we will report the details of development of this new millimeter-wave spectrometer, assembly condition at this time, results of performance assessment and so on.

地球の大気環境は、様々な要因で変化する。例えば極域においては、プロトンイベントや磁気嵐の影響で高エネルギー粒子が大気中に降り込むと、窒素酸化物（NO_X）が増加し、これによりオゾンが破壊される。一方、紫外線によって NO_X は光解離し、オゾン破壊の進行を止める。また NO_X が下方輸送された場合、紫外線はより上空で吸収されるため、NO_X の光化学寿命が延び、長期間にわたりオゾンに影響を与える。さらに、紫外線は NO_X だけでなく、オゾンの生成・消滅にも直接影響を及ぼす。このように大気組成は、多くの物理的・化学的要因が複雑に絡み合って変動する。そこで我々は、どのような条件下でどのような物理・化学過程がより支配的に組成変動に影響を与えるかを観測的に理解するため、南極・昭和基地において大気分子の長期的なモニタリングを行っている。

モニタリングには、ミリ波分光法を用いている。この方法では、大気分子の回転遷移によって放射されるミリ波スペクトルを受信・分光することで、大気分子の存在量と鉛直分布を導出できる。しかし、従来の我々のミリ波分光計は観測周波数の帯域幅が 1 GHz に制限されていたため、高エネルギー粒子の降り込みによる大気組成変動の理解のために重要な O_3(237.146 GHz) と NO(250.796 GHz) を同時に観測することができず、時分割して周波数を切り替え、交互に観測しなければならなかった。しかし上述したように、大気中の分子は非常に複雑に関係し合って変動している。そこで我々は、2019 年度から南極・昭和基地で従来の O_3 と NO に加え、CO, NO_2, HO_2 の 5 分子を同時に観測するため、新たなミリ波分光計の開発を行っている。

そのために我々はこれまで（１）広い周波数帯域に渡って、大気信号を効率よく集光する周波数無依存ビーム伝送光学系の設計開発、（２）光学系によって集光された信号を、観測分子の周波数に応じて分配し、１つ１つの検出器へと導くマルチプレクサ（合分波器）の開発、（３）検出器からの信号を最終段のデジタルフーリエ変換分光計に導く IF（中間周波数）系の開発を進めてきた。(1) ではビーム伝送系シミュレータ (GRASP) を用い、179 GHz から 254 GHz までの 71 GHz の帯域にわたり 39.3(+-)1.7 %の開口能率が得られるビーム伝送光学系の設計に成功した。また、(2) では電磁界シミュレータ (HFSS) を用い、179 GHz から 254 GHz までの帯域を 4 つのチャンネルに分割するマルチプレクサの設計製作を行い、情報通信研究機構のベクトルネットワークアナライザを用いた単体評価でほぼ設計通りの周波数特性（ただし低周波帯での挿入損失において 1-2 dB 程度の悪化が見られる）が確認できた。(3) では、新たに導入した 2 GHz 帯域幅のデジタルフーリエ変換分光計を３つの IF 帯域に分割し、５つの分子スペクトルを同時に取得するための回路設計を行なった。現在、これらの開発で製作してきたコンポーネントを実機へと組み上げつつ、段階的な性能評価を行なっている。

発表では、この新しいミリ波分光計の開発の詳細と現時点でのアセンブリ状況、性能評価結果などについて報告する。

アルゼンチン・リオガジェゴスでのミリ波を用いた成層圏オゾンの観測

關 博則 [1]; 水野 亮 [1]; 長濱 智生 [1]; 中島 拓 [1]; 大山 博史 [1]
[1] 名大・宇地研

Observation of stratospheric ozone with a millimeter-wave radiometer in Rio Gallegos, Argentina

Hironori Seki[1]; Akira Mizuno[1]; Tomoo Nagahama[1]; Taku Nakajima[1]; Hirofumi Ohyama[1]
[1] ISEE, Nagoya Univ.

http://skx1.stelab.nagoya-u.ac.jp/

Argentine Rio Gallegos (51.6 S, 69.3 W) is located at the southernmost tip of South American Continent and is located near the boundary area of the ozone hole which occurs in the sky over Antarctica. Therefore, the city is often inside ozone hole in winter to early spring season. As ultraviolet flux at the surface increases, the ozone hole has become a serious risk of environmental problems closely related to life for residents living in this region. For these reasons, our research group has been working together with collaborators in Argentina and Chile as parts of the international science and technology cooperation project (SATREPS) to solve to global environmental problems in the southernmost region of South America as the "blank area" of the earth observation network since 2013. We have been developing and operating the monitoring system of stratospheric ozone, aerosols and ultraviolet rays to construct communicating information systems about atmospheric data to domestic and foreign country.Continuous monitoring of stratospheric ozone with a ground-based millimeter wave spectrometer aims to investigate a vertical distribution of ozone and to detect its long-term and short-term variations. We observe an emission spectrum of ozone at 110.83 GHz. A heterodyne receiver with a superconducting mixer element (SIS) is used for millimeter wave detection with the radiometer. A receiver noise temperature Trx is estimated at 200 K in double side band (DSB). A digital FFT spectrometer is used for the radio wave spectrometer. Its frequency resolution is 70 kHz and the band width is 1 GHz. In the observation, three directions of the sky cold, blackbody, and cold blackbody cooled by liquid nitrogen are observed every 2 minutes, respectively, to calibrate a spectral intensity. The ozone emission spectrum is acquired every 7 minutes. We derive the vertical distribution of ozone by using a retrieval method from the observed ozone spectrum. In the retrieval, we use the temperature and pressure data taken from MERRA 2 reanalysis data, spectral parameters of molecules from HITARAN 2008 database, and climatological ozone distributions over Rio Gallegos with Aura / MLS ozone data as an initial estimate of the ozone distribution. For the retrieval, we use the Levenberg marquardt method for retrieval, and we obtain the vertical distributions from altitude 20 to 60 km from the observed spectra averaged every hour.As results from 2015, we detected sharp decreases of the stratospheric ozone mixing ratio from September to October, when the ozone hole occurs near the upper stratosphere, indicating the observation site is inside the ozone hole. In the presentation, we report the observation details and characteristics of ozone variations observed since 2013.

アルゼンチン・リオガジェゴス (51.6 S, 69.3 W) は南米大陸最南端に位置しており、南極上空に発生するオゾンホールの境界領域付近にあることから、冬～早春にかけて極渦の影響によりしばしばオゾンホールの内側に入り込む。それによって地表での紫外線量が増加するため、この地域の住民にとってオゾンホールは日常生活に密着した環境問題となっている。そこで我々研究グループは、地球観測網の「空白域」である南米南端域での環境問題の対応へ向け、2013 年より地球規模課題対応国際科学技術協力事業 (SATREPS) の一環としてアルゼンチン・チリと共に大気質データの国内外へ向けた情報伝達システムの構築をめざし、成層圏オゾンにエアロゾルや紫外線も含めた大気モニタリングの環境開発及び運用を行ってきた。その中で、地上ミリ波分光計による連続的なオゾンモニタリングは、成層圏オゾンの高度分布情報の取得とその長期的・短期的な動態を明らかにすることを目標としている。観測周波数 110.83 GHz のオゾンの回転遷移による放射スペクトルを観測している。ミリ波放射分光計のミリ波検出には超伝導ミクサ素子（SIS 素子）を用いたヘテロダイン受信機を用いており、その雑音温度 Trx(DSB) は~200 K である。電波分光器にはデジタル FFT 分光計を用い、その周波数帯域 1 GHz で周波数分解能は 70 kHz である。観測では空の方向に加え、常温黒体及び液体窒素を利用した冷却黒体の 3 つの方向を 2 分ごとにそれぞれ観測し、電波強度の校正を行っている。オゾン放射スペクトルは 7 分ごとに取得される。観測されたオゾンスペクトルからリトリーバルによってオゾンの高度分布を導出する。リトリーバルには MERRA2 再解析データから気温・気圧データを、HITARAN2008 データベースから分子の分光パラメータを、オゾン高度分布の初期推定値として Aura/MLS のオゾンデータによるリオガジェゴス上空での気候値を用いている。また、リトリーバルには Levenberg marquardt 法を用いたアルゴリズムを用い、1 時間ごとに平均したスペクトルから高度 20 から 60 km までの高度分布を得ている。これまでに解析を行った 2015 年以降については、上部成層圏の高度 40km 付近で成層圏オゾンの季節変動に加え、オゾンホールの発生する 9 月~10 月にオゾン混合比の急激な減少が見られ、観測サイトがオゾンホールの範囲内に入り込んでいる様子を検出することができた。発表では、観測の詳細と得られたオゾン変動の特徴について報告する。

Feasibility study for artificial aurora experiments at the EISACT Tromso site

Takuo Tsuda[1]; Michael Rietveld[2]; Michael J. Kosch[3]; Shin-ichiro Oyama[4]; Keisuke Hosokawa[1]; Satonori Nozawa[5]; Tetsuya Kawabata[5]; Akira Mizuno[5]; Yasunobu Ogawa[6]
[1] UEC; [2] EISCAT; [3] SANSA; [4] ISEE, Nagoya Univ.; [5] ISEE, Nagoya Univ.; [6] NIPR

We report a brief survey on conditions for artificial aurora optical experiments in *F* region heating with O-mode at the EISCAT Tromso site using dynasonde data from 2000 to 2017. The results obtained in our survey indicate the following: The possible conditions for conducting artificial aurora experiments are concentrated in twilight hours in both evening and morning, compared with late-night hours; the possible conditions appear in fall, winter, and spring, while there is no chance in summer, and the month-to-month variation among fall, winter, and spring is not clear. The year-to-year variation is well correlated with the solar cycle, and experiments during the solar minimum would be almost hopeless. These findings are useful for planning future artificial aurora optical experiments.

南極昭和基地における近赤外波長領域（1.0-1.6 microns）の広帯域/高波長分解能・分光観測

西山 尚典 [1]; 田口 真 [2]; 鈴木 秀彦 [3]; 坂野井 健 [4]
[1] 極地研; [2] 立教大・理・物理; [3] 明治大; [4] 東北大・理

A ground-based observation of imaging spectrum in near infrared wavelength (1.0-1.6 microns) at Syowa Station

Takanori Nishiyama[1]; Makoto Taguchi[2]; Hidehiko Suzuki[3]; Takeshi Sakanoi[4]
[1] NIPR; [2] Rikkyo Univ.; [3] Meiji univ.; [4] Grad. School of Science, Tohoku Univ.

The motivation of this study is further understanding of dayside magnetosphere and terrestrial atmosphere coupling system by using continuous observation with high temporal and spatial resolutions. Dayside aurora, polar patch, and airglow should be key phenomena for the understanding. In particular, those phenomena in near infrared (NIR) wavelength are crucially important because lower background sky luminosity by Rayleigh scattering may allow us to conduct ground-based optical observation even in dayside. Continuous dayside optical monitoring in aurora region and cusp give us a clue to understanding of substorm pre-onset sequences at cusp region, magnetopause dynamics related to solar wind shocks, and wave-particle interactions due to electromagnetic ion cyclotron waves and whistler mode chorus. However, NIR aurora has a total lack of its spectral information with enough resolution to make a feasibility study in comparison to that in visible wavelength.

We designed a narrow field spectrometer with medium-high spectral resolution that mainly consists of Czerny-Turner type imaging spectrometer (HORIBA, iHR320) with one entry port and two exit ports. This spectrometer has two mirrors and three diffractive gratings in a rotating turret. A toroidal mirror for collimating corrects for astigmatism so that the tangential (resolution optimized) and sagittal (imaging optimized) focal planes cross at the center of the focal plane. Another larger focus mirror allows the entire flat field to be used without vignetting. Collecting optics, equipped outside the spectrometer, are a gold coated off-axis parabolic mirror and a NIR longpass filter for removal of secondary diffracted light in visible wavelength. Two detectors for two exit ports are NIR-photomultiplier tube (PMT) module with thermoelectric (TE) cooling system (Hamamatsu, H10330C-75) and InGaAs camera with 640 x 512 pixels and TE cooling in 4 stages (Photon etc., ZephIR 1.7). NIR-PMT module in combination with an exit slit measures precisely individual emission spectrum with high resolution of 0.006 nm. On the other hand, InGaAs camera covers wider spectral ranges (200 nm, 45 nm, 25 nm) and medium spectral resolutions (0.31 nm, 0.070 nm, 0.038 nm) depending on the three gratings (150 gr/mm, 600 gr/mm, 900 gr/mm). The two detectors cannot be operated simultaneously but can be easily switched by a software.

We started ground-based spectroscopic observation in NIR wavelength ranging from 1.0 to 1.6 microns, which covers auroral emissions in N_2 1st Positive (1.2 microns) and N_2^+ Meinel (1.1 and 1.5 microns) [*Jones* 1974; *Zhou et al*., 2007], at Syowa Station (69.0^{o}S, 39.6^{o}E) in Antarctica from March 2018. In this presentation, we are going to report initial results based on one year observation.

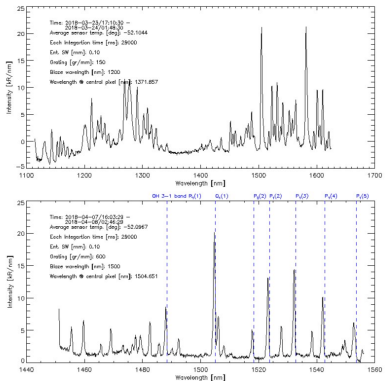

北欧ライダー拠点を目指して：AO高速周波数切替システムと磁気光学狭帯域フィルタ開発

川原 琢也 [1]; 野澤 悟徳 [2]; 斎藤 徳人 [3]; 津田 卓雄 [4]; 和田 智之 [3]; 高橋 透 [5]; 川端 哲也 [2]
[1] 信州大・工; [2] 名大・宇地研; [3] 理化学研究所基幹研; [4] 電通大; [5] 極地研

Na lidar in the EISCAT radar site: future upgrades

Takuya Kawahara[1]; Satonori Nozawa[2]; Norihito Saito[3]; Takuo Tsuda[4]; Satoshi Wada[3]; Toru Takahashi[5]; Tetsuya Kawabata[2]
[1] Faculty of Engineering, Shinshu University; [2] ISEE, Nagoya Univ.; [3] ASI, RIKEN; [4] UEC; [5] NIPR

An Nd:YAG laser-based sodium temperature/wind lidar was developed for the measurement of the northern polar mesosphere and lower thermosphere at Tromso (69.6N, 19.2E), Norway. The highly stable laser system is first of its kind to operate virtually maintenance-free during the observation season (from late September to March) since 2010. The lidar data is currently important and is going to be getting more important if the EISCAT_3D project starts or if we join the joint project of the Whole Atmosphere Community Climate Model (WACCM). In this talk, we summarize our current status and the future prospect of the lidar.

我々はノルウェー・トロムソ（北緯69）に位置するEISCATレーダーサイトに設置したナトリウム温度・風ライダーで極夜の観測を継続している。2010年に観測を開始してから、ほぼメンテナンスフリーの準自動観測を継続してきた。今後のEISCAT_3D計画や、英米の大気の鉛直輸送モデルWhole Atmosphere Community Climate Model (WACCM)への鉛直風データの提供などで、より重要性が増して行く状況にある。本発表ではライダー本来のパフォーマンスを最大限まで高めるAO高速周波数切替システムのシステムと、昼間観測のための磁気光学狭帯域フィルタ開発の途中経過に関して展望を示す。

Relationship between the By component of Interplanetary Magnetic Field and occurrence of polar cap patches

Michitaro Nagata[1]; Keisuke Hosokawa[1]; Kazuo Shiokawa[2]; Yuichi Otsuka[2]
[1] UEC; [2] ISEE, Nagoya Univ.

Polar cap patches are regions of high density plasma in the polar cap F region ionosphere. The electron density within patches is known to be 2 to 10 times higher than that in the surrounding region. It has been suggested that patches are produced by long distance transportation of high-density plasma from the dayside sunlit area towards the dark central polar cap region by the anti-sunward convection during negative Bz conditions. Polar cap patches have been observed in many places in the polar cap. In the past, however, most of the observation stations were located at magnetic latitudes around 80 degrees (e.g., Resolute Bay in Canada and Longyearbyen in Norway). Thus, continuous observations at a fixed point in the magnetic coordinate system have not yet been done due to the rotation of the Earth. This has made it difficult to follow the statistical characteristics of patches, especially seasonal and UT dependence of their occurrence. In this study, we statistically investigate the occurrence distribution of polar cap patches by using data from a station near the magnetic pole and clarify the factors controlling the generation of patches.

We have used 630.0 nm all-sky images from Eureka, Canada (80.0 N, 85.9 W, 87.7 MLAT) for almost three winter seasons from 2015 to 2017. The amount of data used is 85 days in 2015, 108 days in 2016 and 47 days in 2017, respectively. We automatically identified the appearance of patches from a time-series of the optical intensity at zenith and made a list of patches. Then, we manually checked all the patches in the list and discarded other phenomena such as polar cap aurorae which have been miss-identified by the automated detection. By using this list of patches, we analyzed how the occurrence of patches depends on UT, season, and IMF. As a result of the statistics, generation of patches is dominated not only by the Bz component of IMF but also season, UT and IMF By. In particular, we found that polar cap patches were observed more often when the IMF By was positive, which has not suggested in the previous studies. In actual, the occurrence of patches was 3 times higher during positive IMF By periods. That means more patches should be observed during intervals of away sector of the IMF (IMF By is positive and Bx is negative in the away sector). To interpret this result, first we suspected a bias in the occurrence of toward and away sectors. However, there was not such a difference during the period of statistical analysis. We also tried to explain the result by the so-called Russell-McPherron effect by comparing the distribution of the polar cap patches in autumn and spring. But, the bias due to the Russell-McPherron effect was not clear. Therefore, at this stage, we speculate that the shape of polar cap convection pattern is favorable for capturing and transporting dense plasma in the duskside sunlit region during the positive IMF By intervals. To evaluate this scenario, we visualize the average pattern of plasma convection in the polar cap area during intervals of positive IMF By patches by analysing data from the SuperDARN radars in a statistical way. In the presentation we will present the results of this analysis and discuss the origin of the observed preference of patch occurrence for positive IMF By intervals.

Investigation of interhemispheric asymmetry of polar cap patch occurrence

Akiko Kagawa[1]; Keisuke Hosokawa[1]; Yasunobu Ogawa[2]; Akira Kadokura[2]; Yusuke Ebihara[3]; Hidekatsu Jin[4]; Kazuo Shiokawa[5]; Yuichi Otsuka[5]
[1] UEC; [2] NIPR; [3] RISH, Kyoto Univ.; [4] NICT; [5] ISEE, Nagoya Univ.

Polar cap patches are defined as regions of plasma density enhancements in the polar cap F region ionosphere. The electron density inside patches is 2 to 10 times larger than the background level. When discussing the generation mechanism of patches, it is important to consider the spatial distribution of 1) the daytime high-density plasma and 2) the high-latitude plasma convection. That is, to produce patches, there should be a spatial overlap of the above-mentioned two factors especially on the dayside. Taking this into account, if the distance (i.e., offset) between the geographic and geomagnetic poles (Altitude adjustment corrected geomagnetic coordinates) is sufficiently large, there should be a period when the entire polar cap is within the dark hemisphere and the intake of daytime high-density plasma (i.e., high-density patches) never happens. Thus, it is predicted that the production of patches deeply depends on the offset between the two poles. However, there has been no study that examined the dependence of patch occurrence (for example, UT distribution and seasonal distribution) on the offset because almost all of the past studies were targeted for patches in the northern hemisphere (NH) where the offset is smaller (˜7 degrees) than that in southern hemisphere (SH) which is ˜15 degrees. In this study, we reveal the role played by the offset in the patch production process by investigating the interhemispheric asymmetry of patch occurrence characteristics.

In order to perform statistics of patches in both hemispheres, we made use of 630.0 nm airglow images from all-sky imagers operated at Resolute Bay, Canada (OMTIs: 74.7 N, 265.1 E) and McMurdo, Antarctica (AWI: 77.5 S, 166.4 E) during local winter in 2015. In addition, to visualize the spatial distribution of the plasma density in the entire polar cap, we employed the GAIA (Ground-to-Topside Model of Atmosphere and Ionosphere for Aeronomy) model. As a result of statistical analysis, it was found that almost no patches were observed in McMurdo during a few hours from 14 to 17 UT. In this time period, the entire high-latitude plasma convection system in the SH is in the dark hemisphere and there should be no interaction with the high-density plasma in the sunlit area. Such a configuration prevents the intake of sunlit high-density plasma which is the primary reason for the absence of patches in the SH in this specific time period. Similar UT dependence of patch occurrence was not seen in the NH because of the small offset between the poles. This indicates the difference in the offset between the poles indeed introduces an interhemispheric asymmetry in the climatology of patches. In addition to the analysis of UT dependence, we investigated the effect of the offset on the seasonal distribution of patches by using in-situ plasma density data from the Swarm satellites. We found that the occurrence rate of patches is higher during equinoctial periods, especially in the SH. This tendency can partly be explained by the so-called Russel-McPherron (R-M) effect, but the reason for the slight interhemispheric asymmetry is still unclear. In the presentation, by taking both the R-M effect and the difference in the offset into account, we discuss the interhemispheric asymmetry in the seasonal variation of patch occurrence rate.

オーロラ領域における熱圏大気ダイナミクスの数値シミュレーション

大井川 智一 [1]; 品川 裕之 [2]; 田口 聡 [1]
[1] 京大理; [2] 情報通信研究機構

Numerical simulation of the thermospheric dynamics in the auroral region

Tomokazu Oigawa[1]; Hiroyuki Shinagawa[2]; Satoshi Taguchi[1]
[1] Grad school of Science, Kyoto Univ.; [2] NICT

www-step.kugi.kyoto-u.ac.jp

The thermosphere and ionosphere in the polar region have been studied for a long time. Recent results of the ground and satellite measurements have suggested that local dynamics of the auroral thermosphere and ionosphere are extremely complicated. In particular, in the auroral region, various processes, such as Joule heating, particle precipitation heating, and ion-neutral drag force enhanced by particle precipitation, are strongly coupled. Previous observations have shown some characteristic mesoscale phenomena such as neutral vertical winds and increasing neutral density in the auroral region. However, the behavior of such phenomena is still not well understood. In order to study the mesoscale thermosphere dynamics in the auroral region, nonhydostatic atmosphere models are required instead of traditional hydrostatic atmosphere models. We will report on how the vertical neutral wind and the neutral density depend on typical parameters in the auroral region, such as electric field, electron density and width of heating region using a two-dimensional nonhydrostatic neutral atmospheric model.

極域の熱圏・電離圏は長年にわたって研究されてきたが、近年の地上や衛星からの観測により、そのダイナミクスは極めて複雑であることが明らかになっている。特にオーロラ領域においては、ジュール加熱や粒子の降り込みによる加熱や電離、さらに電離によって密度の増加したイオンによるイオンー中性ドラッグ等の様々な過程が相互作用しており、オーロラ領域の熱圏鉛直流や密度上昇といった特徴的なメソスケール現象も観測されている。しかしその振る舞いはまだ十分には理解されていない。数値シミュレーションはそうしたオーロラ領域のメソスケール現象を解明するための有力な手段であるが、その定量的な取り扱いには、従来からよく用いられてきた静水圧モデルではなく、非静水圧平衡モデルを用いる必要がある。本講演では、熱圏の２次元非静力学大気モデルを用いることにより、オーロラ領域の主なパラメータである電場の大きさや電子密度および加熱領域の幅等に対する、中性大気の鉛直流や密度上昇の依存性について調べた結果を報告する。

高エネルギー降下粒子がNa層に与える影響の化学モデル計算

滝沢 響吾 [1]; 津田 卓雄 [1]
[1] 電通大

Chemical model calculations on Na layer variation induced by energetic particle precipitation

Kyogo Takizawa[1]; Takuo Tsuda[1]
[1] UEC

Metallic atom and ion layers, such as Na/Na^+, K/K^+, Fe/Fe^+, and Ca/Ca^+ layers, exist in the mesosphere and lower thermosphere (MLT). The height range of the MLT region corresponds to the ionospheric D and E regions, and in the polar region energetic particles precipitating from the magnetosphere can often penetrate into the E region and even into the D region. Therefore, the influence of energetic particles on the metallic atom and ion layers is of interest regarding changes in atmospheric composition accompanied by auroral activity or geomagnetic activity.

There are several previous studies on energetic particle effects to Na atom. Decreases in Na density during energetic particle precipitations were reported from Na resonance scattering lidar and incoherent scatter radar observations during nighttime at high-latitudes, i.e., wintertime. Using sunlight-induced Na emission data by a low-orbit-satellite, it was revealed that Na densities were low during the geomagnetically active periods in the polar daytime, i.e., summertime, compared with those during the quiet periods. Some models based on the Na chemistry indicated that charge exchange reactions Na atoms and background ions (NO^+, $O_2{}^+$), which can be enhanced by ionization due to energetic particles, play important role in mechanism for Na densities decrease induced by the energetic particle precipitation. However, our understanding on energetic particle effects to the Na layer is still limited. In particular, more quantitative evaluations on the Na chemical processes are needed.

In this study, we have developed a numerical model to understand importance of the Na chemical processes triggered by ionization, i.e., enhancements of electron and ion densities, due to energetic particle precipitation. The model describes simply continuity equations related with Na chemical reactions. To investigate the ionization effects to the Na layer, we have perfomred two calcurations using the model. One is the case of higher electron and ion densities, i.e., the case of ionization induced by energetic particle precipitation, and the other is the case of lower electron and ion densities, i.e., the case of no ionization or no particle precipitation. Such calculations have been done in the two background conditions, which are summertime and wintertime. As the results, we have found that the calculrated Na densities in the cases of ionization were lower than those in the cases of no ionization in both summertime and wintertime. Under the winter condition, amount of Na density decrease was ~3700 cm^{-3} at 95 km height while that under the summer condition was ~2400 cm^{-3} at 94 km height. These summr and winter results would be fairly consistent with the previous observational results. Thus, the enhancements of electron and ion densities can induce Na density decrease through the Na chemical process. In the presentation, we will introduce our model and present the calculated results. Furtheremore, we will discuss important chemical processes and background parameters in the Na decrease due to energetic particles, based on comparisons between results in the summertime and wintertime.

太陽陽子降り込みイベントに伴う極域中間圏オゾン減少の統計解析

石島 陸 [1]; 長濱 智生 [2]; 水野 亮 [2]
[1] 名大・理・宇地研; [2] 名大・宇地研

A statistical analysis of ozone depletion in the polar mesosphere caused by precipitating solar protons

Riku Ishijima[1]; Tomoo Nagahama[2]; Akira Mizuno[2]
[1] ISEE, Nagoya Univ.; [2] ISEE, Nagoya Univ.

It is known that energetic particle precipitation (EPP) into the polar mesosphere induces generation of NO_x and HO_x due to dissociation and/or ionization of nitrogen and oxygen molecules, leading ozone (O_3) depletion in the upper stratosphere and mesosphere. In particular, O_3 depletion in the stratosphere and mesosphere was reported at the large solar proton events (SPEs) that the energetic protons from the sun precipitate into the atmosphere (e.g. Jackman et al. 2005). However, the response of the stratospheric and mesospheric O_3 at the SPEs with the medium and the small proton flux is not revealed. To understand relationship between the O_3 depletion and SPEs in the upper stratosphere and mesosphere, we investigated changes of mesospheric O_3 mixing ratio before and after the SPEs that the maximum of the proton flux over 10 MeV exceeds 10 pfu during a period in 2012-2015 which are listed by NOAA SPACE ENVIRONMENT SERVICES CENTER, by using the O_3 dataset observed with Aura/MLS (version 4.2) (Ishijima et al. JpGU2018). We examined the temporal change of the zonal average of the O_3 mixing ratio at an altitude of 60 km every 3 degrees from 50 to 80 degrees in geomagnetic latitude over 5 days before and after the 6 SPEs with the maximum of the proton flux over 100 pfu during the period, and found significant ozone depletion in a region where the geomagnetic latitude is more than 70 degrees, and suggested the relationship between the proton flux and the O_3 depletion reduction rate of O_3. Furthermore, we found that the temporal variation of the zonal averaged O_3 in two polar areas showed a difference in time about 12-24 hours, implying it may be due to difference in time of precipitation of the solar proton in both the poles. To confirm them statistically, we examine the mesospheric O_3 depletion at the SPEs extended from 2004 to 2017. During 13 years, there are 53 SPEs with the maximum of the proton flux ranging from 12 to 6530 pfu. For all the SPEs, we estimate the time at which the O_3 at 60 km most decreases from the average value before the event with the geomagnetic latitude every 3 degrees, and also estimate the correlation between the maximum of the proton flux at the SPE and the O_3 depletion rate. In the presentation, we report on the details of these features as well as the feature of the O_3 depletion with the geomagnetic latitude. In addition, the time difference of the O_3 depletion in both the polar areas through a solar cycle is discussed.

極域中間圏では高エネルギー粒子の降り込み (Energetic Particle Precipitation: EPP) によって窒素分子や酸素分子が解離・電離して NO_x や HO_x を生成し、それらによりオゾン (O_3) が減少することが知られている。特に、太陽からの陽子が地球大気に降り込む太陽陽子イベント (Solar Proton Event: SPE) においては、大きな SPE 時に成層圏・中間圏の O_3 減少が報告されている (例えば、Jackman et al. 2005)。しかし、中・小規模な SPE まで含めたイベント時における成層圏・中間圏 O_3 の応答についてはこれまで十分には解明されていない。我々はこれまでに、2012-2015 年の期間で NOAA SPACE ENVIRONMENT SERVICES CENTER による 10 MeV 以上の陽子フラックスが 10 pfu を超える SPE に着目し、Aura/MLS で観測された O_3 データ（version 4.2）を利用して、SPE 前後における中間圏 O_3 への変動を調べた（石島ほか、JpGU2018）。期間中に陽子フラックスの最大値が 100 pfu を超えた 6 つの SPE に関して、高度 60 km における O_3 混合比について磁気緯度 50-80 度までの 3 度ごとの帯状平均を求め、その時間変化をイベント前後 5 日間にわたって調べたところ、磁気緯度が 70 度以上の高緯度領域で有意な O_3 減少を見出した。さらに、陽子フラックスと SPE 前後での O_3 減少率の関連を示唆する結果を得た。その一方で、磁気緯度帯ごとの O_3 の時間変動には両極で半日から 1 日程度の差があり、北極側と南極側では SPE の降り込み方やそれに対する O_3 の影響に違いによる可能性が考えられる。

そこで本研究では、前回利用した Aura/MLS の O_3 データを 2004-2017 年の 13 年間に拡張し、1 太陽周期における SPE が中間圏 O_3 に与える影響を調べた。期間中に陽子フラックスが 10 pfu を超える SPE は 53 回発生し、フラックスの最大値は 12 から 6530 pfu の範囲であった。全ての SPE において、高度 60 km における O_3 混合比がイベント前の平均値から最も減少する時刻をそれぞれの磁気緯度で求め、陽子フラックスとの関連について解析を行い、前回得られた SPE と O_3 の関係性、北極側と南極側の違いを磁気緯度帯ごとにより詳細を得た。発表では、これらを示すとともに、ほぼ同じ強さの SPE でも太陽活動度が異なる期間で中間圏 O_3 の減少傾向の違いについても報告する予定である。

Ionospheric heating in the dayside polar region during solar minimum and geomagnetically quiet equinox periods.

Hitoshi Fujiwara[1]; Satonori Nozawa[2]; Yasunobu Ogawa[3]; Yasunobu Miyoshi[4]; Hidekatsu Jin[5]; Hiroyuki Shinagawa[5]; Chihiro Tao[5]; Ryuho Kataoka[3]; Huixin Liu[6]
[1] Faculty of Science and Technology, Seikei University; [2] ISEE, Nagoya Univ.; [3] NIPR; [4] Dept. Earth & Planetary Sci, Kyushu Univ.; [5] NICT; [6] None

The localized and rapid changes in the polar cap ionosphere seem to be one of the important issues for the future space weather predictions. From the observations with the European Incoherent Scatter (EISCAT) radar system, some interesting features of the dayside polar cap ionosphere have been revealed even during geomagnetically quiet (small Kp) periods. In order to understand dayside polar ionosphere/thermosphere, we have performed simultaneous observations with the EISCAT UHF radar (at Tromsoe) and EISCAT Svalbard radar (ESR) (at Longyearbyen). In this study, we report on two examples of significant ionospheric disturbances observed in the dayside polar region at around or higher than 80 deg latitude with the ESR 32 m antenna (elevation angle of 30 deg) on March 20 and 21, 2018. The quiet ionosphere was observed in the same periods with ESR 42 m antenna (field-aligned direction) and the EISCAT UHF radar (at Tromsoe). The solar and geomagnetic activities were quite low, F10.7=69 and Kp=0-1-, during the observational periods (07:00-13:00 UT) on both days.

In the first case (March 20), the IMF Bz component fluctuated around 0 nT before 10:00 UT while the IMF Bz showed negative values after about 10:00 UT. Strong ion flows were widely seen higher than 80 deg latitude during 09:00-12:00 UT. Before 09:00 UT, quasi periodic variations of the localized ion flows were seen at around 80 deg latitude. The ion temperature was about 1000 K at around 80 deg latitude with some rapid enhancements during the observational period. The electron density showed quasi periodic variations (about 10 minutes) in association with strong ion flows. In the second case (March 21), strong ion flows and increases in the ion temperature were observed during the periods of positive Bz. Strong shears of the ion flows and reversals of the flow direction were remarkable at around 08:30 and 09:00 UT. The rapid increase in the ion temperature was seen after 09:00 UT when strong ion flows were observed. The ion temperature was changed from about 900 K to 2000 K within 10 minutes at around 09:04-09:14 UT. These data sets will be examples which would show features of the dayside polar cap ionosphere during the solar minimum condition. We will compare the present data with the IPY 2007-2008 data which were obtained from continuous observations with the ESR during the last solar minimum periods.